



**National Library  
of Canada**

**Bibliothèque nationale  
du Canada**

**Canadian Theses Service**

**Service des thèses canadiennes**

**Ottawa, Canada  
K1A 0N4**

## **NOTICE**

The quality of this microform is heavily dependent upon the quality of the original thesis submitted for microfilming. Every effort has been made to ensure the highest quality of reproduction possible.

If pages are missing, contact the university which granted the degree.

Some pages may have indistinct print especially if the original pages were typed with a poor typewriter ribbon or if the university sent us an inferior photocopy.

Reproduction in full or in part of this microform is governed by the Canadian Copyright Act, R.S.C. 1970, c. C-30, and subsequent amendments.

## **AVIS**

La qualité de cette microforme dépend grandement de la qualité de la thèse soumise au microfilmage. Nous avons tout fait pour assurer une qualité supérieure de reproduction.

S'il manque des pages, veuillez communiquer avec l'université qui a conféré le grade.

La qualité d'impression de certaines pages peut laisser à désirer, surtout si les pages originales ont été dactylographiées à l'aide d'un ruban usé ou si l'université nous a fait parvenir une photocopie de qualité inférieure.

La reproduction, même partielle, de cette microforme est soumise à la Loi canadienne sur le droit d'auteur, SRC 1970, c. C-30, et ses amendements subséquents.



National Library  
of Canada

Bibliothèque nationale  
du Canada

Canadian Theses Service

Service des thèses canadiennes

Ottawa, Canada  
K1A 0N4

The author has granted an irrevocable non-exclusive licence allowing the National Library of Canada to reproduce, loan, distribute or sell copies of his/her thesis by any means and in any form or format, making this thesis available to interested persons.

The author retains ownership of the copyright in his/her thesis. Neither the thesis nor substantial extracts from it may be printed or otherwise reproduced without his/her permission.

L'auteur a accordé une licence irrévocable et non exclusive permettant à la Bibliothèque nationale du Canada de reproduire, prêter, distribuer ou vendre des copies de sa thèse de quelque manière et sous quelque forme que ce soit pour mettre des exemplaires de cette thèse à la disposition des personnes intéressées.

L'auteur conserve la propriété du droit d'auteur qui protège sa thèse. Ni la thèse ni des extraits substantiels de celle-ci ne doivent être imprimés ou autrement reproduits sans son autorisation.

ISBN 0-315-55584-X

Canada

THE UNIVERSITY OF ALBERTA  
APPLICATION OF GOVUNOV'S SCHEME TO THE PROPAGATION  
OF WAVES IN NONLINEAR ELASTIC STRING

*by*



Kenzu Abdella

A THESIS SUBMITTED TO  
THE FACULTY OF GRADUATE STUDIES AND RESEARCH  
IN PARTIAL FULFILLMENT OF THE REQUIREMENTS  
FOR THE DEGREE OF  
MASTER OF SCIENCE  
IN  
APPLIED MATHEMATICS

DEPARTMENT OF MATHEMATICS

EDMONTON, ALBERTA

FALL, 1989

THE UNIVERSITY OF ALBERTA

RELEASE FORM

NAME OF AUTHOR: Kenzu Abdella

TITLE OF THESIS: APPLICATION OF GODUNOV'S SCHEME TO THE PROPAGATION  
OF WAVES IN NONLINEAR ELASTIC STRING

DEGREE FOR WHICH THESIS WAS PRESENTED: M.Sc.

YEAR THIS DEGREE GRANTED 1989

Permission is hereby granted to THE UNIVERSITY OF ALBERTA LIBRARY to reproduce single copies of the thesis and to lend or sell such copies for private, scholarly or scientific research purposes only.

The author reserves other publication rights, and neither the thesis nor extensive extracts from it may be printed or otherwise reproduced without the author's written permission.

SIGNED

PERMANENT ADDRESS:


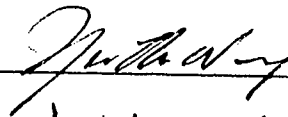

Department of Applied Mathematics  
University of Western Ontario  
London, Ontario, Canada.

Date 7/09/1989

THE UNIVERSITY OF ALBERTA  
THE FACULTY OF GRADUATE STUDIES AND RESEARCH

The undersigned certify that they have read, and recommend to the Faculty of Graduate Studies and Research, for acceptance, a thesis entitled APPLICATION OF GODUNOV'S SCHEME TO THE PROPAGATION OF WAVES IN NONLINEAR ELASTIC STRING submitted by Kenzu Abdella in partial fulfilment of the requirements for the degree of Master of Science.

Supervisor

Date 5/09/1989

*I dedicate this thesis to  
my father Abdella Sultan  
and to  
my mother Zeineba Ali*

## ABSTRACT

In this thesis the propagation and reflection of waves on a nonlinear hyperelastic string, using a general strain-energy function, is investigated. The Riemann problem for the longitudinal motion is investigated and an iterative Riemann solver is proposed. Up to shock formation characteristic methods are used to investigate breakdown and envelopes of characteristics for fairly general initial, boundary value problems. Thereafter a numerical algorithm is required and Godunov's scheme combined with the solutions to the Riemann problems are used to investigate solutions after shock formation. A number of physical examples have been examined.

## **ACKNOWLEDGEMENTS**

I would like to express my special thanks to Dr. R.J. Tait for the excellent guidance and supervision provided during the course of writing this thesis. I also would like to thank W.G. Aiello for his helpful suggestions in the computer work.

I would like to thank V. Spak for her patience and the excellent typing of this thesis. Further thanks are due to the NSERC for their support during the course of this research.



## TABLE OF CONTENTS

Chapter	Page
I Introduction	1
II Conservation Laws	
and Numerical Method of Conservation Laws	4
2.1. Introduction to Hyperbolic Conservation Laws	4
2.2. Conservative Numerical Schemes	11
2.3. Godunov's Scheme	18
2.4. The Artificial Compression Method	23
III Formulation of the Equations of Motion	
and Solution to the Riemann Problem	32
3.1. Governing Equations	32
3.2. Constitutive Relations	36
3.3. The Riemann Problem for the Mooney-Rivlin String	39
3.4. The Riemann Problem for the Three-Term Stress-Stretch Relation	48

Chapter	Page
IV Numerical Algorithms	
and Approximate Solution to the Riemann Problem	64
4.1. Algorithms for the Exact Solution	
of the Riemann Problem	64
4.2. An Iterative Riemann Solver	75
4.3. Algorithm for Solving Initial, Boundary Value	
Problems by Godunov's Scheme	97
V Numerical Illustrations and Conclusion	107
5.1. Numerical Illustrations	107
5.2. Conclusion	123
Bibliography	125

## CHAPTER I

### INTRODUCTION

Over the past few decades there has been considerable interest in models for physical phenomena which involve a system of hyperbolic conservation laws. In this thesis we consider a class of conservation laws arising from a motion of a nonlinear elastic string, and we investigate the propagation and reflection of longitudinal waves.

Since, in general, solutions of the equations of motion develop discontinuities, a generalized (weak) solution is required. This causes both numerical and analytical difficulties when solving these equations, especially when reflections are involved [3]. Moreover, if realistic forms of the strain energy function associated with the elastic string are used, problems of degeneracy occur.

For certain initial, boundary conditions it is possible to describe the behaviour of the string when both longitudinal and transverse waves are present [17], at least up to reflection. However, these are essentially extensions of the Riemann problem. However if general initial, boundary conditions are imposed, the solutions can no longer be found using similarity solutions or elementary characteristic theory. An attempt to investigate such a problem by perturbation methods and the difficulties generated by the degeneracies is described in [10]. In this thesis we will consider fairly general initial boundary value problems.

This thesis is composed of five chapters. The second chapter consists of two parts. The first part describes the theory of hyperbolic conservation

laws. Basic features such as entropy conditions and breakdowns of smooth solutions are explained. The second part of the chapter investigates numerical techniques for solving hyperbolic conservation laws. The main properties of conservative schemes, monotone schemes and upwind schemes are discussed. Godunov's scheme, which is based on the exact solution of the Riemann problem is described and the idea of Riemann solvers is introduced. Also in this part of the chapter Harten's Artificial Compression Method (ACM) [5] is described and an automatic switch for turning the ACM on and off is presented.

In Chapter III the system of Lagrangian governing equations of the plane motion of the nonlinear elastic string is formulated in conservation form. The longitudinal equation of motion is obtained as a special case of these equations. The constitutive relations for Mooney-Rivlin and Ogden three-term strain energy functions are presented. In formulating these relations, the thermodynamic effects are neglected. Intuitively this is a good approximation since rubberlike materials are relatively poor conductors of heat. Moreover it has been shown that temperature variations are small for the deformation of hyperelastic strings [17]. Also in Chapter III the Riemann problem for the longitudinal equations of motion is investigated. The solution is described both for strings with Mooney-Rivlin strain energy function and for Ogden's three-term strain energy function.

Later on in this thesis these solutions to the Riemann problem are used in the application of Godunov's scheme to solve problems of longitudinal wave propagation in hyperelastic string. The exact solution to the Riemann problem

has proven very expensive to solve. Therefore an appropriate, simplified approximate solution is required. Such an approximation is proposed in Chapter IV, when an iterative method is used to obtain the solution. In certain cases this iterative technique converges in a few iterations to the exact solution.

In Chapter V we shall consider fairly general initial, boundary value problems for which internal shocks occur, and for which elementary characteristic theory breaks down. Therefore, it is necessary to investigate other numerical methods. As previously mentioned Godunov's method is employed.

In general, shock fronts smear substantially leaving the difficulty of differentiating between shock waves and expansion waves. Sometimes this is of importance when dealing with reflections. In order to sharpen the shocks, Harten's Artificial Compression Method (ACM) and an automatic switch to turn on and off the ACM are incorporated with the existing scheme. Finally some concluding remarks are presented at the end of Chapter V.

# CHAPTER II

## CONSERVATION LAWS

### AND NUMERICAL METHOD OF CONSERVATION LAWS

#### 2.1. Introduction to Hyperbolic Conservation Laws

Let  $u \in \mathbb{R}$  be the density and let  $\hat{f}(u) \in \mathbb{R}^n$  be the flux of certain physical quantities. Then in the absence of sinks and sources we have the hyperbolic conservation law

$$(2.1) \quad \frac{d}{dt} \int_{\Omega} u dx = - \int_{\partial\Omega} \hat{f} \cdot \mathbf{n} dS$$

for any fixed domain  $\Omega$  in the  $x$  space with a boundary  $\partial\Omega$ . Here  $\mathbf{n}$  denotes the outward normal to  $\Omega$  and  $dS$  the surface element on  $\partial\Omega$ . (2.1) is called the *integral form* of the Conservation laws. It expresses the fact that the rate of change of the quantity  $u$  contained in  $\Omega$  is equal to the flux entering  $\Omega$  through the boundary  $\partial\Omega$ . By applying the divergence theorem and by taking  $d/dt$  under the integral sign we obtain

$$(2.2) \quad \int_{\Omega} \left( \frac{\partial u}{\partial t} + \operatorname{div} \hat{f} \right) dx = 0.$$

If we divide (2.2) by  $VOL(\Omega)$  and then shrink  $\Omega$  to a point where all partial derivatives of  $u$  and  $\hat{f}$  are continuous, then we obtain

$$(2.3) \quad \frac{\partial u}{\partial t} + \operatorname{div} \hat{f} = 0.$$

This is called the *divergence form* of the conservation law and it expresses the divergence free character of the scalar field  $u$ . We shall consider systems of conservation laws

$$u_t^j + \operatorname{div} \hat{f}^j = 0 \quad j = 1, \dots, n,$$

where  $\hat{f}^j$  is some nonlinear function of  $u^1, \dots, u^n$ . In the one space dimension  $x \in \mathbb{R}$  and  $\hat{f}^j = f, i$ , (2.3) becomes

$$(2.4) \quad \frac{\partial u}{\partial t} + \frac{\partial f(u)}{\partial x} = 0 \quad t \geq 0,$$

where  $u = (u_1, u_2, u_3, \dots, u_n)^T$  and  $f = (f_1, f_2, f_3, \dots, f_n)^T$ . Examples of conservation laws include, compressible Euler equations, elasticity models and shallow water wave equations. Later on in this thesis both the derivations and the solutions of several elasticity models will be discussed.

If  $A(u)$  denote the *jacobian matrix* for  $f(u)$ , that is

$$(2.5a) \quad A(u) = \frac{\partial f}{\partial u},$$

then we can write (2.4) in the following matrix form:

$$(2.5b) \quad \frac{\partial u}{\partial t} + A(u) \frac{\partial u}{\partial x} = 0.$$

Following P.D. Lax's [9] definition, the system (2.4) will be *strictly hyperbolic* if all the eigenvalues of  $A$  are real and distinct,

$$(2.6) \quad \begin{aligned} A(u)r_i(u) &= \lambda_i(u)r_i(u) \\ \lambda_1(u) &< \lambda_2(u) < \dots < \lambda_n(u). \end{aligned}$$

Equation (2.4) is called *genuinely nonlinear*, if for  $i \in \{1, 2, 3, \dots, n\}$

$$(2.7) \quad \nabla \lambda_i(\mathbf{u}) \cdot \mathbf{r}_i(\mathbf{u}) \neq 0 \quad \text{for all } \mathbf{u}.$$

We say the system is *linearly degenerate* or *exceptional* if

$$(2.8) \quad \nabla \lambda_i(\mathbf{u}) \cdot \mathbf{r}_i(\mathbf{u}) \equiv 0, \quad \text{for some } i.$$

For a genuinely nonlinear system, it turns out that because of the dependence of the *characteristic values*  $\lambda_i(\mathbf{u})$  on the variable  $\mathbf{u}$ , singularities tend to develop in the solution. This causes both analytical and numerical difficulties. In order to illustrate these nonlinearity features, let us consider the scalar conservation law  $u \in \mathbb{R}$  with the smooth initial data  $u(x, 0) = u_0(x)$ . Along the characteristic curves

$$(2.9) \quad \frac{dx}{dt} = \lambda(u) = f'(u),$$

we must have  $(du)/(dt) = u_t + u_x (dx)/(dt) = u_t + f'(u)u_x = 0$ . Therefore  $u$  is constant along the characteristic. Hence the characteristics are straight lines with the slope  $1/f'(u_0(x))$ . If  $\lambda(u_0(x))$  is an increasing function of  $x$  then  $u(x, t)$  will be an expansion wave which is also called a *rarefaction wave*. A rarefaction wave is a continuous solution of the form  $u = u(x/t)$ , (see Fig. 2.1). On the otherhand if  $\lambda(u_0(x))$  is a decreasing function of  $x$ , then  $u(x, t)$  will be a compression wave which eventually will become multivalued, (see Fig 2.1).



Therefore classical solutions cease to exist in a finite time and the solution becomes discontinuous. To overcome these difficulties we must generalize the notion of solution to include such discontinuous and nondifferentiable solutions in such a way that they still satisfy the original differential equations in some sense. This will be done by employing the idea of weak solutions.

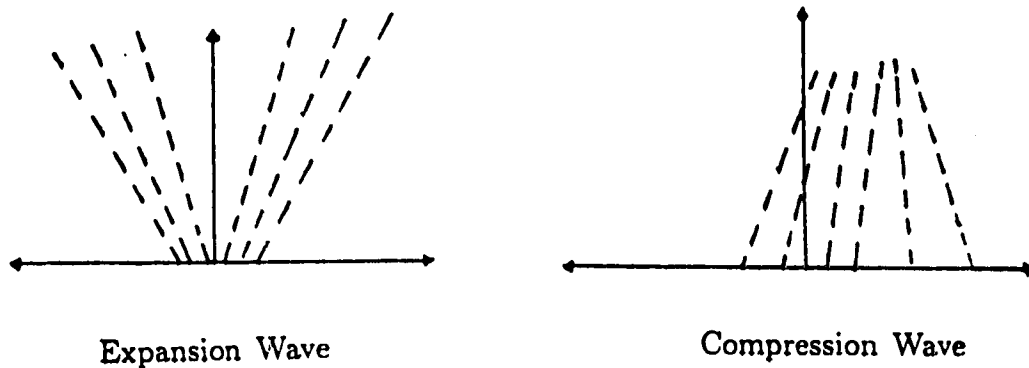


Figure 2.1.

To this end we write the divergence form of the conservation law in one dimension (2.4) as

$$(2.10) \quad \nabla \cdot (u, f(u)) = 0$$

where the operator  $\nabla \equiv (\partial_t, \partial_x)$ . Let  $\phi(x, t)$  be any smooth test function with compact support in  $t \geq 0$ . Then multiplying (2.10) by  $\phi$  and integrating over  $t > 0$  we obtain,

$$(2.11) \quad \iint_{t \geq 0} \phi(\nabla \cdot (u, f(u))) dx dt = 0.$$

Then by applying the divergence theorem to (2.11) we obtain

$$(2.12) \quad \iint_{t \geq 0} (\nabla \phi) \cdot (u, f(u)) dx dt + \int u(0, x) \phi(x, 0) dx = 0.$$

A bounded measurable function  $u(x, t)$  satisfying (2.12) for any test function  $\phi$  with compact support in  $t \geq 0$  is called a *weak solution* of (2.4).

As a result of this new notion of solution, every piecewise continuous weak solution of (2.4) must satisfy the *Rankine-Hugoniot* relation across the line of discontinuity  $x = \psi(t)$ ,

$$(2.13) \quad \sigma[u] = [f(u)]$$

where  $[u] = (u_+ - u_-)$ ,  $[f(u)] = [f(u_+) - f(u_-)]$ ,  $u_{\pm} = u(\psi(t) \pm 0, t)$  Fig (2.2), and  $\sigma$  is the speed of propagation.

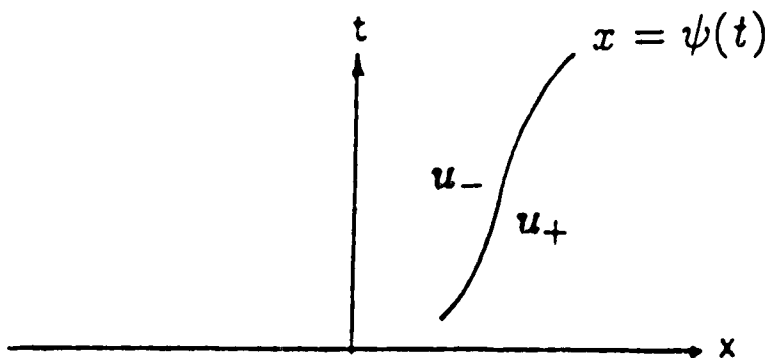


Figure 2.2 Discontinuity along  $x = \psi(t)$ .

An interesting feature of shock wave theory is that there can be an infinite

number of weak solutions of (2.4) with same initial data  $u_0(x)$ . Therefore an *admissibility criterion*, the *entropy condition*, is needed to select a physically relevant solution. The simplest problem having this property is the Riemann problem, which is an initial value problem for (2.4) with the initial data

$$(2.14) \quad u(x, 0) = \begin{cases} u_l & \text{for } x < 0 \\ u_r & \text{for } x > 0 \end{cases}$$

for given constant states  $u_l$  and  $u_r$ . Assuming (2.4) to be genuinely non-linear, Lax [9] showed that the following entropy condition must be satisfied for some  $i \in [1, 2, \dots, n]$ ;

$$(2.15) \quad \begin{aligned} \lambda_i(u_l) &> \sigma > \lambda_i(u_r) \\ \lambda_{i-1}(u_l) &< \sigma < \lambda_{i+1}(u_r). \end{aligned}$$

These inequalities are called *entropy inequalities*. Discontinuities satisfying these inequalities are called *i-shock waves*.

Another approach in settling the admissibility criterion is to use a viscosity principle [9]. Therefore those solutions that are limits as  $\varepsilon \rightarrow 0$  of solutions  $u(\varepsilon)$  of the parabolic viscous equations.

$$(2.16) \quad u_t + f(u)_x = \varepsilon u_{xx} \quad \varepsilon > 0$$

are admissible. The existence and uniqueness of the solutions  $u(\varepsilon)$  of (2.16) has been established by using the maximum principle for parabolic equations [9]. Moreover as  $\varepsilon \rightarrow 0$ ,  $u(\varepsilon)$  converges to the solution  $u(x, t)$  of (2.4).

Consider the system of conservation laws (2.4) that has an *entropy function*  $U(u)$  with the following properties.

(i)  $U$  is a convex function of  $u$ , that is:

$$(2.17a) \quad U_{uu} > 0$$

and

(ii)  $U$  satisfies

$$(2.17b) \quad U_u f_u = F_u$$

where  $F$  is some other function called the *entropy flux*. Therefore by multiplying (2.4) by  $U_u$  and by using (2.17) we see that every smooth solution of (2.4) satisfies

$$(2.18) \quad U(u)_t + F(u)_x = 0.$$

Lax[9] showed that the limit solutions of (2.16) satisfy

$$(2.19a) \quad U(u)_t + F(u)_x \leq 0.$$

Therefore by using the divergence theorem we have

$$(2.19b) \quad - \int_0^\infty \int_{-\infty}^\infty (\phi_t U + \phi_x F) dx dt - \int_{-\infty}^\infty \phi(x, 0) U(u_0(x)) dx \leq 0,$$

where  $\phi(x, t)$  is a smooth test function with a compact support in  $t \geq 0$ . This is equivalent to requiring that for all rectangles  $[a, b] \times [t_1, t_2]$  the inequality obtained by integrating (2.19a) over the rectangle should hold:

$$(2.19c) \quad \int_a^b U(u(x, t_2)) dx - \int_a^b U(u(x, t_1)) dx + \int_{t_1}^{t_2} F(u(b, t)) dt - \int_{t_1}^{t_2} F(u(a, t)) dt \leq 0.$$

If  $u$  is piecewise smooth with discontinuities, then (2.18) holds pointwise in the smooth region, and across the discontinuities we have,

$$(2.19d) \quad F(u_r) - F(u_l) \leq \sigma(U(u_r) - U(u_l)).$$

Relations (2.19) are called *entropy conditions*.

These conditions for selecting physically relevant solutions are only adequate if the entropy function  $U$  and its corresponding entropy flux can be constructed. Nevertheless, as we will see later on, these conditions are useful in checking the admissibility of numerical schemes and in obtaining a priori estimates.

## 2.2 Conservative Numerical Schemes

In this section we will consider the numerical solutions of the one dimensional system of conservation laws (2.4)

$$(2.4) \quad u_t + f(u)_x = 0 \quad t \geq 0 \quad -\infty < x < \infty$$

where  $u(x, t) \in \mathbb{R}^n$ ,  $f(u(x, t)) \in \mathbb{R}^n$ . To do this we will look at finite difference schemes which can be put into the following conservation form. Consider a point  $x$  and let  $u_i^n = u(x + ih, t_n)$ , where  $t_n$ ,  $n = 0, 1, \dots$  are discrete time levels and  $h$  a step size in the  $x$  direction. A finite difference method is said to be in *conservation form* if it can be written in the form

$$(2.20) \quad u(x, t_{n+1}) = u(x, t_n) + \Lambda \left( G^n(x + \frac{h}{2}) - G^n(x - \frac{h}{2}) \right) \quad \Lambda = \frac{t_{n+1} - t_n}{h} = \frac{\tau}{h}$$

where  $G(x + \frac{h}{2}) = G(u_{-q+1}^n, u_{-q+2}^n, \dots, u_q^n)$  and  $G(x - \frac{h}{2}) = G(u_{-q}^n, u_{-q+1}^n, \dots, u_{q-1}^n)$ . Here  $G$  is a vector valued function of  $2q$  arguments. It is called a *numerical flux*. In order for (2.20) to be in agreement with (2.4), we require the following consistency condition;

$$(2.21) \quad G(u, u, \dots, u) = f(u).$$

In other words, the numerical flux must be consistent with the physical flux.

The discrete analogue of the entropy condition (2.19a) will be

$$(2.22) \quad U_i^{n+1} \leq U_i^n + \Lambda (F_E^n(x + \frac{h}{2}) - F_E^n(x - \frac{h}{2}))$$

where  $U_i^n = U(u_i^n)$  and  $F_E^n(x + \frac{h}{2}) = F_E(u_{-q+1}^n, \dots, u_q^n)$ .  $F_E(u, u, \dots)$  is a *numerical entropy flux* which must be consistent with the entropy flux;

$$(2.23) \quad F_E(u, u, \dots, u) = F(u).$$

From the following theorem, proved by Lax and Wendroff [10], we see that a finite difference approximation to a conservation law should be in conservation form.

**THEOREM 2.1.** *Let  $u(x, t_n)$  be a solution to a finite difference scheme in conservation form. If  $u(x, t_n)$  converges boundedly almost everywhere to some function  $v(x, t)$  as  $h$  and  $\tau$  tend to zero, then  $v(x, t)$  is a weak solution of (2.4).*

**PROOF:** Let  $\phi(x, t)$  be a test function with compact support in  $t \geq 0$ . Multiply (2.20) by  $\phi(x, t)$ , integrate with respect to  $x$  and sum over all values of  $t$  that are integer multiples of  $k$  to obtain the following:

$$\begin{aligned}
 (2.24) \quad & \sum_n \int_{-\infty}^{\infty} \phi(x, nk) \left( \frac{u(x, (n+1)k) - u(x, nk)}{k} \right) dx k \\
 & = - \sum_n \int_{-\infty}^{\infty} \phi(x, nk) \left( \frac{G(x + \frac{h}{2}) - G(x - \frac{h}{2})}{k} \right) dx k.
 \end{aligned}$$

Applying summation by parts to the left side we have

$$\begin{aligned}
 (2.25) \quad & \sum_n \int_{-\infty}^{\infty} \phi(x, nk) \left( \frac{u(x, (n+1)k) - u(x, nk)}{k} \right) dx k \\
 & = - \int_{-\infty}^{\infty} \phi(x, 0) u(x, 0) dx \\
 & \quad - \sum_{-\infty}^{\infty} \left( \frac{\phi(x, nk) - \phi(x, (n-1)k)}{k} \right) u(x, nk) dx k.
 \end{aligned}$$

Now using (2.25) and a simple change of variable, (2.23) becomes

$$\begin{aligned}
 (2.26) \quad & \sum_n \int_{-\infty}^{\infty} \left( \frac{\phi(x, nk) - \phi(x, (n-1)k)}{k} \right) u(x, nk) dx \, k \\
 & + \sum_n \int_{-\infty}^{\infty} [\phi(x + \frac{n}{2}, nk) - \phi(x - \frac{n}{2}, nk)] G(x) dx \, k \\
 & + \int_{-\infty}^{\infty} \phi(x, 0) u(x, 0) dx = 0.
 \end{aligned}$$

where  $G(x) = G(u_{-q}^n, \dots, u_q^n)$  and the values  $u_{-q}^n, \dots, u_q^n$  are the values of  $u$  at the  $2q$  points symmetrically distributed about the point  $(x, nk)$ . If  $u(x, nk)$  tends boundedly almost everywhere to a function  $v(x, t)$ , so do  $u_{-q}^n, \dots, u_q^n$  and thus  $G(x)$  tends to  $G(u, u, \dots, u)$  which by the consistency requirement (2.21) equals  $f(v)$ . Hence the limit of (2.26) is the desired limit

$$(2.27) \quad \int_0^{\infty} \int_{-\infty}^{\infty} (\phi_t v + \phi_x f(v)) dx dt + \int_{-\infty}^{\infty} \phi(x, 0) v(x, 0) dx = 0.$$

Therefore  $v(x, t)$  is a weak solution of (2.4).  $\square$

Theorem 2.1 does not indicate whether or not the limit solution is the physically relevant solution. In order to ensure that the entropy condition is satisfied, we will look at the so called monotone schemes. Let a finite difference scheme of the scalar conservation law be in the following form:

$$(2.28) \quad u_i^{n+1} = Qu_i^n = H(u_{i-q}^n, \dots, u_{i+q}^n).$$



This difference scheme is said to be *monotone* if  $H$  is a monotone increasing function of each of its arguments. In other words

$$(2.29) \quad H_j = \frac{\partial H}{\partial u_j^n} \geq 0.$$

The operator  $Q$  in (2.28) is called *monotone preserving* if for any monotone mesh function  $V, W = QV$  is also monotone.

Harten, Hyman, and Lax [6] proved the following theorems concerning monotone and monotone preserving schemes.

**THEOREM 2.2.** *Let (2.28) be a monotone finite difference method in conservation form. If the solution of this finite difference method,  $u_i^n$  converges boundedly almost everywhere to some function  $v(x,t)$  as  $\tau$  and  $h$  approach to zero with  $\Lambda$  fixed, then  $v(x,t)$  is a weak solution of (2.4) and the entropy condition is satisfied at all discontinuities of  $v$ .*

**THEOREM 2.3.** *A monotone finite difference method in conservation form is first order.*

**THEOREM 2.4.** *A monotone finite difference method is monotone preserving.*

Therefore monotone schemes satisfy the entropy condition and they are non oscillatory.

The notion of monotone finite difference methods can be extended to the vector case, by taking the inequality (2.29) to mean that all the eigenvalues of

the matrix  $H_j$  are nonnegative for every  $j \in \{-q, \dots, q\}$ . However the notion of monotone preserving, unlike the notion of monotone, cannot be extended to nonlinear systems.

Before we conclude this section let us note that when a conservative system is approximated by a conservative difference scheme, shocks which fall between mesh points can at best be represented by transitions over two intervals. In other words a shock of the form

$$(2.30) \quad u(x) = \begin{cases} u_l & \text{for } x < x_s \\ u_r & \text{for } x > x_s \end{cases}$$

where  $x_{j-\frac{1}{2}} < x_s < x_{j+\frac{1}{2}}$  can at best be represented by a transition of the form

$$(2.31) \quad u_i^n = \begin{cases} u_l & \text{for } i < j \\ u_m & \text{for } i = j \\ u_r & \text{for } i > j \end{cases}$$

where  $u_m(x_{j+\frac{1}{2}} - x_{j-\frac{1}{2}}) = u_l(x_s - x_{j-\frac{1}{2}}) + u_r(x_{j+\frac{1}{2}} - x_s)$ ,  $x_{j+\frac{1}{2}} = (x_{j+1} + x_j)/2$ .

However, in most practical computations, shocks are spread over far more than two intervals. This difficulty of poor resolution of shocks is known to be less severe if we use upwind difference schemes. These schemes attempt to discretize the conservation law by using differences based in the direction determined by the sign of the characteristic speed.

We conclude this section by giving the definition of a general three point upwind scheme.

**DEFINITION:** A difference scheme in conservation form is said to be *upwind*, if the following two conditions hold.

- i) For the nearby states  $u_1$  and  $u_2$ , the following is a linear approximation to the numerical flux  $G(u_1, u_2)$

$$(2.32) \quad G(u_1, u_2) = A^+ u_1 + A^- u_2$$

where  $A(u)$  is the Jacobian matrix of  $f(u)$  and

$$(2.33) \quad A^\pm = \frac{1}{2}(A \pm |A|).$$

If  $u_1$  and  $u_2$  are near some state  $u_*$  then the requirement (2.32) is equivalent to requiring that,

$$(2.34) \quad \begin{aligned} G(u_1, u_2) = & f(u_*) + A^+(u_*)(u_1 - u_*) \\ & + A^-(u_*)(u_2 - u_*) + O(|u_1 - u_*| + |u_2 - u_*|). \end{aligned}$$

- ii) When all signal speeds associated with the numerical flux  $G(u_1, u_2)$  are positive, then  $G(u_1, u_2) = f(u_1)$ . When all signal speeds associated with the numerical speed are negative, then  $G(u_1, u_2) = f(u_2)$ .

### 2.3 Godunov's Scheme

Consider the initial value problem for the one dimensional hyperbolic system of conservation laws (2.4)

$$(2.35) \quad \frac{\partial \mathbf{u}}{\partial t} + \frac{\partial f(\mathbf{u})}{\partial x} = 0 \quad -\infty < x < \infty$$

$$\mathbf{u}(x, t_0) = \mathbf{u}_0(x)$$

where  $\mathbf{u}(x, t)$  is a column vector of  $n$  variables and  $f(\mathbf{u})$  is a vector valued function of  $n$  components.

To solve the above initial value problem, Godunov constructed a first order upwind finite difference scheme based on successive solutions of local Riemann problems. In the derivation of his scheme, Godunov considered a numerical approximation of  $\mathbf{u}(x, t_n)$  of the discrete time levels  $t_n$ ,  $n = 0, 1, 2, \dots$  to be a piecewise constant function of  $x$ ;

$$(2.36) \quad \mathbf{u}(x, t_n) = \mathbf{u}_i^n \quad (i - \frac{1}{2})h \leq x \leq (i + \frac{1}{2})h$$

where  $h$  is a step size in the  $x$  direction. In order to calculate  $\mathbf{u}$  at time  $t_{n+1} = t_n + \tau$ , we solve (2.35) in each interval  $[ih, (i+1)h]$  with the following initial conditions:

$$(2.37) \quad \mathbf{u}(x, t_n) = \begin{cases} \mathbf{u}_i^n & x \leq (i - \frac{1}{2})h \\ \mathbf{u}_{i+1}^n & x > (i + \frac{1}{2})h. \end{cases}$$

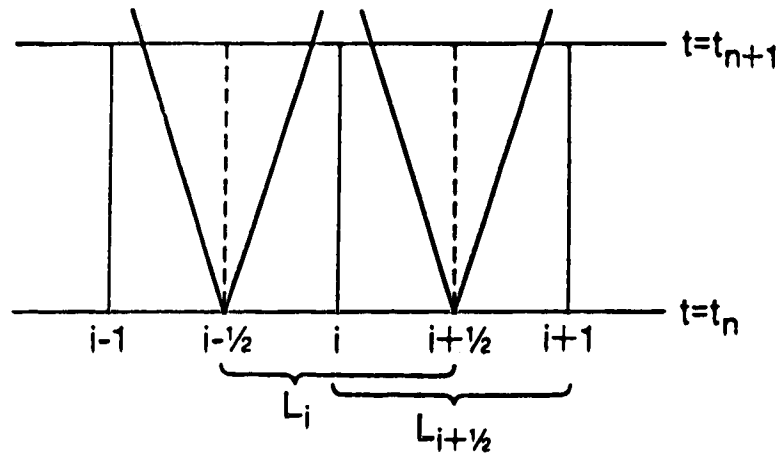
This initial value problem defines a sequence of Riemann problems. The waves generated by neighbouring Riemann problems will not interact if the *CFL* condition

$$(2.38a) \quad \gamma \leq \frac{1}{2}$$

is satisfied (see Figure 2.3). Here  $\gamma$  is the Courant number given by

$$(2.38b) \quad \gamma = |\lambda_{\max}| \frac{\tau}{h}$$

where  $|\lambda_{\max}|$  is the largest signal speed.



where  $L_i = \{x : (i - 1/2)h < x < (i + 1/2)h\}$

Figure 2.3

Thus the solution  $u^e(x, t)$  for  $t_n < t \leq t_{n+1}$  can be expressed exactly in terms of the solution of local Riemann problems. Let  $R(\frac{x}{t}, u_l, u_r)$  denote the solution of the Riemann problem for system (2.4) with the initial data,

$$(2.39) \quad u(x, 0) = \begin{cases} u_l & x < 0 \\ u_r & x > 0. \end{cases}$$

Then  $u^e(x, t)$  is given by

$$(2.40) \quad u^e(x, t) = R\left(\frac{x - (i + \frac{1}{2})h}{t - t_n}, u_i^n, u_{i+1}^n\right) \quad ih \leq x \leq (i+1)h.$$

Godunov then obtains  $u_i^{n+1}$  by averaging  $u^e(x, t)$  over  $[(i - \frac{1}{2})h, (i + \frac{1}{2})h]$

$$(2.41) \quad u_i^{n+1} = \frac{1}{h} \int_{(i-\frac{1}{2})h}^{(i+\frac{1}{2})h} u^e(x, t_{n+1}) dx.$$

Since  $u^e(x, t)$  is the exact solution of (2.35), we can integrate (2.35) over the rectangle  $[(i - \frac{1}{2})h, (i + \frac{1}{2})h] \times [t_n, t_{n+1}]$  to obtain

$$(2.42) \quad \begin{aligned} & \int_{(i-\frac{1}{2})h}^{(i+\frac{1}{2})h} \int_{t_n}^{t_{n+1}} \left( \frac{\partial u^e(x, t)}{\partial t} + \frac{\partial f(u^e(x, t))}{\partial x} \right) dt dx \\ &= \int_{(i-\frac{1}{2})h}^{(i+\frac{1}{2})h} u^e(x, t_{n+1}) dx - \int_{(i-\frac{1}{2})h}^{(i+\frac{1}{2})h} u^e(x, t_n) dx \\ &+ \int_{t_n}^{t_{n+1}} f(u^e((i + \frac{1}{2})h, t)) dt - \int_{t_n}^{t_{n+1}} f(u^e((i - \frac{1}{2})h, t)) dt = 0. \end{aligned}$$

From (2.40) we see that  $u^e((i - \frac{1}{2})h, t) = R(0, u_{i-1}^n, u_i^n)$  and  $u^e((i + \frac{1}{2})h, t) = R(0, u_i^n, u_{i+1}^n)$  and therefore (2.42) becomes

$$(2.43) \quad \begin{aligned} & \int_{(i-\frac{1}{2})h}^{(i+\frac{1}{2})h} u^e(x, t_{n+1}) dx = \int_{(i-\frac{1}{2})h}^{(i+\frac{1}{2})h} u^e(x, t_n) dx \\ &+ \int_{t_n}^{t_{n+1}} f(R(0, u_{i-1}^n, u_i^n)) dt - \int_{t_n}^{t_{n+1}} f(R(0, u_i^n, u_{i+1}^n)) dt. \end{aligned}$$

Using (2.41) we obtain

$$(2.44) \quad u_i^{n+1} = u_i^n - \frac{\tau}{h} (f(R(0, u_i^n, u_{i+1}^n)) - f(R(0, u_{i-1}^n, u_i^n))).$$

Therefore

$$u_i^{n+1} = u_i^n - \Lambda (f_{i+\frac{1}{2}}^n - f_{i-\frac{1}{2}}^n)$$

where  $\Lambda = \frac{\tau}{h}$ ,  $u_{i+\frac{1}{2}}^n = R(0, u_i^n, u_{i+1}^n)$  and  $f_{i+\frac{1}{2}}^n = f(u_{i+\frac{1}{2}}^n)$ . (2.45) is Godunov's scheme and it is clearly in a conservation form. Godunov's scheme is monotone preserving and Harten, Lax and Van Leer [7] showed that it is also upwind.

It is clear that Godunov's scheme does not use all the information derived from the exact solution of the Riemann problem. Instead it uses the data at a selected point in the relevant interval. However, the Riemann problem can be very expensive to solve and in many cases it is impossible to obtain the exact solution. Harten, Lax and Van Leer [7] proposed the replacement of the exact solution  $R(x/t, u_l, u_r)$  of the Riemann problem (2.39) by an approximate solution  $r(x/t, u_l, u_r)$ . This approximate solution can be structurally much less complex as long as it is in a conservation form and as long as it satisfies the entropy inequalities. They proved the following theorem which shows that this type of an approximation is consistent.

**THEOREM 2.5.** *Let  $r(x/t, u_l, u_r)$  be an approximation to the solution of the Riemann problem (2.39) that satisfies the following conditions:*

i) consistency with the integral form of the conservation law:

$$(2.46) \quad \int_{-h/2}^{h/2} r\left(\frac{x}{\tau}, u_l, u_r\right) dx = \frac{h}{2}(u_l + u_r) - \tau(f(u_r) - f(u_l))$$

for  $\frac{h}{2} > \tau|\lambda_{\max}|$ .

ii) consistency with the integral form of the entropy condition:

$$(2.47) \quad \int_{-h/2}^{h/2} U\left(r\left(\frac{x}{t}, u_l, u_r\right)\right) dx \leq \frac{h}{2}(U(u_l) + U(u_r)) - \tau(f_E(u_r) - f_E(u_l))$$

for  $\frac{h}{2} > \tau|\lambda_{\max}|$ .

Then the Godunov type scheme, defined as follows

$$(2.48) \quad u_i^{n+1} = \frac{1}{h} \int_0^{h/2} r\left(\frac{x}{\tau}, u_{i-1}^n, u_i^n\right) dx + \frac{1}{h} \int_{-h/2}^0 r\left(\frac{x}{\tau}, u_i^n, u_{i+1}^n\right) dx$$

is in conservation form consistent with (2.39), and satisfies the entropy approximating inequality (2.22).

We note that Godunov's scheme is of Godunov's type. Then by using a classical result of Lax [7] we see that limit solutions of Godunov's scheme which uses the above approximate solution; obeys the conservation law and satisfies the entropy condition. In Chapter IV we will consider some particular approximate solutions  $r\left(\frac{x}{t}, u_l, u_r\right)$  to the Riemann problem corresponding to



an elasticity conservation law. Approximate solutions to the Riemann problem satisfying Theorem 2.5 are called *Riemann solvers*.

## 2.4 The Artificial Compression Method

Consider the scalar conservation law

$$(2.49) \quad u_t + f(u)_x = 0$$

with the initial data

$$u(0, x) = u_0(x).$$

Suppose the solution  $u(x, t)$  has a discontinuity denoted by  $(u_\ell(t), u_r(t), \sigma(t))$  where  $u_\ell(t)$  and  $u_r(t)$  are the state to the left and to the right of the shock respectively, and  $\sigma(t)$  is the shock speed. Oleinik [12] gave the following admissibility criterion:

$$(2.50) \quad S(u, u_\ell) = \frac{f(u) - f(u_\ell)}{u - u_\ell} \geq \sigma \geq \frac{f(u) - f(u_r)}{u - u_r} \\ = s(u, u_r) \quad \forall u \in (u_\ell, u_r).$$

This can be restated in the following convenient form:

$$(2.51) \quad [g_0(u) - c] \operatorname{sgn}(u_r(t) - u_\ell(t)) \geq 0 \quad \forall u \in (u_\ell, u_r)$$

where  $g_0(u) = f(u) - \sigma u$  is the *flux function* in the coordinate system moving with the discontinuity. The constant  $c = g_0(u_\ell) = g_0(u_r)$ . Jennings [8]

showed that in the case of strict inequality in (2.51), which corresponds to a shock wave, every monotone scheme in conservation form possesses a viscous profile and the number of cells  $W(u_\ell, u_r)$  occupied by values between  $u_\ell$  and  $u_r$  in the profile is inversely proportional to  $g_0(u) - c$ . However in the case of strict equality in (2.51), which corresponds to *contact discontinuity*, Jennings showed that such a profile does not exist and that  $W(u_\ell, u_r)$  is unbounded in time. Therefore we need to modify the standard finite difference methods so as to prevent the smearing of contact discontinuities and improve the resolution of shocks. In this thesis we shall discuss one such modification, *Artificial Compression Method (ACM)*, which was introduced by Harten [4]. ACM can be used in conjunction with an already existing finite difference scheme.

Consider a function  $g(u, t)$  which has the following properties:

$$(2.52a) \quad g(u, t) \equiv 0 \quad \text{for all } u \notin (u_\ell(t), u_r(t))$$

$$(2.52b) \quad g(u, t) \operatorname{sgn}(u_r(t) - u_\ell(t)) > 0 \quad \text{for all } u \in (u_\ell(t), u_r(t)).$$

Such a function  $g$  is called *Artificial Compression Flux (ACF)*.

**THEOREM 2.6.** *If  $u(x, t)$  is the solution of the original conservation law (2.49), then it is also the solution of the modified conservation law:*

$$(2.53) \quad u_t + [f(u) + g(u, t)]_x = 0.$$

PROOF: Since  $u(x, t)$  does not take any values between  $u_\ell(t)$  and  $u_r(t)$ , property (2.52a) tells us that  $\hat{f} = f + g \equiv f$  and (2.53) is reduced to the original equation (2.49).

The Rankin-Hugoniot condition for the modified equation (2.53) will be:

$$\begin{aligned}
 \hat{f}(u_r(t)) - \hat{f}(u_\ell(t)) &= [f(u_r(t) + g(u_r(t), t)) - [f(u_\ell(t)) + g(u_\ell(t), t)] \\
 (2.54) \qquad &= f(u_r(t)) - f(u_\ell(t)) \quad \text{by property (2.52a)} \\
 &= \sigma(t)(u_r(t) - u_\ell(t)) \quad \text{by (2.13).}
 \end{aligned}$$

Therefore  $(u_\ell(t), u_r(t), \sigma(t))$  is also a discontinuity for (2.53). To complete the proof we show that  $u(x, t)$  is an admissible discontinuity for (2.53). Let  $\hat{g}_0(u, t) = \hat{f}(u, t) - \sigma u$  be the flux function in the coordinate system moving with the discontinuity  $(u_\ell(t), u_r(t), \sigma(t))$ . Then by (2.52a)  $\hat{c} = \hat{g}_0(u_\ell(t)) = \hat{g}_0(u_r(t)) = c$ . Therefore using (2.51) and (2.52b) we obtain the following inequality:

$$\begin{aligned}
 (\hat{g}_0 - \hat{c})\text{sgn}(u_r - u_\ell) &= (f + g - \sigma u - c)\text{sgn}(u_r - u_\ell) \\
 (2.55) \qquad &= (f - \sigma u - c)\text{sgn}(u_r - u_\ell) + g(u, t)\text{sgn}(u_r - u_\ell) \\
 &= (g_0(u) - c)\text{sgn}(u_r - u_\ell) + g(u, t)\text{sgn}(u_r - u_\ell) > 0.
 \end{aligned}$$

Thus the modified equation satisfies the entropy condition. However, note that the entropy condition (2.55) is a strict inequality. Therefore both contact discontinuities and shocks for the original equation will be shocks for the modified equation. Note also that  $|\hat{g}_0(u, t) - c| > |g_0(u, t) - c|$  so that the spread of shocks for the modified equation which is inversely proportional to  $|\hat{g}_0(u, t) - c|$ , is reduced.

If we approximate the modified equation by a monotone finite difference scheme then we have a more restrictive CFL condition.

$$(2.56) \quad \max_u |\partial_u f + \partial_u g| \Delta \leq 1.$$

To overcome this difficulty Harten suggested the use of *split flux method* where the artificial compression is separated from the main calculation. Let the modified scheme  $\hat{L}$  be such that

$$(2.57) \quad \hat{L} = CL$$

where  $L$  is a finite difference approximation to the solution operator of the original conservation law and  $C$ , the *artificial compressor* is some finite difference approximation to the solution operator of the equation,

$$(2.58) \quad u_t + g(u)_x = 0.$$

Observe that if  $(u_l, u_r, \sigma)$  is an admissible solution of the original problem then by (2.52a) we obtain

$$\frac{g(u_r(t)) - g(u_l(t))}{u_r(t) - u_l(t)} = 0.$$

Thus  $(u_l, u_r, 0)$  is a stationary shock of (2.58).

The split flux ACM,  $\hat{L} = CL$  is a corrective type two step scheme. In the first step,  $L$  smears discontinuity as it propagates it. In the second step  $C$  compresses the smeared transition towards a sharp discontinuity. Since the

application of  $C$  does not involve any physical motion, it does not alter the physical time in the solution obtained by the first step. Therefore the time step  $\tau' = \Lambda'h$  should be regarded as a dummy time step.

The split flux approach allows us the freedom to choose  $C$  independently of the main calculation. Harten [4] chose  $C$  to be the upwind scheme in conservation form:

$$(2.59) \quad u_j^{n+1} = u_j^n - \frac{\Lambda'}{2}(\hat{G}_{j+\frac{1}{2}}^n - \hat{G}_{j-\frac{1}{2}}^n),$$

where  $\hat{G}_{j+\frac{1}{2}} = g_j^n + g_{j+1}^n - |g_{j+1}^n - g_j^n| \text{sgn}(u_{j+1}^n - u_j^n)$  and  $g_j^n = g(u_j^n, t)$ . He showed that if the discrete CFL condition

$$(2.60) \quad \Lambda' \max_{u_j \neq u_{j+1}} \left| \frac{g_{j+1} - g_j}{u_{j+1} - u_j} \right| \leq 1,$$

then the upwind scheme (2.59) is monotone preserving. Harten showed by the following theorem that this upwind scheme possesses stationary shock-like profiles.

**THEOREM 2.7.** *Let  $g(u, t)$  be an ACF (2.52) for the discontinuity  $(u_l, u_r, \sigma)$ . The finite difference solution of the upwind scheme (2.59) to the initial data*

$$(2.61) \quad u_j^0 = \begin{cases} u_l & \text{for } j \leq J_L \\ u_{\sigma, j} & \text{for } J_L < j < J_r \\ u_r & \text{for } J_r > j \end{cases}$$

where  $u_{\bullet j}$  is a monotone function of  $j$ , converges pointwise to the stationary shock-like solution

$$(2.62) \quad u_j^\infty = \begin{cases} u_\ell & \text{for } j < J_\infty \\ u_\ell + \alpha(u_r - u_\ell) & \text{for } j = J_\infty \\ u_r & \text{for } j > J_\infty \end{cases}$$

where the integer  $J_\infty$  and  $\alpha$ ,  $0 \leq \alpha \leq 1$ ,  $J_\ell \leq J_\infty \leq J_r$  are uniquely determined by the conservation relation

$$(2.63) \quad \sum_{j=j_\ell}^{j_r} u_j^0 = \sum_{j=j_\ell}^{j_r} u_j^\infty = (J_\infty - \alpha - J_\ell + 1)u_\ell + (J_r - J_\infty + \alpha)u_r.$$

Equation 2.62 is the maximum resolution possible for the conservation scheme  $L$ .

In general  $u_\ell$  and  $u_r$ , which are used in the construction of  $g$  in (2.51), are not known in advance. Harten [5] showed that this information can be extracted directly from the numerical solution  $u^n$  itself. He defines  $g_i^n$  as follows:

$$(2.64) \quad g_i^n = S_{j+\frac{1}{2}}^n \cdot \max[0, \min(|\Delta_{j+\frac{1}{2}}^n u_j^n|, S_{j+\frac{1}{2}}^n \Delta_{j-\frac{1}{2}}^n u_j^n)]$$

where  $\Delta_{j+\frac{1}{2}}^n u = u_{j+1}^n - u_j^n$  and  $S_{j+\frac{1}{2}}^n = \text{sgn}(\Delta_{j+\frac{1}{2}}^n u)$ . Therefore  $|g_{j+1}^n - g_j^n| \leq |u_{j+1}^n - u_j^n|$ , and the CFL condition (2.60) becomes  $\Lambda' \leq 1$ .

The artificial compression operator  $C_\Delta$  is the upwind scheme (2.59) with  $g_i^n$  defined by (2.64). The analogue of Theorem 2.7 holds where the artificial compressor  $C$  is replaced by the numerical compressor  $C_\Delta$ .

**THEOREM 2.8.** Let  $u^{n+1} = C_{\Delta} u^n$ ,  $n \geq 0$  where  $C_{\Delta}$  is the artificial compressor (2.59), (2.64) with  $\Lambda' \leq 1$ , and  $u_n^0$  is the initial data (2.61). As  $n \rightarrow \infty$ ,  $u^n$  converges pointwise to the stationary shock like solution (2.62), (2.63).

The artificial compression method can be extended to the system of conservation law. The method described for the scalar case can be applied componentwise to the system of conservation laws. However, the artificial compressor  $g$  in this case is approximated by the vector

$$(2.65) \quad g_i^n = \alpha_i^n (u_{i+1}^n - u_{i-1}^n)$$

where the nonnegative scalar  $\alpha_i^n = \alpha_i(u^n)$  is defined by

$$(2.66) \quad \alpha_i^n = \max \left[ 0, \min_{1 \leq j \leq p} \frac{\min[|\Delta_{i,j+\frac{1}{2}}^n u|, S_{i,j+\frac{1}{2}}^n \Delta_{i,j-\frac{1}{2}}^n u]}{|\Delta_{i,j+\frac{1}{2}}^n u| + |\Delta_{i,j-\frac{1}{2}}^n u|} \right]$$

where  $\Delta_{i,j+\frac{1}{2}}^n u = u_{i,j+1}^n - u_{i,j}^n$ ,  $S_{i,j+\frac{1}{2}}^n = \text{sgn}(\Delta_{i,j+\frac{1}{2}}^n u)$  and  $u_{i,j}^n$  denotes the  $j$ 's component of  $u_i^n$  for  $j = 1, 2, \dots, p$ . This modification constructs the numerical artificial compression flux in the correct direction.

The artificial compression method is essentially a modification of the characteristic field of the given initial value problem by the addition of the convergent characteristic field  $\frac{dx}{dt} = g'$  (2.53) of a stationary shock. In this process ACM improves resolution of the solution in the neighbourhood of admissible discontinuities. If the ACM is used in smooth regions (bounded  $u_{xx}$ ), then the characteristic speeds are modified by a term which is  $O(h)$ . This will

cause any compression wave to develop into a shock earlier than it should, and any expansion wave to expand with  $O(h)$  delay. Moreover if applied to an inadmissible discontinuity, (eg. a rarefaction wave developing from initial discontinuities) the ACM might make it become an admissibility discontinuity in the modified equation (2.53). Therefore it is necessary to design some sort of automatic switch that eliminates the application of ACM in rarefaction regions.

We modify the upwind scheme  $C_\Delta$  by  $C'_\Delta$  which is given by

$$(2.67) \quad u_i^{n+1} = u_i^n - \frac{\lambda}{2} (\theta_{i+\frac{1}{2}}^n \hat{G}_{i+\frac{1}{2}}^n - \theta_{i-\frac{1}{2}}^n \hat{G}_{i-\frac{1}{2}}^n)$$

where  $\theta_{i+\frac{1}{2}}^n$  is an *automatic switch* such that  $0 \leq \theta_{i+\frac{1}{2}} \leq 1$  and  $\theta_{i+\frac{1}{2}}^n \approx 1$  for shocks and contact discontinuities, but  $\theta_{i+\frac{1}{2}}^n = O(h)$  in smooth regions. In order to construct the switch  $\theta_{i+\frac{1}{2}}^n$  we must be able to identify the discontinuities. There are two possible ways to detect a discontinuity on a fixed mesh:

- i) to look for a large variation of the solution
- ii) to look for abrupt changes in the variation of solutions; such that abrupt changes occur at the end points of transitions.

There are many such switches that can be constructed using these two ideas [5]. In this thesis we will use the following automatic switch constructed by Harten [5] using the second idea

$$(2.68) \quad \theta_{i+\frac{1}{2}}^n = \max(\hat{\theta}_i^n, \hat{\theta}_{i+1}^n)$$



where

$$(2.69) \quad \hat{\theta}_i^n = \begin{cases} \frac{|\Delta_{i+\frac{1}{2}}^n \beta| - |\Delta_{i-\frac{1}{2}}^n \beta|}{|\Delta_{i+\frac{1}{2}}^n \beta| + |\Delta_{i-\frac{1}{2}}^n \beta|} & \text{for } \|\Delta_{i+\frac{1}{2}}^n \beta\| + |\Delta_{i-\frac{1}{2}}^n \beta| > \varepsilon \\ 0 & \text{otherwise.} \end{cases}$$

Here  $\beta = \beta(u)$  is a scalar function of the vector  $u$  which has a jump discontinuity when  $u$  is a shock or contact discontinuity. Otherwise it is smooth. We choose  $\varepsilon > 0$  so that a variation in  $\beta(u)$  which is less than  $\varepsilon$  is negligible. Clearly  $0 \leq \theta_{i+\frac{1}{2}}^n \leq 1$  and it satisfies the required properties.

Note that the switch detects abrupt changes in the variation of  $\beta(u)$ , independent of their size. Its values for the numerical solution might fluctuate and, in so doing, trigger the switch. Such an occurrence can be prevented by choosing an appropriate tolerance  $\varepsilon$  in (2.69). In Chapter V we will present several examples of computations with ACM using the artificial compressor  $C'_\Delta$  given by (2.6). As we will see, these computations exhibit oscillation free transitions with an excellent resolution of shocks.

# CHAPTER III

## FORMULATION OF THE EQUATIONS OF MOTION AND SOLUTION TO THE RIEMANN PROBLEM

### 3.1. Governing Equations

Consider a perfectly flexible uniform incompressible hyperelastic string. Suppose that in its reference configuration the string has its unstressed natural length at temperature  $T_0$ , and occupies the interval  $[0, L_0]$  on the  $x_1$  axis of a rectangular coordinate system. The  $x_1$  coordinate of a particle in its reference configuration is denoted by  $X \in [0, L_0]$ . Therefore the motion of the string is given by

$$(3.1) \quad \mathbf{x} = \mathbf{x}(X, t) = (x_1(X, t), x_2(X, t))^T$$

where  $\mathbf{x}$  is the position at time  $t$  of a particle that occupies position  $X$  in the reference configuration and the superposed  $T$  denotes the transpose.

If  $S(\mathbf{x}, t)$  denotes the arc length measured from  $\mathbf{x} = \mathbf{x}(0, t)$  in the deformed configuration then the stretch  $\lambda(X, t)$  is given by

$$(3.2) \quad \lambda(X, t) = \frac{\partial S}{\partial X}.$$

Therefore we have the following compatibility relations,

$$(3.3) \quad \frac{\partial(\lambda \cos \theta)}{\partial t} = \frac{\partial u}{\partial X} \quad \text{and} \quad \frac{\partial(\lambda \sin \theta)}{\partial y} = \frac{\partial v}{\partial X}$$

where  $u = \dot{x}_1, v = \dot{x}_2$  and  $\theta = \theta(X, t)$  is the angle that the tangent to the string makes with  $x_1$  axis as indicated in Figure 3.1.

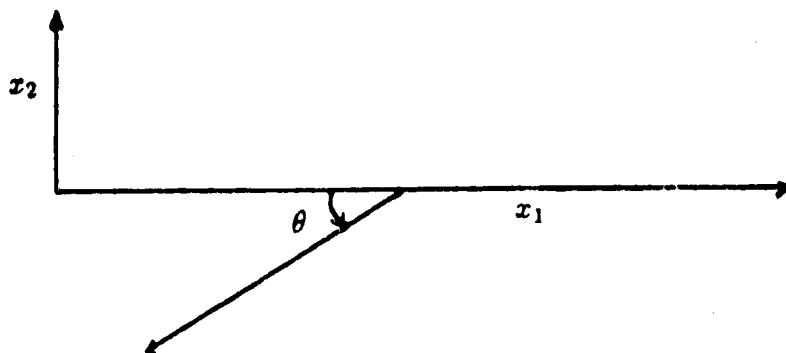


Figure 3.1

Since we have assumed that the string is perfectly flexible, the tensile force  $P$  per unit sectional area of the string in the reference configuration is tangential to the string. Therefore if the body forces are neglected, then the Lagrangian equations of motions will be as follows;

$$(3.4) \quad \frac{\partial(P \cos \theta / \rho_0)}{\partial X} = \frac{\partial u}{\partial t} \quad \text{and} \quad \frac{\partial(P \sin \theta / \rho_0)}{\partial X} = \frac{\partial v}{\partial t},$$

where  $\rho_0$  is the constant density in the reference configuration.

System (3.3) and (3.4) are in the following conservation form;

$$(3.5) \quad \frac{\partial G}{\partial t} + \frac{\partial H(G)}{\partial X} = 0,$$

where  $\mathbf{G} = (\lambda \cos \theta, \lambda \sin \theta, u, v)^T$ ,  $\mathbf{H} = (u, v, P \cos \theta / \rho_0, P \sin \theta / \rho_0)^T$ . We write (3.5) in the following convenient form,

$$(3.6) \quad \frac{\partial \mathbf{G}}{\partial t} + \mathbf{B} \frac{\partial \mathbf{G}}{\partial X} = 0.$$

If the isentropic approximation is adopted and  $P = P(\lambda)$  is the adiabatic nominal stress-stretch relation, then the matrix  $\mathbf{B}$  is given by

$$(3.7) \quad \mathbf{B} = \begin{pmatrix} 0 & | & -I \\ -C & | & 0 \end{pmatrix}$$

where  $I$  is the  $2 \times 2$  identity matrix, and  $C$  is a  $2 \times 2$  matrix with the following components;

$$(3.8) \quad \begin{aligned} C_{11} &= (C_L^2 \cos^2 \theta + C_T^2 \sin^2 \theta) \\ C_{12} &= C_{21} = (C_L^2 - C_T^2) \sin \theta \cos \theta \\ C_{22} &= C_L^2 \sin^2 \theta + C_T^2 \cos^2 \theta \\ C_L^2 &= \frac{1}{\rho_0} \frac{\partial P}{\partial \lambda} \\ C_T^2 &= \frac{P}{\rho_0 \lambda}. \end{aligned}$$

The eigenvalues of  $\mathbf{B}$  are  $\pm C_L$  and  $\pm C_T$ . Therefore the system will be strictly hyperbolic if  $C_L^2 > 0, C_T^2 > 0$  and  $C_L^2 \neq C_T^2$ .

If system (3.5) is subjected to certain initial and boundary conditions then solutions can be found (see for example [14] [16]). However these are essentially solutions to the Riemann problems. In this thesis we will consider fairly general initial boundary value problems for the special case of (3.5) with

$\theta = 0$  and  $v = 0, \forall (X, t) \in \{(X, t) : 0 \leq X \leq L_0, t > 0\}$ . This is a simple longitudinal stretch of a string which occupies the interval  $[0, L_0]$  of the  $x_1$  axis in the undeformed natural reference state at temperature  $T_0$ . Therefore the governing system of partial differential equations (3.5) is reduced to a system of two equations:

$$(3.9a) \quad u_t + f(u)_X = 0$$

where  $u = (u, \lambda)^T$  and  $f = \left(\frac{-P(\lambda)}{\rho_0}, -u\right)^T$ . If equation (3.9a) is non-dimensionalised by setting  $\hat{x} = \frac{x}{L}$ ,  $\hat{X} = \frac{X}{L}$ ,  $\hat{P} = \frac{P}{\mu}$ ,  $\hat{t} = \frac{t(\mu/\rho_0)^{1/2}}{L}$ ,  $\hat{u} = \frac{u}{(\rho_0/\mu)}$ , where  $L$  is a typical length, then dropping the hats, we obtain the conservation law

$$(3.9b) \quad u_t + f(u)_X = 0$$

where  $u = (\lambda, u)^T$  and  $f = (-P, -u)^T$  where  $u = \frac{\partial x_1}{\partial t}$ .

In Chapter V we will consider a number of initial, boundary value problems for (3.9). In general these problems develop internal shocks and it is not possible to find analytic solutions beyond a finite time  $t_b$ . Consequently it is necessary to investigate other numerical methods. In this thesis Godunov's method which is described in Section 2.4, will be employed. Godunov's scheme is based on the exact solution of the Riemann problem for (3.9). Therefore later on in this Chapter we shall discuss solutions of the Riemann problem. But first we shall describe the constitutive relations required in order to solve (3.9).

### 3.2. Constitutive Relations

In this thesis we shall consider the problem of simple tension of an incompressible hyperelastic string. For these problems the strain energy function is given as a function of  $\lambda$ , so that

$$(3.10) \quad W(\lambda) = W(\lambda, \frac{1}{\sqrt{\lambda}}, \frac{1}{\sqrt{\lambda}}),$$

where  $\lambda$  is the stretch in the direction of the tension. We obtain results for special cases of the Mooney-Rivlin and three term Ogden strain energy functions. For Ogden's three term strain energy function we have

$$(3.11) \quad W(\lambda) = \sum_{i=1}^3 \frac{\mu_i}{a_i} (\lambda^{a_i} + 2\lambda^{-a_i/2} - 3),$$

where  $\mu_3$  is the infinitesimal shear modulus,  $0 \leq a_i \leq 1$  and  $\sum_{i=1}^3 \mu_i a_i = 2\mu$ .

For isothermal tension Ogden [11] has shown that the nominal stress-stretch relation,

$$(3.12) \quad P(\lambda) = \sum_{i=1}^3 \mu_i (\lambda^{a_i-1} - \lambda^{-\frac{a_i}{2}-1})$$

obtained from

$$(3.13) \quad P(\lambda) = \frac{dW}{d\lambda},$$

gives a close fit with experimental data for simple tension of certain rubber up to stretches of about 7 when the  $\mu_i$  and  $a_i$  take the values

$$(3.14) \quad \begin{array}{lll} \frac{\mu_1}{\mu} = 1.491 & \frac{\mu_2}{\mu} = 0.003 & \frac{\mu_3}{\mu} = -0.0237 \end{array}$$

$$a_1 = 1.3 \quad a_2 = 5.0 \quad a_3 = -2.0.$$

With these parameters (3.12) gives an s-shaped curve with an inflection point  $i = 2.624$  [see Fig. 3.2]. The Mooney-Rivlin strain energy function is a special case of (3.11) with

$$(3.15) \quad \begin{array}{lll} \frac{\mu_1}{\mu} = \alpha & \frac{\mu_2}{\mu} = -(1 - \alpha) & \mu_3 = 0 \end{array}$$

$$a_1 = 2.0 \quad a_2 = -2 \quad 0 \leq \alpha \leq 1,$$

and the corresponding nominal stress stretch relation is

$$(3.16) \quad P(\lambda) = \mu(\alpha + (1 - \alpha)/\lambda)(\lambda - \frac{1}{\lambda^2}).$$

With  $\alpha = 0.6$  (3.16) gives a close fit with simple tension experimental data for  $\lambda$  upto about 3.5. The Neo-Hookian stress stretch relation is a special case of (3.16) with  $\alpha = 1$ ,

$$(3.17) \quad P = \mu(\lambda - \lambda^{-2}).$$

For the problems we will consider in this thesis we will use the stress stretch relations (3.12), (3.16) and (3.17). These relations are generally used

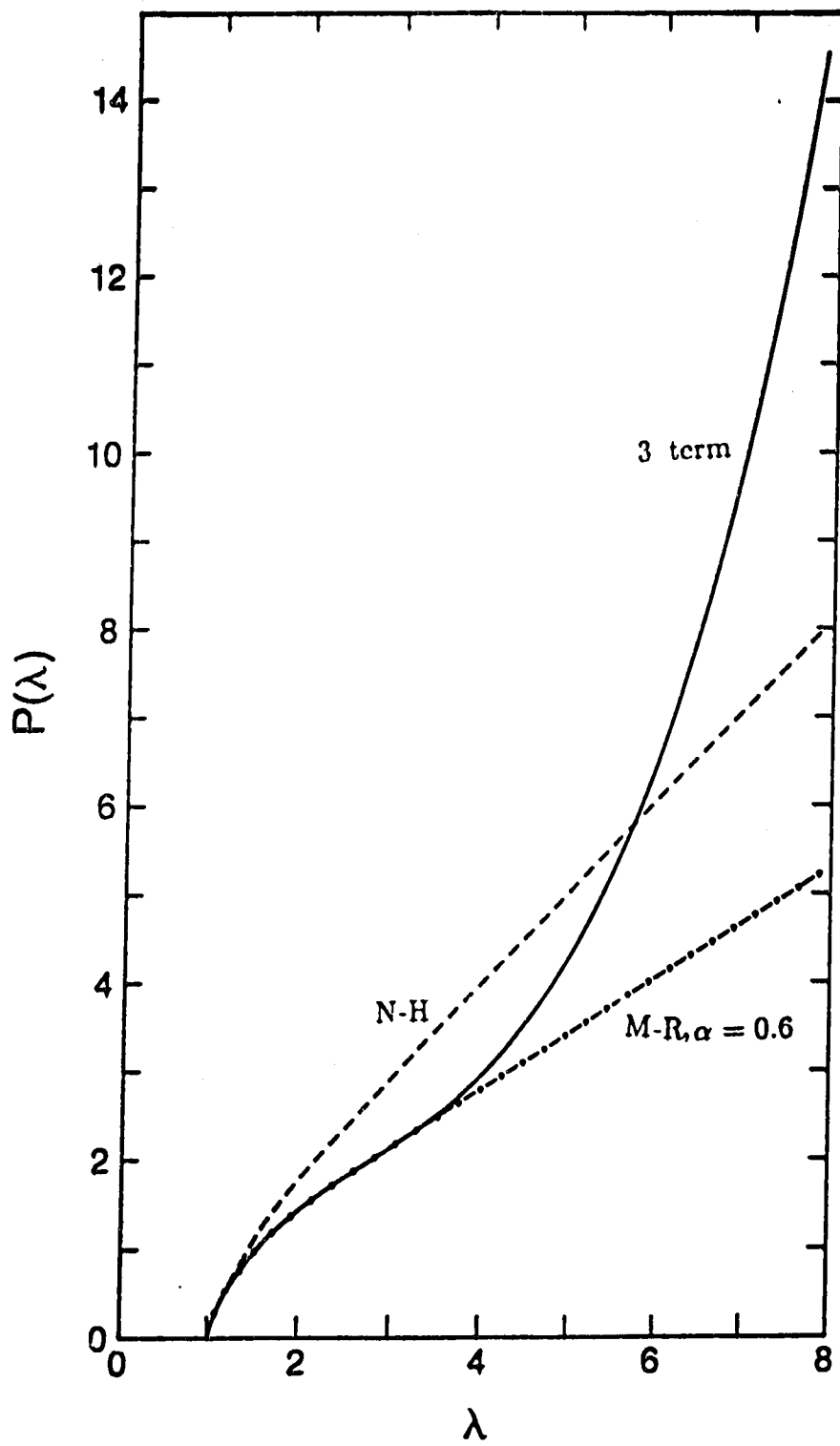


Figure 3.2



for isothermal deformations. The thermodynamic effects are investigated in [17], where it is verified that for rubber like materials the error caused by neglecting these effects on the  $P - \lambda$  relation is negligible.

### 3.3. The Riemann problem for the Mooney-Rivlin String

Consider the conservation system (3.9)

$$(3.18) \quad \frac{\partial \mathbf{u}}{\partial t} + \frac{\partial \mathbf{f}(\mathbf{u})}{\partial X} = 0$$

where  $\mathbf{u} = (\lambda, u)^T$  and  $\mathbf{f} = (-u, -P(\lambda))^T$ . For now we will consider the Mooney-Rivlin string which has the convex stress stretch relation given by

$$(3.19) \quad P(\lambda) = \mu \{ \alpha(\lambda - \lambda^{-2}) + (1 - \alpha)(1 - \lambda^{-3}) \}, \quad \alpha = 0.6.$$

We may write (3.18) as

$$(3.20) \quad \mathbf{u}_t + A \mathbf{u}_x = 0$$

where  $A = \begin{pmatrix} 0 & -1 \\ -C_L^2 & 0 \end{pmatrix}$  and  $C_L = \sqrt{P'(\lambda)} > 0$ . The eigenvalues of  $A$  are;

$$(3.21) \quad \begin{aligned} \alpha_1 &= C_L = \sqrt{P'(\lambda)} > 0 \\ \alpha_2 &= -C_L = -\sqrt{P'(\lambda)} < 0. \end{aligned}$$

These are both real and distinct. Therefore (3.9) is strictly hyperbolic.

We consider the Riemann problem for (3.9) subject to the initial condition

$$(3.22) \quad u(0, X) = (\lambda(0, X), u(0, X))^T = \begin{cases} u_\ell = (\lambda_\ell, u_\ell)^T & X < 0 \\ u_r = (\lambda_r, u_r)^T & X > 0 \end{cases}$$

where  $u_\ell$  and  $u_r$  are constant states. The solution of the Riemann problem (3.9), (3.13) for a general function  $P$ , with  $P'' < 0$  and  $P' > 0$ , consists of constant states separated by either shock waves or by rarefaction waves (see [14]).

Now we will discuss shock wave curves. Let  $u = (\lambda, u)^T$  be a state connected to  $u_\ell = (\lambda_\ell, u_\ell)^T$  on the right by an  $i$ -shock. Then  $u$  satisfies the following jump condition (2.13),

$$(3.23) \quad V \begin{bmatrix} u \\ \lambda \end{bmatrix} = \begin{bmatrix} -P(\lambda) \\ -u \end{bmatrix}$$

where  $[F] = F_r - F_\ell$  denotes the jump in the quantity  $F$  from the right state to the left state, and  $V$  is the shock speed. Thus solving for  $V$  we obtain the following:

$$(3.24) \quad V = \pm \sigma(\lambda)$$

$$\text{where } \sigma(\lambda) = \sqrt{\frac{P(\lambda) - P(\lambda_\ell)}{\lambda - \lambda_\ell}}.$$

Eliminating  $V$  in (3.23) we obtain

$$(3.25) \quad [u] = \pm \sqrt{[P][\lambda]}.$$

The  $i$ -shock must satisfy the usual shock inequality (2.15)

$$(3.26) \quad \alpha_i(\lambda) \leq V_i \leq \alpha_i(\lambda_\ell).$$

Hence for the 1-shock  $V_1 = -\sigma(\lambda) < 0$  and for 2-shock  $V_2 = \sigma(\lambda) > 0$ , since  $\alpha_1 < 0 < \alpha_2$ .

We now consider the possible states  $u$  that can be connected to  $u_\ell$  on the right by a 1-shock. In this case (3.26) implies

$$(3.27) \quad -\sqrt{P'(\lambda)} < -\sqrt{P'(\lambda_\ell)}$$

which gives  $P'(\lambda) > P'(\lambda_\ell)$ . Thus  $\lambda_\ell > \lambda$  since  $P'' < 0$ . From (3.25) we have

$$(3.28) \quad V_1(\lambda - \lambda_\ell) = -(u - u_\ell) \quad \text{and} \quad V_2(\lambda - \lambda_\ell) = -(u - u_\ell).$$

Hence since  $V_1 < 0 < V_2$  and  $(\lambda - \lambda_\ell) < 0$  we conclude that  $[u] = u - u_\ell < 0$ . Therefore in (3.25) we must choose the negative sign. Therefore any state that can be connected to  $u_\ell$  by a 1-shock on the right will lie on the 1-shock curve given by the following;

$$(3.29) \quad S^- : u - u_\ell = (\lambda - \lambda_\ell) \sqrt{\frac{P(\lambda) - P(\lambda_\ell)}{\lambda - \lambda_\ell}} = s^-(\lambda, u_\ell) \quad \lambda < \lambda_\ell.$$

Note that  $\frac{ds^-}{d\lambda} = \frac{(P(\lambda_\ell) - P(\lambda) + P'(\lambda)(\lambda_\ell - \lambda))}{2\sqrt{[P]([\lambda])}} > 0$ . Hence  $s^-$  is monotone increasing. It can be shown that in region  $\lambda < \lambda_\ell$ ,  $s^-$  is starlike about the point  $(\lambda, u)$  (i.e. any straight line through  $(\lambda_\ell, u_\ell)$  crosses the curve  $s^-$

at most at one point). Hence in the  $(\lambda, u)$  plane the  $s^-$  curve will be as shown in Fig. 3.3a.

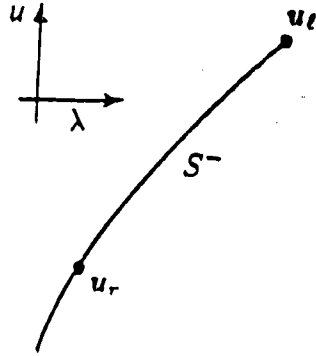


Figure 3.3a

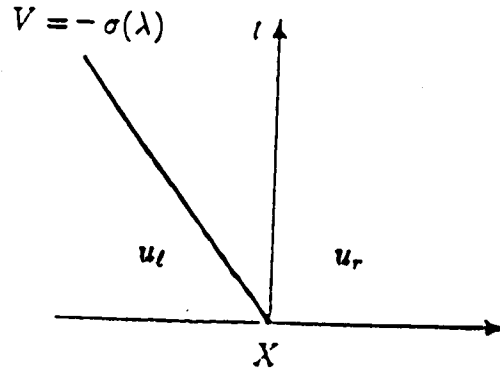


Figure 3.3b

If  $u_r$  is any point on this curve then the Riemann problem can be solved by connecting 1-shock on the right (see Fig. 3.3b).

Similarly we consider the possibility of connecting 2-shock wave to the right of state  $u_l$ . In this case the shock inequalities (3.26) require

$$\sqrt{P'(\lambda)} < \sqrt{P'(\lambda_l)}.$$

Hence  $\lambda > \lambda_l$ . Then using a similar argument as above we obtain the 2-shock curve which is given by,

$$(3.30) \quad S^+ : u - u_l = -(\lambda - \lambda_l) \sqrt{\frac{P(\lambda) - P(\lambda_l)}{\lambda - \lambda_l}} = s^+(\lambda, u_l) \quad \lambda > \lambda_l.$$

Here  $s^+$  is monotone decreasing and it is starlike about the point  $(\lambda_\ell, u_\ell)$  (see Fig. 3.4a).

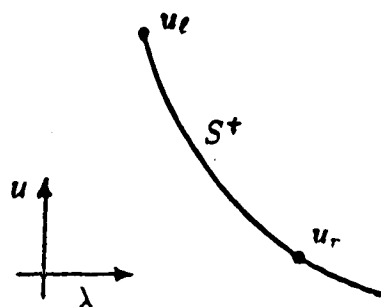


Figure 3.4a

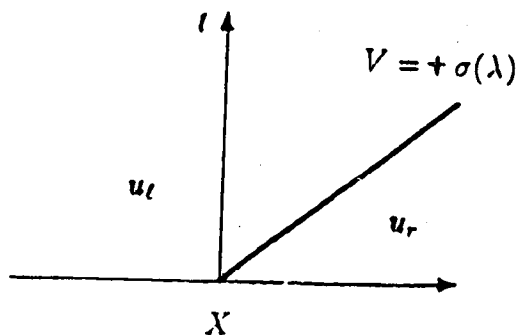


Figure 3.4b

Thus for any  $u_r$  on this curve the solution to the Riemann problem will be as depicted in Fig. 3.4b.

Let us now find all the possible states  $u = (\lambda, u)^T$  that can be connected to the right of  $u_\ell$  by a rarefaction wave. Rarefaction waves are the continuous solution to the Riemann problem of the form  $u = u(X/t)$ . Here we have two families of rarefaction waves corresponding to each characteristic values  $\alpha_i$ . For  $k = 1, 2$  a  $k$ -rarefaction wave must be such that  $\alpha_k(u(X/t))$  is an increasing function of  $X/t$ .

If  $z = X/t$ , for  $u = u(z)$  we obtain  $u_z = \frac{u_t}{t}$  and  $u_t = -\frac{u_z X}{t}$ .

Hence (3.20) becomes

$$(3.31) \quad (A - zI)u_z = 0.$$

If  $u_z \equiv 0$  then  $u$  is constant. Therefore suppose  $u_z \neq 0$ . In this case  $u_z$  will be a right eigenvector of  $A$  corresponding to the eigenvalue  $z$ . Hence corresponding to each eigenvalue, we obtain a rarefaction wave which satisfies

$$\begin{pmatrix} -\alpha_k & -1 \\ C_L^2 & -\alpha_k \end{pmatrix} \begin{pmatrix} \lambda_z \\ u_z \end{pmatrix} = \begin{pmatrix} 0 \\ 0 \end{pmatrix}.$$

From this we obtain  $\frac{u_z}{\lambda_z} = -\alpha_k$  or,

$$(3.32) \quad \frac{du}{d\lambda} = -\alpha_k \quad \text{for } k = 1, 2,$$

which by integration gives the  $k$  rarefaction curve given by

$$R^\pm : u = u_\ell + \int_{\lambda_\ell}^{\lambda} \alpha_k(y) dy, \quad k = 1 \text{ and } 2.$$

Then the requirement  $\alpha_k(\lambda) > \alpha_k(\lambda_\ell)$  gives  $P'(\lambda) > P'(\lambda_\ell)$  for 1-rarefaction wave and  $P'(\lambda) < P'(\lambda_\ell)$  for 2-rarefaction waves. Therefore since  $P'' < 0$  we have

$$(3.33) \quad R^- : u - u_\ell = \int_{\lambda_\ell}^{\lambda} C_L(s) ds = r^-(\lambda, u_\ell) \quad \lambda > \lambda_\ell$$

$$R^+ : u - u_\ell = - \int_{\lambda_\ell}^{\lambda} C_L(s) ds = r^+(\lambda, u_\ell) \quad \lambda < \lambda_\ell.$$

Note that  $\frac{dr^-}{d\lambda} = C_L(\lambda) > 0$  and  $\frac{d^2 r^-}{d\lambda^2} = \frac{P''(\lambda)}{2C_L(\lambda)} < 0$ . Similarly  $\frac{dr^+}{d\lambda} = -C_L(\lambda) < 0$  and  $\frac{d^2 r^+}{d\lambda^2} = -\frac{P''(\lambda)}{2C_L(\lambda)} > 0$ . Therefore the rarefaction waves can be depicted as in Fig. (3.5a).

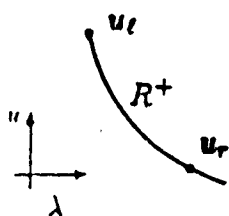
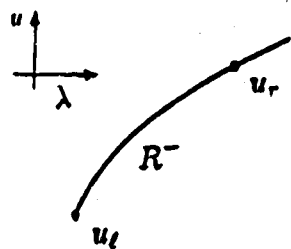


Figure 3.5a

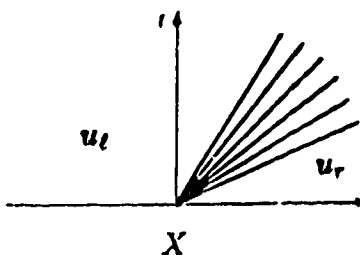
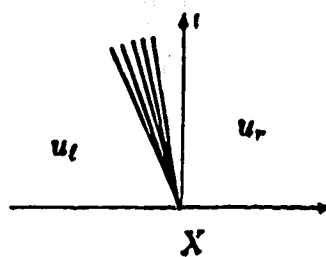


Figure 3.5b

The corresponding solution of the Riemann problem will then be as shown in Fig. (3.5b).

Hence given the initial condition (3.22) one can solve the Riemann problem by connecting  $u_\ell$  to  $u_r$  by a rarefaction wave as follows. For instance if  $\alpha_1(\lambda_\ell) < \alpha_1(\lambda_r)$  then we obtain  $\lambda(X/t)$  from  $X/t = \alpha_1(\lambda(X/t)) = -\sqrt{P'(\lambda(X/t))}$  which will then be used to find  $u(X/t)$  from  $u = u_\ell + \int_{\lambda_\ell}^{\lambda} C_L(s) ds$ .

Note that  $\frac{ds^-}{d\lambda} = \frac{1}{2}(\sigma^2 + P')\frac{1}{\sigma}$ , and  $\frac{d^2s^-}{d\lambda^2} = \frac{P''}{2\sigma} - \frac{(2P' - \sigma - P'^2/\sigma)}{4\sqrt{P'(\lambda)}}$ . Therefore since  $\lim_{\lambda \rightarrow \lambda_\ell} \frac{P(\lambda) - P(\lambda_\ell)}{\lambda - \lambda_\ell} = P'(\lambda_\ell)$  we obtain  $\frac{ds^-}{d\lambda} |_{\lambda=\lambda_\ell} = \sqrt{P'(\lambda_\ell)}$  and  $\frac{d^2s^-}{d\lambda^2} |_{\lambda=\lambda_\ell} = \frac{P''(\lambda_\ell)}{2\sqrt{P'(\lambda_\ell)}}$ . Therefore at  $\lambda = \lambda_\ell$  the  $s^-$  and the  $r^-$  curve have 2<sup>nd</sup> order contact (i.e. their first and second derivative are equal). Similarly we can show that  $s^+$  and  $r^+$  have second order contact at  $\lambda = \lambda_r$ .

Therefore we have four curves dividing the  $(\lambda, u)$  plane into four disjoint regions. They meet smoothly at  $\lambda = \lambda_\ell$  (see Fig. 3.6).

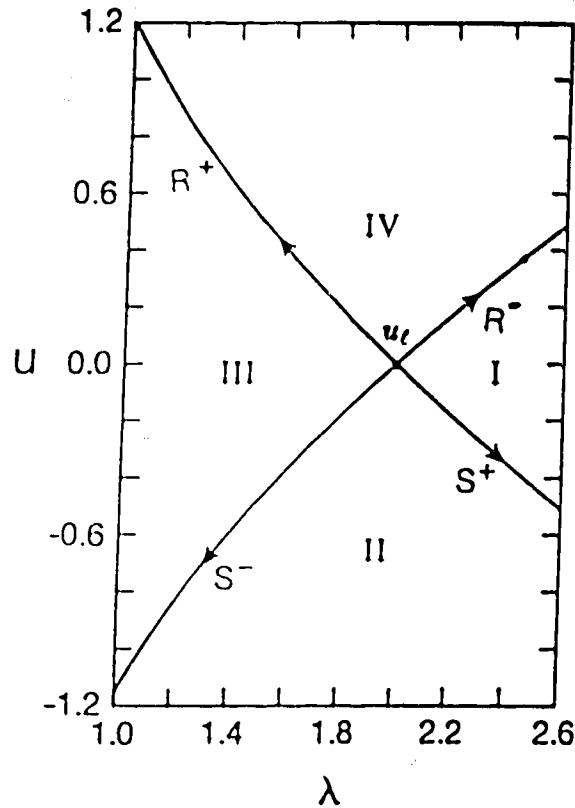


Fig. 3.6

So given any  $u_\ell = (\lambda_\ell, u_\ell)^T \in R^2$  if  $u_r$  lies in one of these curves then the Riemann problem is solved as described above. If  $u_r$  does not lie on one of these curves then we solve the Riemann problem as follows. For  $u \in R^2$  define

$$\begin{aligned}
 S_\pm(\bar{u}) &= \{(\lambda, u) : u - u_\ell = s_\pm(\lambda, \bar{u})\} \\
 R_\pm(\bar{u}) &= \{(\lambda, u) : u - u_\ell = r_\pm(\lambda, \bar{u})\} \\
 W_\pm(\bar{u}) &= S_\pm(\bar{u}) \cup R_\pm(\bar{u}).
 \end{aligned}
 \tag{3.39}$$



If  $u_r = (\lambda_r, u_r)$  is in region I, II or III, then  $\exists$  a unique  $\bar{u} = (\bar{\lambda}, \bar{u})$  such that  $u_r$  lies on  $W_{\pm}(\bar{u})$  and  $\bar{u}$  lies on  $W_-(u_\ell)$  (for details see [15]). If however  $u_r$  is in region IV then such a  $\bar{u}$  exists only if an extra condition is imposed on  $P$ . (For example  $P$  must be such that  $\int_{\lambda_0}^{\infty} \sqrt{P'(y)} dy = +\infty$ .) Therefore for both the Mooney-Rivlin and the Neo-Hookian strings there exists a unique  $\bar{u}$  with the above properties for any  $u_r \in R^2$ . The solution to the Riemann problem is now clear. Suppose for example that  $u_r$  is in region I. Then as we discussed above there exists a unique  $\bar{u} = (\bar{\lambda}, \bar{u})$  such that  $W_+(\bar{u})$  passes through  $u_r$ , and  $W_-(u_\ell)$  passes through  $\bar{u}$ . Hence  $\bar{u}$  is connected to  $u_\ell$  on the right by a 1-rarefaction wave, and  $u_r$  is connected to  $\bar{u}$  on the right by a 2-shock wave (see Fig. 3.7).

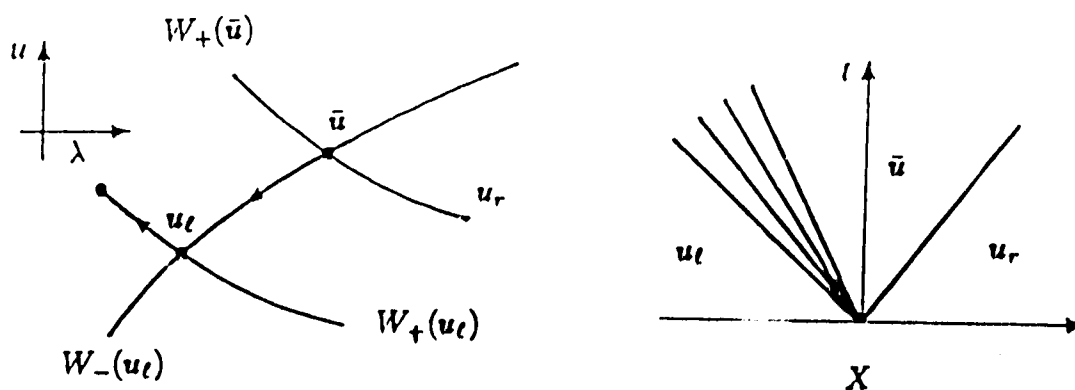


Figure 3.7

The three other cases can also be analyzed similarly.

Note that if  $P'' > 0$ , then obvious changes need to be made, and we find again four curves dividing the  $(\lambda, u)$  plane (see Fig. 3.8).

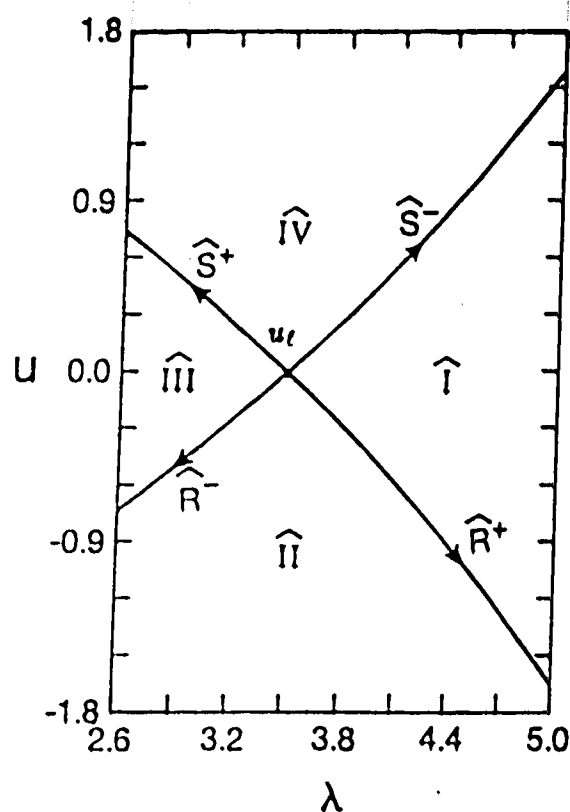


Figure 3.8

### 3.4 The Riemann Problem for the Three-Term Stress-Stretch Relation

We shall now investigate the solution to the Riemann problem for the three-term stress-stretch relation. From Fig. (3.1) we can see that in this case,  $P$  has the following properties:

- i)  $\text{sgn}(P'') = \text{sgn}(\lambda - \lambda_i)$ ,  $\lambda > 1$  where  $\lambda_i = 2.643$  is the only inflection point,
- ii)  $P(1) = 0$ ,  $P'(\lambda) > 0$  and there are exactly two solutions  $\lambda_m, \lambda_M$ ,  $\lambda_m < \lambda_M$  such that the following equation is satisfied

$$\frac{P(\lambda)}{\lambda} = P'(\lambda).$$

The solution we discuss in this section applies not only for this case but also for the case where  $P$  is any function with properties i) and ii) (see [13]).

As before we start our discussion with shock wave curves. Let  $u = (\lambda, u)^T$  be a state that can be connected to  $u_\ell = (\lambda_\ell, u_\ell)^T$  on the right by an i shock. For now consider the case where  $\lambda_\ell < \lambda_i$ .

For the 1-shock curve we require  $P'(\lambda) > \sigma > P'(\lambda_\ell)$ . Therefore we obtain the standard 1-shock curve given by

$$S^- : u - u_\ell = (\lambda - \lambda_\ell) \sqrt{\frac{P(\lambda) - P(\lambda_\ell)}{\lambda - \lambda_\ell}} = s^-(\lambda, u_\ell), \quad \lambda < \lambda_\ell < \lambda_i.$$

For the 2-shock curve the requirement  $P'(\lambda) < \sigma < P'(\lambda_\ell)$  must be satisfied. Therefore proceed as follows. Let  $L$  be a tangent line to the curve  $P = P(\lambda)$  passing through  $(\lambda_\ell, P_\ell)$ . Then let  $(\lambda_{T\ell}, P(\lambda_{T\ell}))$  be the point at which this tangent line touches the curve (see Fig. 3.9). Clearly we have  $\lambda_{T\ell} \geq \lambda_i$  and for  $\lambda_\ell < \lambda < \lambda_{T\ell}$  the requirement for 2-shock curves is satisfied. So for  $\lambda_\ell < \lambda < \lambda_{T\ell}$  we connect  $(\lambda_\ell, u_\ell)$  to  $(\lambda, u)$  on the right by a 2-shock which is given by

$$S^+ : u - u_\ell = -(\lambda - \lambda_\ell) \sqrt{\frac{P(\lambda) - P(\lambda_\ell)}{\lambda - \lambda_\ell}} = s^+(\lambda, u_\ell) \quad \lambda_\ell < \lambda \leq \lambda_i \leq \lambda_{T\ell}.$$

We can proceed with this shock curve only up to  $\lambda = \lambda_{T\ell}$ , since at  $\lambda = \lambda_{T\ell}$  we have  $P' = \sigma$  and then  $P'(\lambda) > \sigma$  for  $\lambda > \lambda_{T\ell}$ . To go beyond  $\lambda_{T\ell}$  we connect  $(\lambda_{T\ell}, u_{T\ell})$  to  $(\lambda, u)$  by a 2-rarefaction wave. This is possible

since for  $\lambda > \lambda_{T\ell}$ ,  $P'(\lambda)$  is increasing. Hence, for  $\lambda > \lambda_{T\ell}$  we have an  $\hat{R}^+$  curve connecting  $(\lambda_{T\ell}, u_{T\ell})$  to  $(\lambda, u)$  given by:

$$\hat{R}^+ : u - u_{T\ell} = - \int_{\lambda_{T\ell}}^{\lambda} C_L(y) dy = \hat{r}^+(\lambda, u_{T\ell}) \quad \lambda > \lambda_{T\ell}.$$

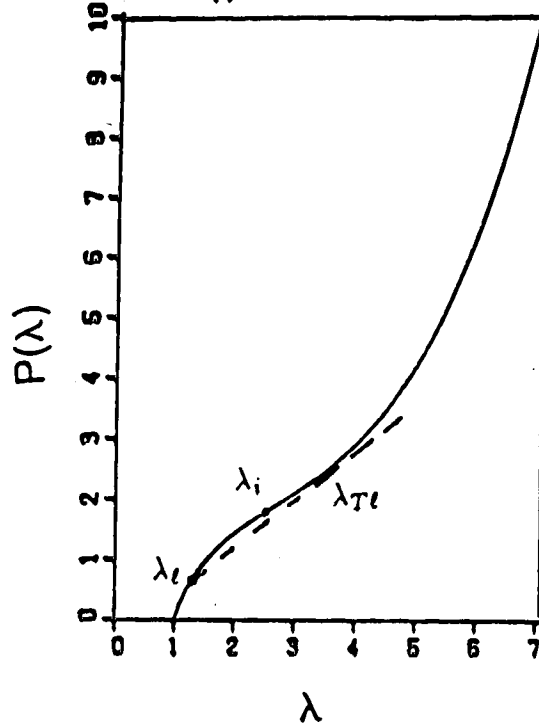


Figure 3.9

Note that  $\frac{ds^+}{d\lambda} = \frac{\text{sgn}(\lambda_{T\ell} - \lambda)}{2\sigma} (P'(\lambda) + \sigma(\lambda))$  and  $\frac{d^2s^+}{d\lambda^2} = \frac{\text{sgn}(\lambda_{T\ell} - \lambda)}{2\sigma} P'' - \frac{(2P' - \sigma - P'^2/\sigma)}{4\sqrt{P}|\lambda|}$ . By the choice of  $\lambda_{T\ell}$  we have  $\sigma(\lambda_{T\ell}) = P'(\lambda_{T\ell})$ . Therefore  $\frac{ds^+}{d\lambda}|_{\lambda=\lambda_{T\ell}} = \sqrt{P'(\lambda_{T\ell})}$  and  $\frac{d^2s^+}{d\lambda^2}|_{\lambda=\lambda_{T\ell}} = \frac{P''(\lambda_{T\ell})}{2\sqrt{P'(\lambda_{T\ell})}}$ . Hence  $s^+(\lambda_{T\ell}, u_{T\ell})$  and  $\hat{r}^+(\lambda, u_{T\ell})$  have a second order contact at  $\lambda = \lambda_{T\ell}$ , (i.e. their first and second derivatives are equal at this point). Therefore on the  $x-t$  plane the solution will be as depicted in Fig. 3.10.

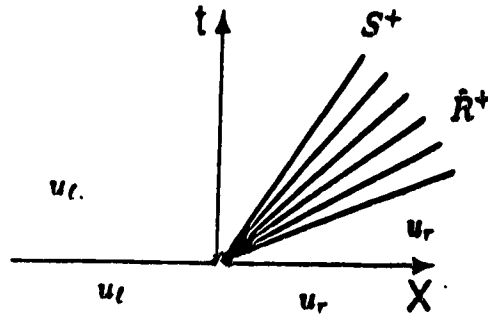


Figure 3.10

Let us now discuss the rarefaction wave curves. For a first rarefaction wave we must have  $P'(\lambda_l) > P'(\lambda)$ . Clearly for  $\lambda_l < \lambda < \lambda_i$  this requirement is satisfied. Hence up to  $\lambda = \lambda_i$  we can connect  $(\lambda_l, u_l)$  to  $(\lambda, u)$  by a 1-rarefaction wave. However we cannot proceed any further with expansion waves since  $P'(\lambda_i) < P'(\lambda)$  for  $\lambda > \lambda_i$ . We also cannot connect  $(\lambda_i, u_i)$  to  $(\lambda, u)$  by a shock curve since the shock speed will be greater than some of the rarefaction characteristic speeds. Therefore we proceed as follows. For each  $\lambda > \lambda_i$  there exists a  $\lambda_T = \lambda_T(\lambda)$  such that  $1 < \lambda_T < \lambda_i$  and,

$$(3.35) \quad \frac{P(\lambda) - P(\lambda_T)}{\lambda - \lambda_T} = P'(\lambda_T).$$

Then if  $\lambda_\ell > \lambda_T$ , we connect  $(\lambda_\ell, u_\ell)$  to  $(\lambda, u)$  by the usual 1-shock curve because in this case we have  $P'(\lambda) > \sigma > P'(\lambda_\ell)$  which is the 1-shock inequality (see Fig. 3.11).

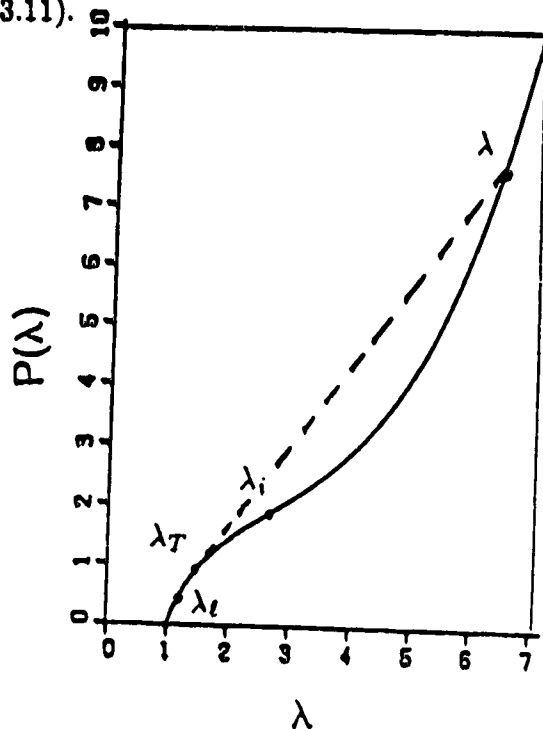


Figure 3.11

But if  $\lambda_\ell < \lambda_T$  then we first connect  $(\lambda_\ell, u_\ell)$  to  $(\lambda_T, u_T)$  by a 1-rarefaction wave which requires  $P'(\lambda_\ell) > P'(\lambda)$ . Then we obtain the  $R^-$  curve given by

$$(3.36) \quad R^- : u - u_\ell = \int_{\lambda_\ell}^{\lambda} C_L(s) ds = r^-(\lambda, u_\ell) \quad \lambda_\ell < \lambda < \lambda_T.$$

Now since  $P'(\lambda) > \sigma > P'(\lambda_T)$  for  $\lambda > \lambda_T$ , we go from  $(\lambda_T, u_T)$  to

$(\lambda, u)$  by a 1-shock, where  $u$  is given by

$$\begin{aligned}
 (3.37) \quad u &= u_T + (\lambda - \lambda_T) \sqrt{\frac{P(\lambda) - P(\lambda_T)}{\lambda - \lambda_T}} \\
 &= u_\ell + \int_{\lambda_\ell}^{\lambda_T} C_L(s) ds + (\lambda - \lambda_T) C_L(\lambda_T).
 \end{aligned}$$

The form of the solution will be as shown in Figure 3.12. There is a jump at the right edge of the rarefaction.

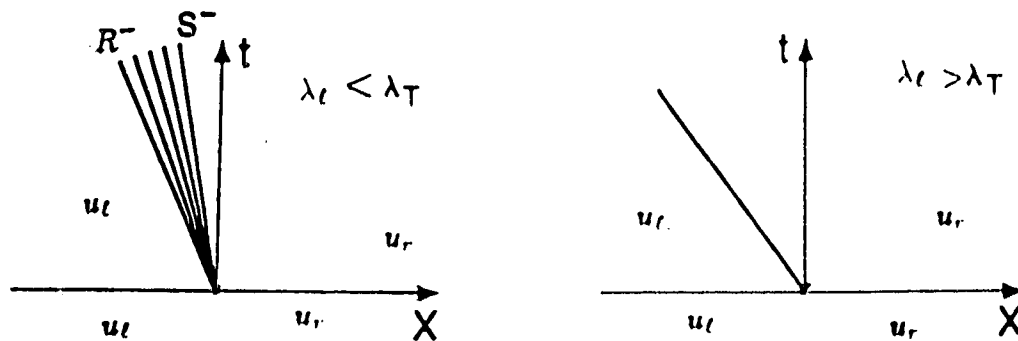


Figure 3.12

Finally we consider the 2-rarefaction wave. Here we require  $P'(\lambda_\ell) < P'(\lambda)$ . So we obtain the standard 2-rarefaction wave curve given by

$$(3.38) \quad R^+ : u - u_\ell = - \int_{\lambda_\ell}^{\lambda} C_L(s) ds = r^-(\lambda, u_\ell) \quad \lambda < \lambda_\ell.$$

As in the convex case, we have four smooth curves which divide the  $(\lambda, u)$  plane as shown in Fig. 3.13.

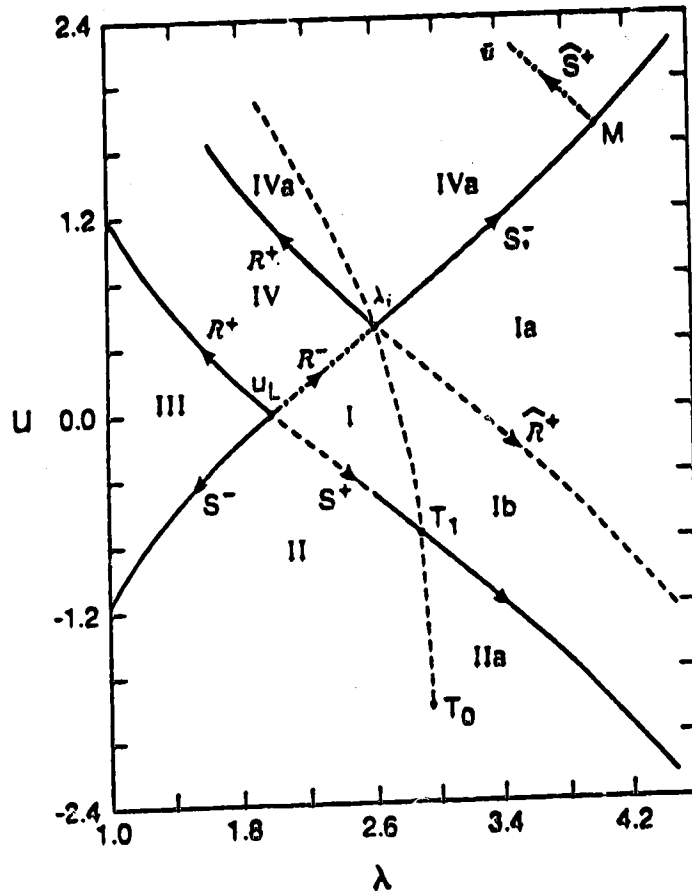


Figure 3.13

The curve  $iT_1T_0$  denotes the locus of the tangent points of the type illustrated in (3.9) for curves emanating from the  $r^-$  curve through  $u_i$  and  $u_i$ ,  $T_1$  being the tangent point associated with  $\lambda_i$ ,  $T_0$  that for  $\lambda = 1$ . The extension of this curve into region IV denotes the locus of tangent points of the type illustrated in Figure 3.11, for curves emanating from the curve  $S_-^-$ . In referring Figure 3.11  $\lambda$  there corresponds to the points on  $S_-^-$ . The



$S_+$  curve represents the locus of points  $(\lambda, u)$  on Figure 3.11 as  $\lambda_T$  varies on the curve  $r^-$  through  $u_\ell$ ,  $\lambda_T \leq \lambda_i$ . The other curves are as indicated previously.

So given any  $u_\ell = (\lambda_\ell, u_\ell)^T \in R^2$  if  $u_r$  lies on one of these curves then the Riemann problem is solved as described above. If  $u_r$  lies in regions I to IV the solution is as described in the Mooney-Rivlin case. The remaining regions require the composite curves of the type illustrated in Figure (3.9) and Figure (3.11). Suppose for example  $u_r$  lies in region IVa. Then we have two possible solutions corresponding to two different cases:

$$(3.39) \quad \begin{aligned} u_r &= \bar{u} - (\lambda_r - \bar{\lambda}) \sqrt{\frac{P(\lambda_r) - P(\bar{\lambda})}{\lambda_r - \bar{\lambda}}} \\ \bar{u} &= u_\ell + \int_{\lambda_\ell}^{\lambda_r} C_L(s) ds + (\bar{\lambda} - \lambda_T) C_L(\lambda_T), \end{aligned}$$

or

$$\begin{aligned} u_r &= \bar{u} - (\lambda_r - \bar{\lambda}) \sqrt{\frac{P(\lambda_r) - P(\bar{\lambda})}{\lambda_r - \bar{\lambda}}} \\ \bar{u} &= u_\ell + (\bar{\lambda} - \lambda_\ell) \sqrt{\frac{P(\bar{\lambda}) - P(\lambda_\ell)}{\bar{\lambda} - \lambda_\ell}} \end{aligned}$$

with

$$P'(\lambda_T) = \frac{P(\bar{\lambda}) - P(\lambda_T)}{\bar{\lambda} - \lambda_T},$$

where referring to Figure 3.11,  $\bar{\lambda}$  corresponds to  $\lambda$  there and  $\lambda_T$  to the tangent point. The first solution corresponds to the case where  $\lambda_T > \lambda_\ell$ . In this case the constant state  $\bar{u} = (\bar{\lambda}, \bar{u})^T$  is connected to  $u_\ell$  by a 1-rarefaction with a jump at the right edge and  $u_r$  is connected to  $\bar{u}$  on the

right by a 2-shock (Figure 3.14a). The second solution corresponds to the case where  $\bar{\lambda}$  lies sufficiently far to the right so that  $\lambda_T < \lambda_\ell$ . In this case  $\bar{u}$  is connected to  $u_\ell$  by a 1-shock and  $u_r$  is connected to  $\bar{u}$  on the right by a 2-shock (Figure 3.14).

If  $\lambda_\ell = \lambda_i$  we can use Fig. 3.8 to obtain Fig. 3.15.

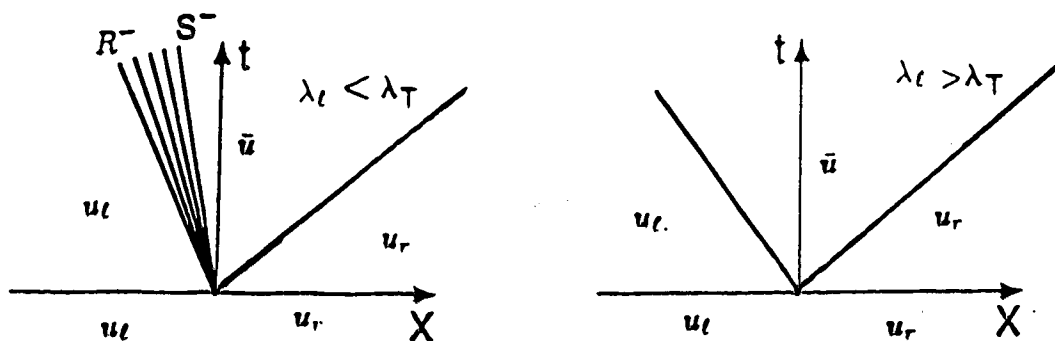


Figure 3.14

Now we consider the case where  $\lambda_\ell > \lambda_i$ . For the 1-shock wave we must have the inequality  $P'(\lambda_\ell) < \sigma < P'(\lambda)$ . This is satisfied when  $\lambda > \lambda_\ell$ , since in this case  $P'' > 0$ . Hence we get the  $S^-$  curve given by

$$(3.41) \quad S^- : u - u_\ell = (\lambda - \lambda_\ell) \sqrt{\frac{P(\lambda) - P(\lambda_\ell)}{\lambda - \lambda_\ell}} = s^-(\lambda, u_\ell) \quad \lambda > \lambda_\ell > \lambda_i.$$

On the  $(\lambda, u)$  plane  $S^-$  is monotone increasing,

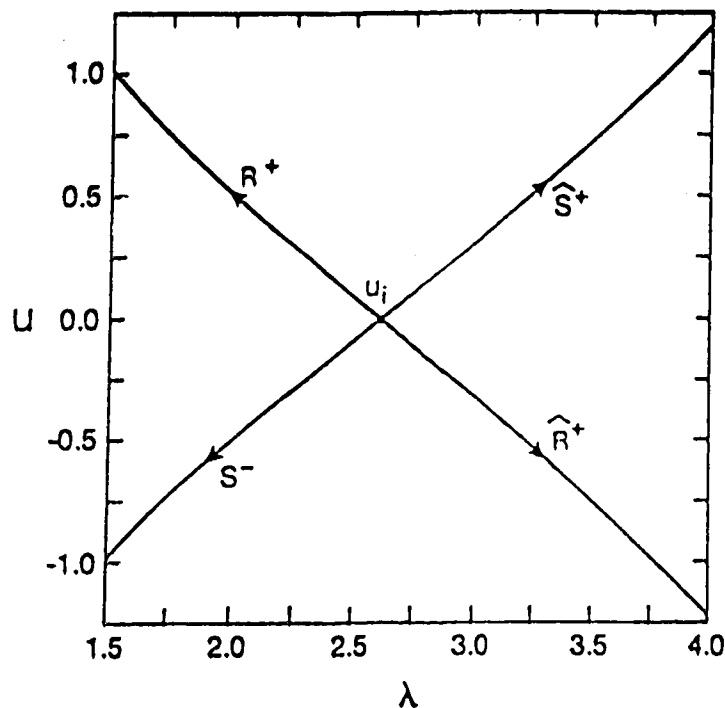


Figure 3.15

For the 2-shock curve we must have  $P'(\lambda) < \sigma < P'(\lambda_\ell)$ . This is satisfied for  $\lambda_{T\ell} < \lambda < \lambda_\ell$  where  $\lambda_{T\ell}$  is the point at which the tangent line  $L$  passing through  $(\lambda_\ell, u_\ell)$  touches the  $P = P(\lambda)$  curve (see Fig. 3.16). Here  $1 < \lambda_{T\ell} < \lambda_i$ . For  $\lambda_{T\ell} < \lambda < \lambda_\ell$  the 2-shock inequality is satisfied. Therefore we connect  $(\lambda_\ell, u_\ell)$  to  $(\lambda, u)$  by a 2-shock curve given by

$$\begin{aligned}
 (3.42) \quad \hat{S}^+ : u - u_\ell &= (\lambda - \lambda_\ell) \sqrt{\frac{P(\lambda) - P(\lambda_\ell)}{\lambda - \lambda_\ell}} \\
 &= \hat{s}^+(\lambda, u_\ell) \quad \lambda_{T\ell} < \lambda < \lambda_i < \lambda_\ell.
 \end{aligned}$$

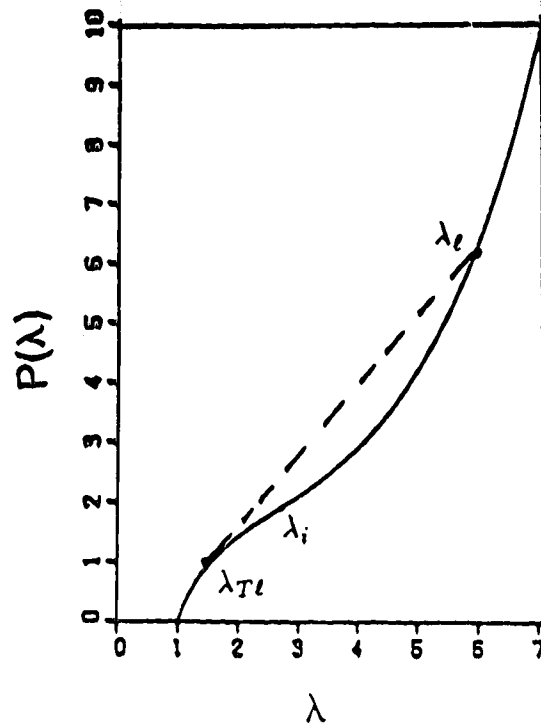


Figure 3.16

At  $\lambda = \lambda_{Te}$  we have  $\sigma(\lambda_{Te}) = P'(\lambda_{Te})$  and  $\sigma(\lambda) < P'(\lambda)$  for  $\lambda < \lambda_{Te}$ . We connect  $(\lambda_{Te}, u_{Te})$  to  $(\lambda, u)$  by 2-rarefaction curve since for  $\lambda < \lambda_{Te}$ ,  $P'(\lambda) > P'(\lambda_{Te})$ . Thus we obtain the  $R^+$  curve given by

$$(3.43) \quad R^+ : u - u_{Te} = - \int_{\lambda_{Te}}^{\lambda} C_L(s) ds = r^+(\lambda, u_{Te}) \quad \lambda < \lambda_{Te} < \lambda_i < \lambda_e.$$

The curves  $\tilde{s}^+$  and  $r^+$  have a 2<sup>nd</sup> order contact at  $\lambda = \lambda_{Te}$  and they are both monotone increasing. The solution to the Riemann problem will then be as shown in Fig. 3.17.

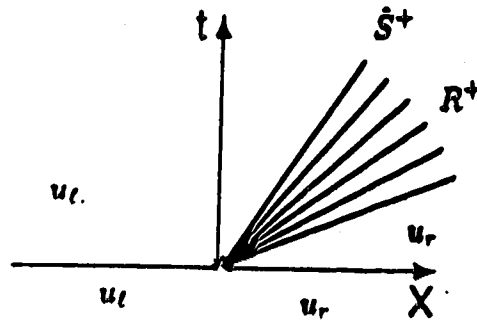


Figure 3.17

Let us now investigate the rarefaction waves. We start with the 1-rarefaction waves where  $P'(\lambda)$  must be less than  $P'(\lambda_\ell)$ . Hence if  $\lambda_i < \lambda < \lambda_\ell$ , we can connect  $(\lambda_\ell, u_\ell)$  to  $(\lambda, u)$  on the right by a 1-rarefaction wave. However for the same reason discussed in the case where  $\lambda_\ell < \lambda_i$  we cannot proceed any further than  $\lambda = \lambda_i$ . Therefore for every  $\lambda < \lambda_i$ , we find a  $\lambda_T$  such that

$$(3.44) \quad \frac{P(\lambda) - P(\lambda_T)}{\lambda - \lambda_T} = P'(\lambda_T)$$

then  $\lambda_i < \lambda_T$  (see Fig. 3.18).

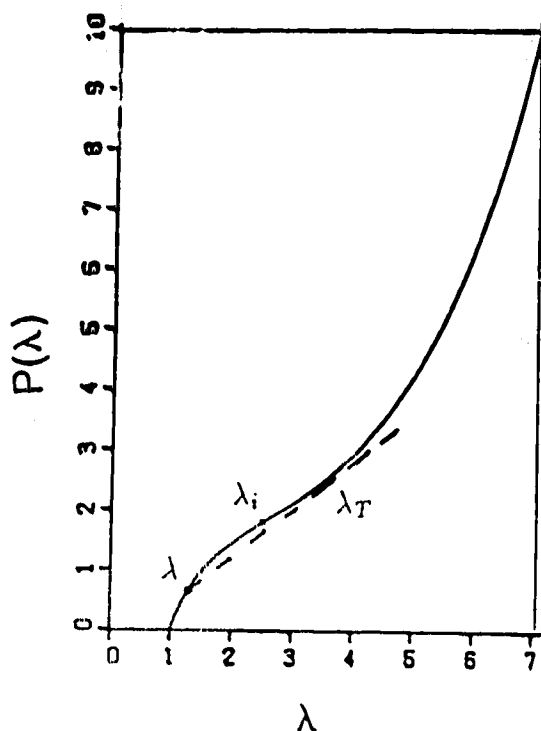


Figure 3.18

If  $\lambda_\ell < \lambda_T$ , the inequality  $P'(\lambda) > \sigma > P'(\lambda_\ell)$  is satisfied. Therefore we connect  $(\lambda_\ell, u_\ell)$  to  $(\lambda, u)$  by a 1-shock curve, which will be given by

$$(3.45) \quad \hat{S}^- : u - u_\ell = (\lambda - \lambda_\ell) \sqrt{\frac{P(\lambda) - P(\lambda_\ell)}{\lambda - \lambda_\ell}} = s^-(\lambda, u_\ell) \quad \lambda < \lambda_i < \lambda_\ell < \lambda_T.$$

However if  $\lambda_\ell > \lambda_T$ , we first connect  $(\lambda_\ell, u_\ell)$  to  $(\lambda_T, u_T)$  by a 1-rarefaction curve given by

$$(3.46) \quad \hat{R}^- : u = u_\ell + \int_{\lambda_\ell}^{\lambda} C(s) ds = \hat{r}^-(\lambda, u_\ell) \quad \lambda_\ell \leq \lambda < \lambda_\ell.$$

Then as in the previous case we connect  $(\lambda_T, u_r)$  to the state  $(\lambda, u)$  by a 1-shock, where  $u$  is given by

$$(3.47) \quad u = u_T + (\lambda - \lambda_T) \sqrt{\frac{P(\lambda) - P(\lambda_T)}{\lambda - \lambda_T}}$$

Then the solution will be as depicted in Figure 3.19.

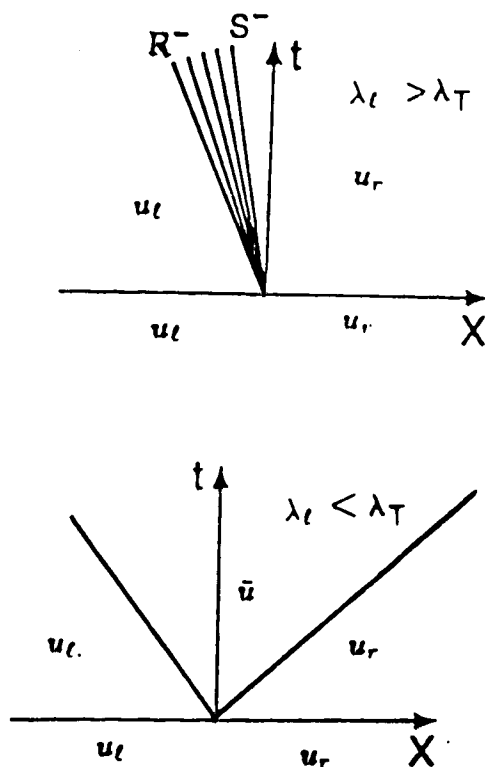


Figure 3.19

Finally we have the 2-rarefaction wave which requires  $P'(\lambda) > P'(\lambda_l)$ . Thus for  $\lambda > \lambda_l$  we connect  $(\lambda_l, u_l)$  to  $(\lambda, u)$  on the right by the 2-rarefaction curve given by

$$\hat{R}^+ : u - u_\ell = - \int_{\lambda_\ell}^{\lambda} C_L(s) ds - r^+(\lambda, u_\ell) \quad \lambda_i < \lambda_\ell < \lambda.$$

This is a monotone increasing curve originating at  $(\lambda_\ell, u_\ell)$  (see Fig. 3.20).

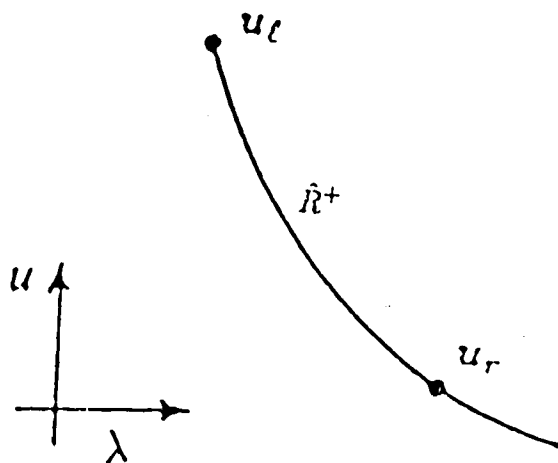


Figure 3.20

As in the previous cases we have four curves which divide the  $(\lambda, u)$  plane as shown in Fig. 3.21.





# CHAPTER IV

## NUMERICAL ALGORITHMS

### AND APPROXIMATE SOLUTION TO THE RIEMANN PROBLEM

#### 4.1. Algorithms for the Exact Solution of the Riemann Problem

ALGORITHM 4.1A: The Riemann problem for the Mooney Rivlin string.

To solve the hyperbolic conservation law,

$$u_t + f_X = 0$$

where  $u = (\lambda, u)^T$  and  $f = (-u, -P)$  subject to the initial condition:

$$u(X, 0) = \begin{cases} u_\ell = (\lambda_\ell, u_\ell)^T & X < 0 \\ u_r = (\lambda_r, u_r)^T & X > 0. \end{cases}$$

Here  $P$  is a convex function given by (3.16).

INPUT:  $u_\ell, u_r$ .

OUTPUT: exact solution  $u_\ell \rightarrow L \rightarrow u_E \rightarrow R \rightarrow u_r$ .

OUTPUT INTERPRETATION: For example if  $L = s^-$  and  $R = r^+$  then we have three constant states  $u_\ell, u_r$  and  $u_E$  separated by a 1-shock and a 2-rarefaction wave (see Fig. 4.1).

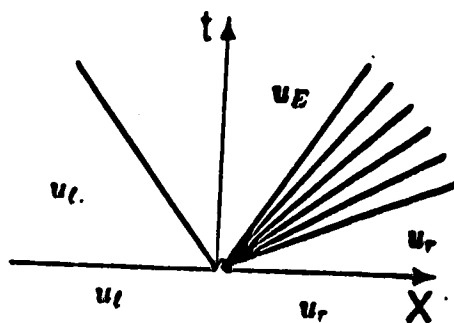


Figure 4.1

STEP 1: Calculating the boundaries of the four regions.

Set

$$UR = u_l + \left| \int_{\lambda_l}^{\lambda_r} C_L(s) ds \right|$$

$$US = u_l - \sqrt{(P(\lambda_r) - P(\lambda_l))(\lambda_r - \lambda_l)}.$$

OUTPUT:  $UR, US$ .

STEP 2: Determining the location of  $u_r$ .

If  $u_r = UR$  then

if  $\lambda_l < \lambda_r$  then  $u_E = (\lambda_r, u_r)^T, L = r^-, R = u_r$

else  $u_E = (\lambda_l, u_l)^T, L = u_l, R = r^+$

Go to Step 6

end if,

else if  $u_r > UR$  then go to Step 3,

if  $u_r = US$  then

if  $\lambda_l < \lambda_r$  then  $u_E = (\lambda_l, u_l)^T, L = u_l, R = s^+$

else  $u_E = (\lambda_r, u_r)^T, L = s^-, R = u_r$

go to Step 6

end if.

else if  $u_r < US$  then go to Step 5,

end if.

else go to Step 4

end if.

end.

STEP 3: Calculation of  $u_E$  in the case where  $u_r$  is in region IV.

Solve for  $u_E = (\lambda_E, u_E)^T$ ,

$$u_E = u_l + \int_{\lambda_l}^{\lambda_E} C_L(s) ds$$

$$u_r = u_E - \int_{\lambda_E}^{\lambda_r} C_L(s) ds$$

$$L = r^-, \quad R = r^+$$

OUTPUT:  $u_E, \lambda_E, L$  and  $R$ .

STEP 4: Calculation of  $u_E$  in the case where  $u_r$  is in region I and region III.

Solve for  $u_E = (\lambda_E, u_E)^T$ ,

if  $\lambda_\ell < \lambda_r$  then

$$u_E = u_\ell + \int_{\lambda_\ell}^{\lambda_E} C_L(s) ds$$

$$u_r = u_E + (\lambda_r - \lambda_E) \sqrt{\frac{P(\lambda_E) - P(\lambda_r)}{\lambda_E - \lambda_r}}$$

$$L = s^-, \quad R = r^+$$

else

$$u_E = u_\ell - (\lambda_E - \lambda_\ell) \sqrt{\frac{P(\lambda_E) - P(\lambda_\ell)}{\lambda_E - \lambda_\ell}}$$

$$u_r = u_E - \int_{\lambda_E}^{\lambda_r} C_L(s) ds$$

$$L = r^-, \quad R = s^+$$

end if.

OUTPUT:  $u_E, \lambda_E, L$  and  $R$ .

STEP 5: Calculation of  $u_E$  in the case where  $u_r$  is in region II.

Solve for  $u^e = (\lambda_E, u_E)^T$

$$u_E = u_\ell + (\lambda_E - \lambda_\ell) \sqrt{\frac{P(\lambda_E) - P(\lambda_\ell)}{\lambda_E - \lambda_\ell}}$$

$$u_r = u_E - (\lambda_r - \lambda_E) \sqrt{\frac{P(\lambda_r) - P(\lambda_E)}{\lambda_r - \lambda_E}}$$

$$L = s^-, \quad R = s^+$$

OUTPUT:  $u_E = (\lambda_E, u_E)^T, L$ , and  $R$ .

**STEP 6: OUTPUT:**

exact solution  $u_l \rightarrow L \rightarrow u_E \rightarrow R \rightarrow u_r.$

stop

end.

**REMARK:**

1. This algorithm furnishes the exact solution for the given Riemann problem with any function  $P$  such that  $P'' < 0$ . If  $P''(\lambda) > 0$  for all  $\lambda$  then to get the exact solution to the Riemann problem, we only need to reverse all the inequalities signs and replace  $US$  by  $US = u_l + \sqrt{(P(\lambda_r) - P(\lambda_l))} (\lambda_r - \lambda_l)$
2. If we want to solve the conservation law (3.9) with a general initial data using Godunov's scheme then the above algorithm gives the value of  $u_{j+\frac{1}{2}}^n$ , where

$$u_l = u_j^n, \quad u_r = u_{j+1}^n, \quad u_{j+\frac{1}{2}}^n = u_E(u_j^n, u_{j+1}^n)$$

where  $u_{j+\frac{1}{2}}^n$  is used in the Godunov's scheme given by

$$u_j^{n+1} = u_j^n + \Delta(f(u_{j+\frac{1}{2}}^n) - f(u_{j-\frac{1}{2}}^n)).$$

**ALGORITHM 4.1B: The Riemann problem for the three-term string.**

To solve the hyperbolic conservation law,

$$u_t + f_x = 0$$

where  $u = (\lambda, u)^T$  and  $f = (-u, -P)^T$  subject to the initial condition

$$u(X, 0) = \begin{cases} u_\ell = (\lambda_\ell, U_\ell)^T & X < 0 \\ u_r = (\lambda_r, U_r)^T & X > 0. \end{cases}$$

Here  $P$  is given by (3.12).

INPUT:  $u_\ell, u_r$  and  $\lambda_i$  where  $\lambda = \lambda_i$  is the only inflection point for the function  $P = P(\lambda)$ . Here we suppose  $\lambda_\ell < \lambda_r$ , and  $\lambda_\ell < \lambda_i$ .

OUTPUT: Exact solution  $u_\ell \rightarrow L \rightarrow u_E \rightarrow R \rightarrow u_r$ , with  $\lambda_T, \lambda_{T\ell}$ .

OUTPUT INTERPRETATION: For example if  $L = r^- s^-$  and  $R = r^+$  then we have three constant states  $u_\ell, u^e, u_r$  separated by 1-rarefaction, 1-shock and 2-rarefaction (see Fig. 4.2).

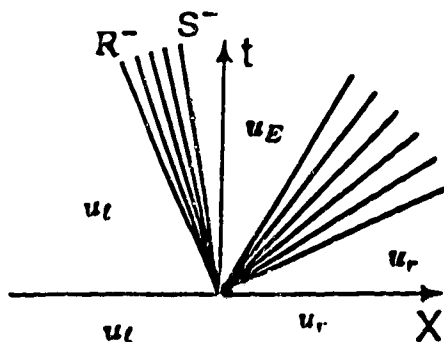


Figure 4.2

**STEP 1: Calculating the boundaries of the four basic regions.**

If  $\lambda_r < \lambda_i$  then let  $\lambda_T = \lambda_{Te} = \lambda_r$ .

else

Calculate the tangents  $\lambda_T$  the tangent to  $\lambda_r$  as shown in Figure (3.11)

where  $\lambda_r$  corresponds to  $\lambda$  there, and  $\lambda_{Te}$  the tangent to  $\lambda_e$  as shown on Figure (3.9).

end if.

if  $\lambda_T > \lambda_e$  then

$$UR = u_e + \int_{\lambda_e}^{\lambda_T} C_L(s) ds + (\lambda_r - \lambda_T) \sqrt{\frac{P(\lambda_r) - P(\lambda_T)}{\lambda_r - \lambda_T}}$$

$$L' = r^- s^-$$

else

$$UR = u_e + (\lambda_e - \lambda_r) \sqrt{\frac{P(\lambda_r) - P(\lambda_e)}{\lambda_r - \lambda_e}}$$

$$L' = s^-$$

end if.

If  $\lambda_{Te} < \lambda_r$  then

$$US = u_e - (\lambda_{Te} - \lambda_e) \sqrt{\frac{P(\lambda_{Te}) - P(\lambda_e)}{\lambda_{Te} - \lambda_e}} - \int_{\lambda_{Te}}^{\lambda_r} C_L(s) ds$$

$$R' = s^+ r^+$$



else

$$US = u_\ell - (\lambda_r - \lambda_\ell) \sqrt{\frac{P(\lambda_r) - P(\lambda_\ell)}{\lambda_r - \lambda_\ell}}$$

$$R' = s^+$$

end if.

end if

OUTPUT:  $UR, US$ .

STEP 2: Determining the location of  $u_r$ .

If  $u_r = UR$  then

$$u_E = (\lambda_r, u_r)^T, L = L', R = u_r$$

go to Step 6

else if  $u_r > UR$  then go to Step 3

if  $u_r = US$  then

$$u_E = (\lambda_\ell, u_\ell)^T, L = u_\ell, R = R'$$

go to Step 6.

else if  $u_r < US$  then go to Step 5

end if

else

go to Step 4

end if

end.

STEP 3: Calculation of  $u_E$  in the case where  $u_r$  is in the IV regions.

Set  $\lambda_E = \lambda_r$ .

\* if  $\lambda_E < \lambda_i$  then

set  $\lambda_m = \lambda_E, \lambda_s = \lambda_r, R = r^+$  and  $L = r^-$

else

Calculate  $\lambda_T$ , the tangent to  $\lambda_E$  as shown on Figure (3.11), where  $\lambda_E$  corresponds to  $\lambda$  there.

if  $\lambda_T < \lambda_\ell$  then

set  $\lambda_m = \lambda_\ell$  and  $L = s^-$

else

set  $\lambda_m = \lambda_T$  and  $L = r^- s^-$

end if.

if  $\lambda_T \leq \lambda_r$  then

set  $\lambda_s = \lambda_r, R = s^+$

else

set  $\lambda_s = \lambda_T, R = s^+ r^+$

end if.

end if.

Then check if the following equations are satisfied,

$$u_E = u_\ell + \int_{\lambda_\ell}^{\lambda_m} C_L(s) ds + (\lambda_E - \lambda_m) \sqrt{\frac{P(\lambda_E) - P(\lambda_m)}{\lambda_E - \lambda_m}}$$

$$u_r = u_E - (\lambda_s - \lambda_E) \sqrt{\frac{P(\lambda_E) - P(\lambda_s)}{\lambda_E - \lambda_s}} - \int_{\lambda_\ell}^{\lambda_r} C_L(s) ds.$$

If not then increase  $\lambda_E$  and go to \*

OUTPUT:  $u_E = (\lambda_E, u_E)^T$ ,  $L, R, \lambda_m$ , and  $\lambda_s$ .

STEP 4: Calculation of  $u_E$  in the case where  $u_r$  is in the I regions.

Set  $\lambda_E = \lambda_\ell$

\* if  $\lambda_E < \lambda_i$  then

set  $\lambda_m = \lambda_e, L = r^-$

Calculate  $\lambda_{T\ell}$  the tangent to  $\lambda_E$  as shown on Figure (3.9) where

$\lambda_E$  corresponds to  $\lambda_\ell$  there.

if  $\lambda_{T\ell} > \lambda_r$  then,

set  $\lambda_s = \lambda_r \quad R = s^+$

else

set  $\lambda_s = \lambda_{T\ell} \quad R = s^+ r^+$

end if

else

set  $\lambda_s = \lambda_E \quad R = r^+$

Calculate  $\lambda_T$  the tangent to  $\lambda_E$  as shown in Figure (3.11) where

$\lambda_E$  corresponds to  $\lambda$  there if  $\lambda_T < \lambda_\ell$  then

set  $\lambda_m = \lambda_\ell, \quad \lambda = s^-$

else

set  $\lambda_m = \lambda_T, \quad \lambda = r^- s^-$

end if

end if

Then check if the following equations are satisfied,

$$u_E = u_\ell + \int_{\lambda_\ell}^{\lambda_m} C_L(s) ds + (\lambda_E - \lambda_m) \sqrt{\frac{P(\lambda_E) - P(\lambda_m)}{\lambda_E - \lambda_m}}$$

$$u_r = u_E - (\lambda_s - \lambda_E) \sqrt{\frac{P(\lambda_E) - P(\lambda_s)}{\lambda_E - \lambda_s}} - \int_{\lambda_s}^{\lambda_r} C_L(s) ds.$$

If not then increase  $\lambda_E$  and go to \*.

OUTPUT:  $u_E = (\lambda_E, u_E)^T, L, R, \lambda_m,$  and  $\lambda_s$ .

STEP 5: Calculation of  $u_E$  in the case where  $u_r$  is in the II regions.

Set  $\lambda_E = \lambda_\ell$

\*  $L = s^-$

Calculate  $\lambda_{T\ell}$ , the tangent to  $L_E$  as shown on Figure (3.9) where

$\lambda_E$  corresponds to  $\lambda_\ell$  there.

if  $\lambda_{T\ell} > \lambda_r$  then

set  $\lambda_s = \lambda_r, \quad R = s^+$

else

set  $\lambda_s = \lambda_{T\ell}, \quad R = s^+ r^+$

end if.

Then check if the following equations are satisfied,

$$u_E = u_\ell + (\lambda_E - \lambda_\ell) \sqrt{\frac{P(\lambda_E) - P(\lambda_\ell)}{\lambda_E - \lambda_\ell}}$$

$$u_r = u_E - (\lambda_s - \lambda_E) \sqrt{\frac{P(\lambda_s) - P(\lambda_E)}{\lambda_s - \lambda_E}} - \int_{\lambda_s}^{\lambda_r} C_L(s) ds.$$

If not then decrease  $\lambda_E$  and go to \*

OUTPUT:  $u_E = (\lambda_E, u_E)^T$ ,  $L$ ,  $R$  and  $\lambda_s$ .

STEP 6: OUTPUT: the exact solution

Stop

end.

REMARK:

1. The algorithm gives the exact solution to the given Riemann problem for the three-term stress-stretch string, if  $\lambda_\ell < \lambda_r$  and  $\lambda_\ell < \lambda_i$ . All the other cases can be done by making simple alterations. For example if  $\lambda_\ell > \lambda_r$  and  $\lambda_r < \lambda_i$  then to get the solution to the Riemann problem, we only need to reverse all the inequalities in this algorithm.
2. Same as Remark 2 in algorithm 4.1.

#### 4.2. An Iterative Riemann Solver

Let  $u_\ell = (\lambda_\ell, u_\ell)^T$  and  $u_r = (\lambda_r, u_r)^T$  be the left and the right states, respectively, in the the Riemann problem for the Mooney-Rivlin string. Then we

construct an iterative approximation to the intermediate state  $u_E = (\lambda_E, u_E)^T$ .

To do this we introduce the following curves:

$$\tilde{S}^+ : u = u_* - (\lambda - \lambda_*) \sqrt{\frac{P(\lambda_*) - P(\lambda)}{\lambda_* - \lambda}} = \tilde{s}^+(\lambda, u_*) \quad \lambda < \lambda_*$$

$$\tilde{S}^- : u = u_* + (\lambda - \lambda_*) \sqrt{\frac{P(\lambda_*) - P(\lambda)}{\lambda_* - \lambda}} = \tilde{s}^-(\lambda, u_*) \quad \lambda > \lambda_*$$

$$\tilde{R}^+ : u = u_* - \int_{\lambda_*}^{\lambda} C_L(s) ds = \tilde{r}^+(\lambda, u_*) \quad \lambda > \lambda_*$$

$$\tilde{R}^- : u = u_* + \int_{\lambda_*}^{\lambda} C_L(s) ds = \tilde{r}^-(\lambda, u_*) \quad \lambda < \lambda_*$$

where  $u_* = (\lambda_*, u_*)^T$  is any point in  $R^2$ ,  $\lambda > 1$ . In the following discussion we shall add a  $*$  suffix to the expansion curves to denote their extension. For example the backward extension of the  $r^-$  curve from  $u_l$  will be denoted by  $r_*^-$  (see Figure (4.3)). Note that from the Schwartz inequality we have,

$$(4.2) \quad \left| \int_{\lambda_*}^{\lambda} C_L(s) ds \right| \leq \sqrt{(P(\lambda) - P(\lambda_*))(\lambda - \lambda_*)},$$

so that the shock curves lie in the convexity of the rarefaction curves (see Figure 4.3).

If  $u_r$  lies on any of the standard shock or rarefaction curves then, as discussed in Chapter III, we do not have any intermediate states. Therefore, let us suppose that  $u_r$  lies in one of the four regions.

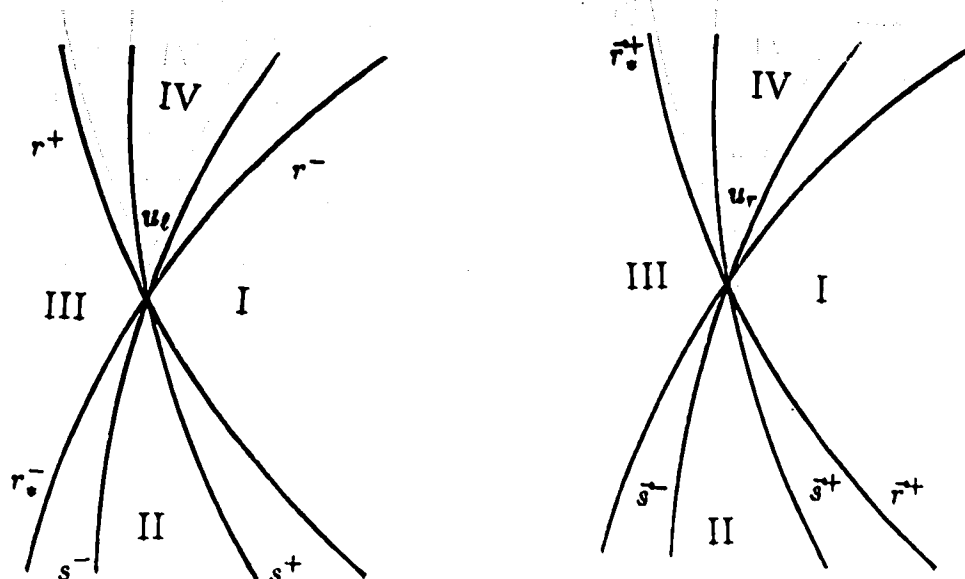


Figure 4.3

### Region I:

Suppose  $u_r$  lies in region I. As a first approximation of  $u_E$  we take  $\bar{u}_1$  which is the value of  $u$  at the intersection of the  $r^-$  curve starting at  $u_l$  and the  $\bar{r}_*^+$  curve starting at  $u_r$  (see Figure 4.4). Then

$$(4.3) \quad u_1 = \frac{1}{2}(u_l + u_r + \int_{\lambda_l}^{\lambda_r} C_L(s) ds).$$

Note that  $\bar{u}_1$  will always be smaller than  $u_E$  since the  $\bar{r}_*^+$  curve emanating at  $u_r$  lies below the  $\bar{s}^+$  curve emanating at  $u_r$  (see Figure 4.4). In order to get a first approximation  $\bar{\lambda}_1$  of  $\lambda_E$  we look at the straight line joining  $u_r$  and  $u_{\ell r 1} = (\lambda_{\ell 1}, u_{\ell r 1})^T$ , where  $\lambda_{\ell 1}$  is the value of  $\lambda$  at the

intersection of the tangent line at  $u_\ell$  and the horizontal line  $u = \bar{u}_1$ , and  $u_{\ell r1}$  is the value of  $u$  on the  $\bar{s}^+$  curve emanating at  $u_r$ . Then,

$$(4.4) \quad \lambda_{\ell1} = \lambda_\ell + \frac{\bar{u}_1 - u_\ell}{C_L(\lambda_\ell)}$$

$$u_{\ell r1} = u_r + (\lambda_r - \lambda_{\ell1}) \sqrt{\frac{P(\lambda_r) - P(\lambda_{\ell1})}{\lambda_r - \lambda_{\ell1}}}.$$

Note that since  $\bar{u}_1 \leq u_E$ , we have  $\lambda_E \geq \lambda_{\ell1}$ . Note also that since the  $\bar{s}^+$  curve is starlike about the point  $u_r$ , the straight line does not cross it at any point between  $\lambda_{\ell1}$  and  $\lambda_r$  (see Figure 4.4). Therefore if we let  $\bar{\lambda}_1$  be the value of  $\lambda$  where the straight line meets the horizontal line  $u = \bar{u}_1$ , then we obtain,

$$(4.5) \quad \bar{\lambda}_1 = \lambda_r + \bar{u}_1 - u_r \sqrt{\frac{\lambda_r - \lambda_{\ell1}}{P(\lambda_r) - P(\lambda_{\ell1})}}$$

Then the starlike property and the fact that at  $u_r$ , the slope of the  $\bar{r}_*^+$  is the same as the slope of the  $\bar{s}^+$  curve, gives us  $\bar{\lambda}_1 \geq \lambda_E$  (see Figure 4.4).

Now let  $u_{r1} = (\bar{\lambda}_1, u_{r1})^T$  denote the point on the  $\bar{s}^+$  curve given by

$$(4.6) \quad u_{r1} = u_r + (\lambda_r - \bar{\lambda}_1) \sqrt{\frac{P(\lambda_r) - P(\bar{\lambda}_1)}{\lambda_r - \bar{\lambda}_1}}.$$

and let  $u_{\ell1} = (\lambda_{\ell1}, u_{\ell1})^T$  denote the point on the  $r^-$  curve through  $u_\ell$  given by

$$(4.7) \quad u_{\ell1} = u_\ell + \int_{\lambda_\ell}^{\lambda_{\ell1}} C_L(s) ds.$$



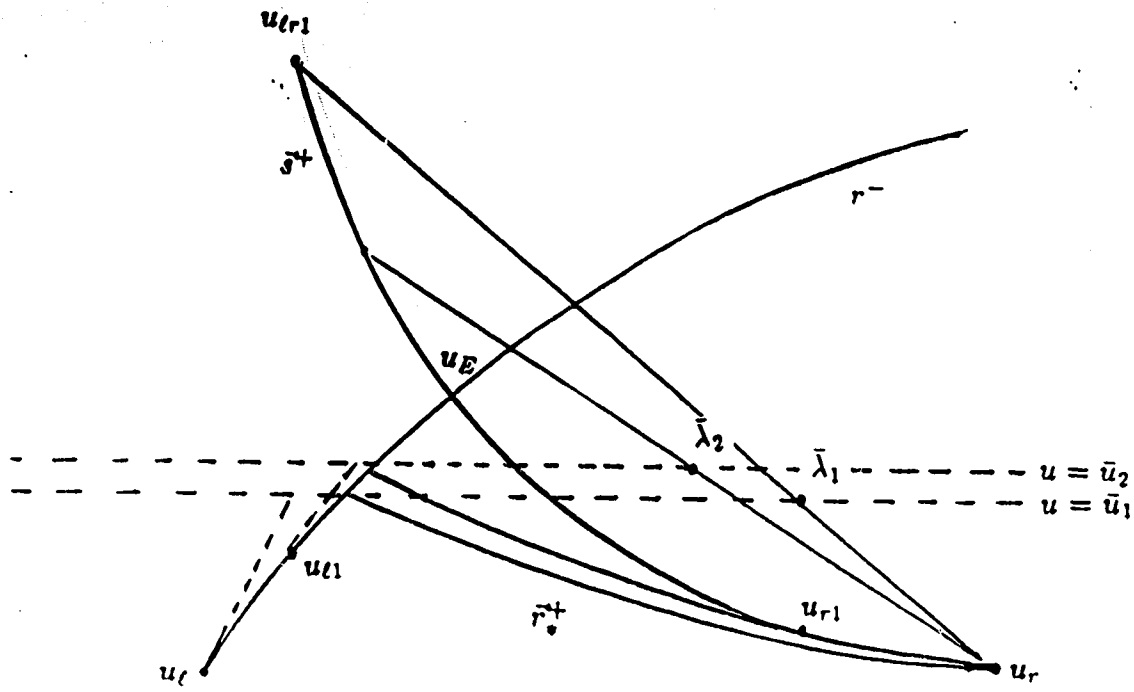


Figure 4.4

As a second approximation of  $u_E$  we shall take  $u_2$  which is the value of  $u$  where the  $r^-$  curve starting at  $u_{l1}$  meets the  $r^+$  curve starting at  $u_{r1}$ . Again  $u_2 \leq u_E$  since the  $r^+$  curve starting at  $u_{r1}$  lies below the  $s^+$  curve starting at  $u_r$ . To see this let  $(\lambda, u_Q)^T$  be a point on the  $r^+$  curve and let  $(\lambda, u_{Q1})^T$  be a point on the  $s^+$  curve, then for fixed  $\lambda_r$  and  $\lambda_{r1}$ ,

$$h(\lambda) = u_{Q1} - u_Q = \sqrt{P(\lambda_r) - P(\lambda)}(\lambda_r - \lambda)$$

(4.8a)

$$- \sqrt{P(\lambda_r) - P(\lambda_{r1})}(\lambda_r - \lambda_{r1}) + \int_{\lambda_{r1}}^{\lambda} C_L(s) ds$$

and

$$(4.8) \quad h'(\lambda) = \sqrt{P'(\lambda)} - \left( \frac{P'(\lambda)}{2\sqrt{\frac{P(\lambda_r) - P(\lambda)}{\lambda_r - \lambda}}} + \frac{\sqrt{\frac{P(\lambda_r) - P(\lambda)}{\lambda_r - \lambda}}}{2} \right).$$

Using the inequality  $a + b \geq 2\sqrt{a} \sqrt{b}$  with  $b = P'(\lambda) > 0$  and  $a = \frac{P(\lambda_r) - P(\lambda)}{\lambda_r - \lambda} > 0$  we get  $h'(\lambda) \leq 0$ . But  $h(\lambda_{r1}) = 0$  so that for any  $\lambda < \lambda_{r1}$ ,  $h(\lambda) = u_{Q1} - u_Q \geq 0$ .

In order to get the second approximation  $\bar{\lambda}_2$  of  $\lambda_E$  we let  $u_{\ell r2} = (\lambda_{\ell2}, u_{\ell r2})^T$  be the point on the  $\bar{s}^+$  curve where  $\lambda_{\ell1}$  is the value of  $\lambda$  where the tangent line at  $u_{\ell1}$  meets the horizontal line  $u = \bar{u}_2$ , and  $u_{\ell r2}$  is the value of  $u$  on the  $\bar{s}^+$  curve emanating at  $u_r$ . Then

$$(4.9) \quad \begin{aligned} \lambda_{\ell2} &= \lambda_{\ell1} + \frac{\bar{u}_1 - u_{\ell1}}{C_L(\lambda_{\ell1})} \\ u_{\ell r2} &= u_r + (\lambda_r - \lambda_{\ell2}) \sqrt{\frac{P(\lambda_r) - P(\lambda_{\ell2})}{\lambda_r - \lambda_{\ell2}}}. \end{aligned}$$

As before  $\bar{\lambda}_E \geq \lambda_E$  since  $\bar{u}_1 \leq u_E$  and  $\lambda_{\ell1} \leq \lambda_E$ . Since  $\lambda_{\ell1} \geq \lambda_{\ell2}$ ,  $\bar{\lambda}_2$  is a better approximation to  $\lambda_E$  than  $\bar{\lambda}_1$ .

This procedure can be applied successively producing points  $u_{\ell i} = (\lambda_{\ell i}, u_{\ell i})^T$  on the  $r^-$  curve where,

$$(4.10) \quad \begin{aligned} \lambda_{\ell i} &= \lambda_{\ell(i-1)} + \frac{\bar{u}_i - u_{\ell(i-1)}}{C_L(\lambda_{\ell(i-1)})} \\ u_{\ell i} &= u_{\ell(i-1)} + \int_{\lambda_{\ell(i-1)}}^{\lambda_{\ell i}} C_L(s) ds, \end{aligned}$$

and producing points  $u_{\ell r i}$  on the  $\tilde{s}^+$  curve where

$$(4.11) \quad u_{\ell r i} = u_r - (\lambda_{\ell i} - \lambda_r) \sqrt{\frac{P(\lambda_{\ell i}) - P(\lambda_r)}{\lambda_{\ell i} - \lambda_r}}.$$

Then the  $i^{\text{th}}$  approximation  $\bar{u}_i$  to  $u_E$  is defined as the value of  $u$  where the  $r^-$  curve starting at  $u_{\ell i}$  meets the  $\tilde{r}_i^+$  curve starting at  $u_{r(i-1)}$  where,

$$(4.12) \quad u_{r i} = u_r + (\lambda_r - \bar{\lambda}_i) \sqrt{\frac{P(\lambda_r) - P(\bar{\lambda}_i)}{\lambda_r - \bar{\lambda}_i}}.$$

Here  $\bar{\lambda}_i$  is the  $i^{\text{th}}$  approximation to  $\lambda_E$  is the value of  $\lambda$  where the straight line joining the point  $u_{\ell r i}$  and  $u_r$  meets the horizontal line  $u = \bar{u}_i$ .

Then the  $i^{\text{th}}$  approximation  $\bar{u}_i = (\bar{\lambda}_i, \bar{u}_i)^T$  of  $u_E$  is given by,

$$(4.13) \quad \bar{u}_i = \frac{1}{2}(u_{\ell(i-1)} + u_{r(i-1)}) + \int_{\lambda_{\ell(i-1)}}^{\lambda_{r(i-1)}} C_L(s) ds$$

and

$$\bar{\lambda}_i = \lambda_r - (\bar{u}_i - u_r) \sqrt{\frac{\lambda_r - \lambda_{\ell i}}{P(\lambda_r) - P(\lambda_i)}}.$$

## Region II:

Let us now suppose that  $u_r$  is in region II. Here we have three different cases to consider.

CASE 1:  $\lambda_{\ell} < \lambda_r$ .

Let  $u_{r*} = (\lambda_\ell, u_{r*})^T$  denote the point on the  $\bar{s}^+$  curve starting at  $u_r$  where,

$$(4.15) \quad u_{r*} = u_r + \sqrt{(P(\lambda_r) - P(\lambda_\ell))(\lambda_r - \lambda_\ell)}.$$

Then as a first approximation of  $u_E$  take  $u_1$  which is the value of  $u$  at the intersection of the  $r_-^-$  curve starting at  $u_\ell$  and  $\bar{r}_+^+$  curve starting at  $u_{r*}$  (see Figure 4.5).

$$(4.16) \quad \bar{u}_1 = (u_\ell + u_{r*})/2.$$

Note that the value of  $u$  where the  $\bar{s}^+$  curve starting at  $u_r$  meets the  $s^-$  curve starting at  $u_\ell$  is equal to  $\bar{u}_1$ . Therefore  $\bar{u}_1 \leq u_E$  since the  $\bar{s}^+$  curve starting at  $u_*$  lies below the  $\bar{s}^+$  curve starting at  $u_r$  (see Figure 4.5). To see this let  $(\lambda, u_P)^T$  be a point on the  $\bar{s}^+$  curve starting at  $u_*$  and let  $(\lambda, u_{P1})^T$  be a point on the  $\bar{s}^+$  curve starting at  $u_r$  (see Figure 4.5). Then for fixed  $\lambda_*$  and  $\lambda_r$  we have

$$(4.17) \quad \begin{aligned} h_1(\lambda) = u_{P1} - u_P = & \sqrt{P(\lambda) - P(\lambda_r)}(\lambda - \lambda_r) - \sqrt{(P(\lambda_\ell) - P(\lambda_r))(\lambda_\ell - \lambda_r)} \\ & - \sqrt{(P(\lambda) - P(\lambda_\ell))(\lambda - \lambda_\ell)} \end{aligned}$$

and

(4.18)

$$\begin{aligned}
h'_1 &= \left( \frac{P'(\lambda)}{2\sqrt{\frac{P(\lambda)-P(\lambda_\ell)}{\lambda-\lambda_\ell}}} + \frac{\sqrt{\frac{P(\lambda)-P(\lambda_\ell)}{\lambda-\lambda_\ell}}}{2} \right) - \left( \frac{P'(\lambda)}{2\sqrt{\frac{P(\lambda)-P(\lambda_r)}{\lambda-\lambda_r}}} + \frac{\sqrt{\frac{P(\lambda)-P(\lambda_r)}{\lambda-\lambda_r}}}{2} \right) \\
&= \frac{\left( \sqrt{\frac{P(\lambda)-P(\lambda_\ell)}{\lambda-\lambda_\ell}} \sqrt{\frac{P(\lambda)-P(\lambda_r)}{\lambda-\lambda_r}} - P'(\lambda) \right) \left( \sqrt{\frac{P(\lambda)-P(\lambda_\ell)}{\lambda-\lambda_\ell}} - \sqrt{\frac{P(\lambda)-P(\lambda_r)}{\lambda-\lambda_r}} \right)}{2\sqrt{\frac{P(\lambda)-P(\lambda_\ell)}{\lambda-\lambda_\ell}} \sqrt{\frac{P(\lambda)-P(\lambda_r)}{\lambda-\lambda_r}}}
\end{aligned}$$

which gives us  $h'_1(\lambda) \leq 0$  for  $\lambda \leq \lambda_\ell$  (see Figure 3.2 for the  $P, \lambda$  relation).

But  $h_1(\lambda_\ell) = 0$  and hence  $h_1(\lambda) \geq 0$  for  $\lambda \geq \lambda_\ell$ .

Now let  $u_{r\ell 1} = (\lambda_{r1}, u_{r1})^T$  be a point on the  $\bar{s}^+$  curve starting at  $u_r$ , where  $\lambda_{r1}$  is the value of  $\lambda$  at the intersection of the tangent line at  $u_r$ , and the horizontal line  $u = \bar{u}_1$  (see Figure 4.5). Then

$$\lambda_{r1} = \lambda_\ell - \frac{(\bar{u}_1 - u_{r*})}{C_L(\lambda_\ell)} \quad (4.19)$$

$$u_{r1} = u_r + \sqrt{(P(\lambda_r) - P(\lambda_{r1}))(\lambda_r - \lambda_{r1})}.$$

As a first approximation of  $\lambda_E$  take  $\bar{\lambda}_1$  which is the value of  $\lambda$  where the line joining  $u_{r1}$  and  $u_r$  meets the horizontal line  $u = \bar{u}_1$  (see Figure 4.5). Then

$$\bar{\lambda}_1 = \lambda_r - (\bar{u}_1 - u_r) \sqrt{\frac{\lambda_r - \lambda_{r1}}{P(\lambda_r) - P(\lambda_{r1})}}. \quad (4.20)$$

As in Region I, since  $\bar{u}_1 \leq u_E$  we have  $\lambda_E \geq \lambda_{r1}$ , and by the starlike property of the  $\bar{s}^+$  curve about  $u_r$  we also have  $\bar{\lambda}_1 \geq \lambda_E$  (see Figure 4.5).

If  $\lambda_r$  is sufficiently close to  $\lambda_E$ , there may be a possibility that  $\bar{\lambda}_1$  lies to the right of  $\lambda_r$ . A large number of numerical experiments were performed to check if such a case can occur. In all the experiments done this case failed to occur. If by any chance such a case occurred we can continue with the iteration by taking a  $\bar{\lambda}_1$  sufficiently close to the left of  $\lambda_r$  so that it does not lie to the left of  $\lambda_E$ . However since in this case  $\lambda_r$  is very close to  $\lambda_E$  any standard techniques for solving nonlinear equations will converge very fast, if  $\lambda_r$  is used as an initial approximation. Therefore in our discussion we shall see that  $\bar{\lambda}_1$  lies on the right of  $\lambda_r$ .

In order to get a second approximation let  $u_{r+1} = (\bar{\lambda}_1, u_{r+1})^T$  be the point on the  $s^+$  curve starting at  $u_r$  where,

$$(4.21) \quad u_{r+1} = u_r + \sqrt{(P(\lambda_r) - P(\bar{\lambda}_1))(\lambda_r - \bar{\lambda}_1)}$$

and let  $u_{\ell+1} = (\bar{\lambda}_1, u_{\ell+1})^T$  be the point on the  $s^-$  curve starting at  $u_\ell$  where,

$$(4.22) \quad u_{\ell+1} = u_\ell - \sqrt{(P(\lambda_\ell) - P(\bar{\lambda}_1))(\lambda_\ell - \bar{\lambda}_1)}.$$

As a second approximation of  $u_E$  take  $\bar{\lambda}_2$  which is the value of  $\lambda$  where the horizontal line  $u = \bar{u}_2$  meets the straight line joining  $u_{r2} = (\lambda_{r2}, u_{\ell+2})^T$  and  $u_r$ . Here  $\lambda_{r2}$  is the maximum of  $\lambda_{r1}$  and the value of  $\lambda$  where

The tangent line at  $u_{r+1}$  meets the horizontal line  $u = \bar{u}_2$  and  $u_{lr2}$  is the tangent line at  $u_{r+1}$  meets the horizontal line  $u = \bar{u}_2$  and  $u_{lr2}$  is a point on the  $s^+$  curve starting at  $u_r$ ,

$$\lambda_{r2} = \max(\lambda_{r1}, \bar{\lambda}_1 - (\bar{u}_2 - u_{r+1})/C_L(\bar{\lambda}_1))$$

(4.24)

$$u_{lr2} = u_r + \sqrt{(P(\lambda_r) - P(\lambda_{r2}))(\lambda_r - \lambda_{r2})}.$$

Then

$$\bar{\lambda}_2 = \lambda_r - (\bar{u}_2 - u_r) \sqrt{\frac{\lambda_r - \lambda_{r2}}{P(\lambda_r) - P(\lambda_{r2})}}$$

(4.25)

so we will repeat the above procedure producing points  $u_{r+i}$  and  $u_{l+i}$  converging to  $u_E$ . Let us now show that the  $i^{\text{th}}$  approximation  $\bar{u}_i$  of  $u_E$  is monotonically increasing from  $\bar{u}_1$  to  $u_E$ . To do this we will show that for a given  $\lambda_\ell, \lambda_r, u_\ell, u_r$  the function  $h_2(\bar{\lambda}_{i-1}) = u_E - \bar{u}_i$  with  $\bar{\lambda}_0 = \lambda_\ell$  is an increasing function. Then

$$\begin{aligned} h_2(\bar{\lambda}_{i-1}) &= \frac{u_r - u_\ell + 2\sqrt{(P(\lambda_r) - P(\lambda_E))(\lambda_r - \lambda_E)}}{2} \\ &+ \frac{\sqrt{(P(\lambda_\ell) - P(\lambda_{i-1}))(\lambda_\ell - \bar{\lambda}_{i-1})}}{2} \\ &- \frac{\sqrt{(P(\lambda_r) - P(\lambda_{i-1}))(\lambda_r - \bar{\lambda}_{i-1})}}{2} \end{aligned}$$

(4.26)

and

$$\begin{aligned}
 h'_2(\bar{\lambda}_{i-1}) &= \frac{1}{4} \left( \frac{P'(\bar{\lambda}_{i-1})}{\sqrt{\frac{P(\lambda_r) - P(\bar{\lambda}_{i-1})}{\lambda_r - \bar{\lambda}_{i-1}}}} + \sqrt{\frac{P(\lambda_r) - P(\bar{\lambda}_{i-1})}{\lambda_r - \bar{\lambda}_{i-1}}} \right) \\
 &\quad - \frac{1}{4} \left( \frac{P'(\bar{\lambda}_{i-1})}{\sqrt{\frac{P(\lambda_\ell) - P(\bar{\lambda}_{i-1})}{\lambda_\ell - \bar{\lambda}_{i-1}}}} + \sqrt{\frac{P(\lambda_\ell) - P(\bar{\lambda}_{i-1})}{\lambda_\ell - \bar{\lambda}_{i-1}}} \right) \\
 &= \left( \sqrt{\frac{P(\lambda_r) - P(\bar{\lambda}_{i-1})}{\lambda_r - \bar{\lambda}_{i-1}}} - \sqrt{\frac{P(\lambda_\ell) - P(\bar{\lambda}_{i-1})}{\lambda_\ell - \bar{\lambda}_{i-1}}} - P'(\bar{\lambda}_{i-1}) \right) \\
 &\quad \times \left( \sqrt{\frac{P(\lambda_r) - P(\bar{\lambda}_{i-1})}{\lambda_r - \bar{\lambda}_{i-1}}} - \sqrt{\frac{P(\lambda_\ell) - P(\bar{\lambda}_{i-1})}{\lambda_\ell - \bar{\lambda}_{i-1}}} \right)
 \end{aligned}$$

which by the  $P - \lambda$  relation gives us  $h'_2(\lambda_{i-1}) \geq 0$ . Therefore since  $\bar{\lambda}_i$  are decreasing monotonically  $h_2(\bar{\lambda}_{i-1})$  will decrease monotonically hence as  $i$  increases  $\bar{u}_i$  goes from  $\lambda_\ell$  to  $\lambda_E$  (see Figure 4.5).

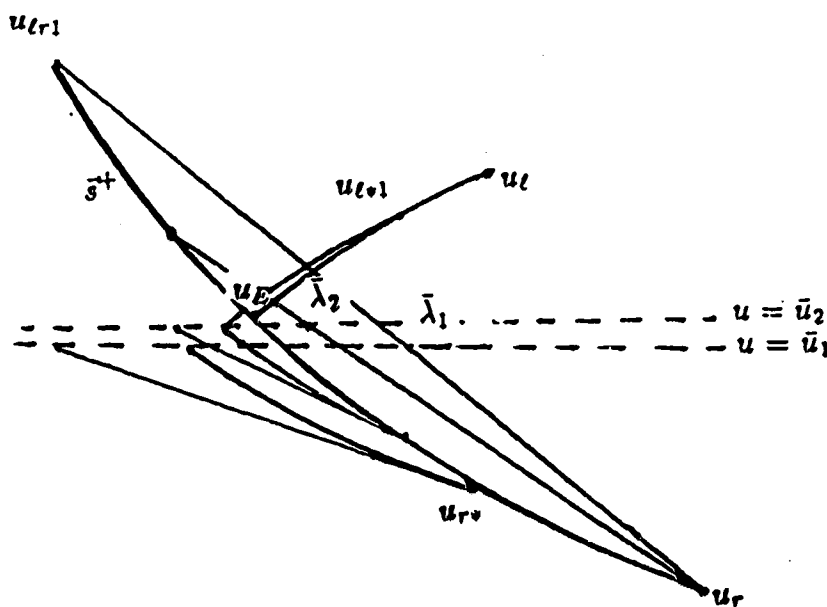


Figure 4.5

CASE 2:  $\lambda_\ell = \lambda_r$ ,



This case is a special case of Case 1. Here the above procedure is used with  $u_r$  as  $u_{re}$ . Note that in this case (4.16) gives the exact value of  $u_E$  already at the first approximation (see Fig. 4.6).

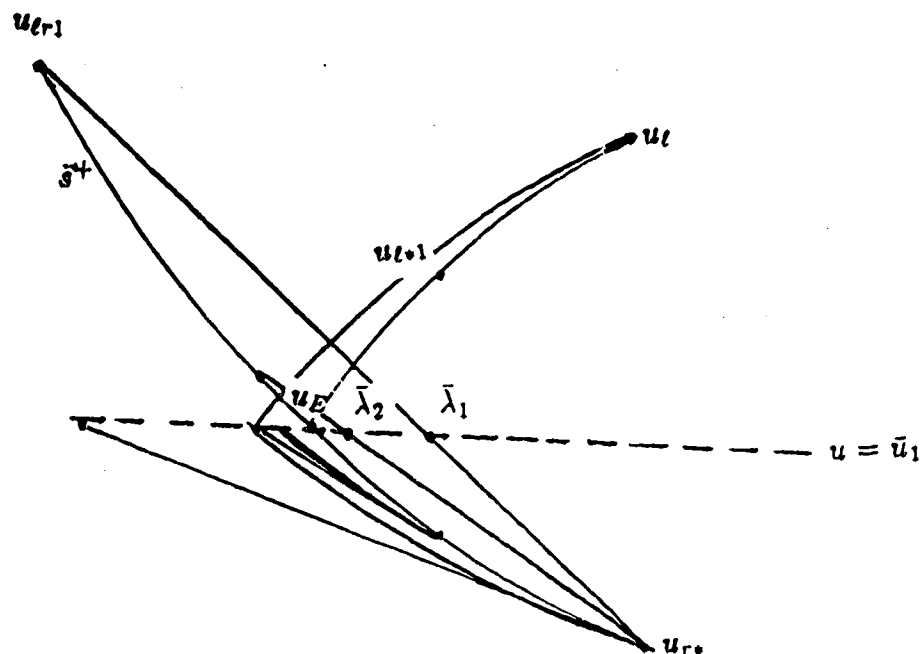


Figure 4.6

CASE 3:  $\lambda_l > \lambda_r$

This case is very similar to Case 1. We need only to interchange the role of  $u_l$  and  $u_r$  (see Figure 4.7). The analysis can be done the same way as in Case 1. The appropriate equations involved in the calculation are given in Algorithm 4.2. Note that in this case  $u_i$  is monotonically decreasing.

### Region III

Region III is very similar to Region I and the method used there can be used with obvious modifications (see Figure 4.7). The equations involved in the calculations are given in Step 3 of Algorithm 4.2.

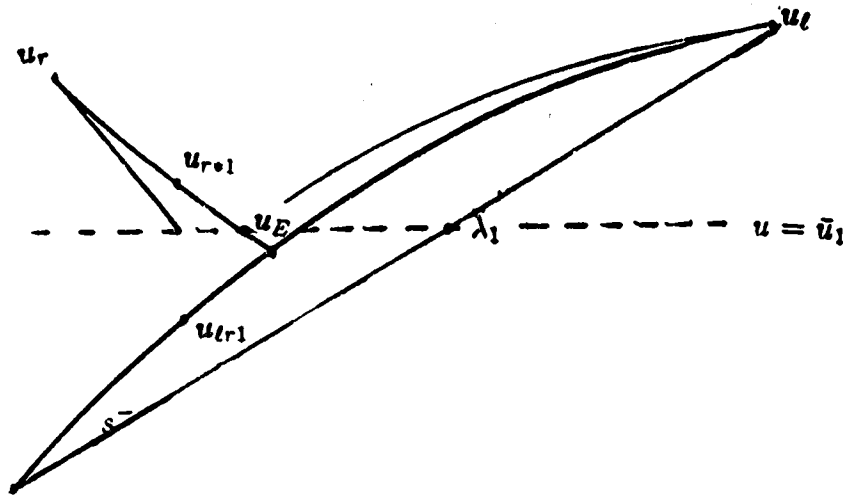


Figure 4.8

#### Region IV

Ideas similar to the one used in Region II can be employed for Region IV, however Region IV is very simple since we have convex and concave curves involved. Therefore we use a simple linear approximation as discussed below.

If  $u_r$  is in Region IV then the exact value  $u_E$  is given by

$$(4.28) \quad u_E = (u_l + u_r + \int_{\lambda_l}^{\lambda_r} C_L(s) ds) / 2.$$

Suppose  $\lambda_l \geq \lambda_r$  then as a first approximation  $\bar{\lambda}_1$  of  $\lambda_E$  we take the value of  $\lambda$  where the tangent line at  $u_l$  meets the horizontal line  $u = u_E$  (see Figure 4.9). Then

$$(4.29) \quad \bar{\lambda}_1 = \lambda_l + \frac{u_E - u_l}{C_L(\lambda_l)}.$$

As a second approximation of  $\lambda_E$  we take  $\bar{\lambda}_2$  the value of  $\lambda$  at the intersection of  $u = u_E$  and the tangent line at  $u_{\ell 1} = (\bar{\lambda}_1, u_{\ell 1})^T$  where  $u_{\ell 1}$  is a point on the  $r^-$  curve starting at  $u_\ell$  with

$$(4.30) \quad u_{\ell 1} = u_\ell + \int_{\lambda_\ell}^{\bar{\lambda}_1} C_L(s) ds$$

because of convexity this procedure is monotone increasing and it will converge to  $\lambda_E$ . If  $\lambda_\ell < \lambda_r$  then we do the above procedure starting with the point  $u_* = (\lambda_r, u_*)^T$  instead of  $u_\ell$ , where

$$(4.31) \quad u_* = u_\ell + \int_{\lambda_\ell}^{\lambda_r} C_L(s) ds.$$

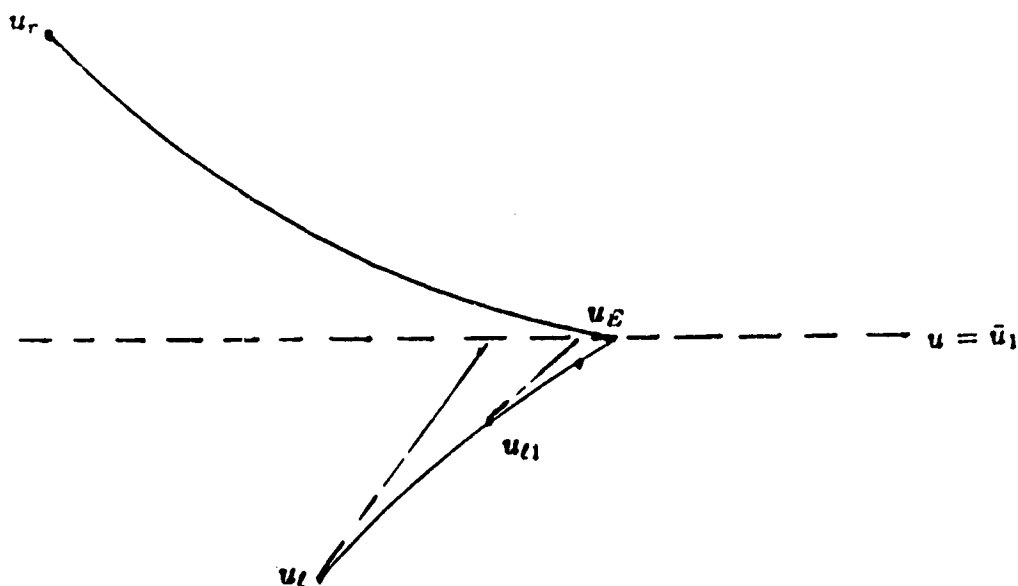


Figure 4.9

**ALGORITHM 4.2.** The iterative Riemann solver for the Mooney Rivline string.

This algorithm is the same as Algorithm 4.1 with Step 3 to Step 5 altered as follows.

STEP 3: Calculation of  $u_E$  when  $u_r$  is in Region IV.

$$\text{Set } u_E = (u_\ell + u_r + \int_{\lambda_\ell}^{\lambda_r} C_L(s) ds) / 2$$

If  $\lambda_\ell \geq \lambda_r$  then

$$\lambda_{*1} = \lambda_\ell$$

$$u_{*1} = u_\ell$$

else

$$u_{*1} = u_\ell + \int_{\lambda_\ell}^{\lambda_r}$$

$$\lambda_{*1} = \lambda_r$$

end if

$$\lambda_{*2} = \lambda_{*1} + \frac{u_E - u_{*1}}{C_L(\lambda_{*1})}$$

\* if  $|\lambda_{*1} - \lambda_{*2}| \geq \text{tolerance (input)}$  then

$$u_{*1} = u_{*1} + \int_{\lambda_{*1}}^{\lambda_{*2}}$$

$$\lambda_{*1} = \lambda_{*2}$$

$$\lambda_{*2} = \lambda_{*1} + \frac{u_E - u_{*1}}{C_L(\lambda_{*1})}$$

go to \*

else

$$\lambda_E = \lambda_{*2}$$

end if

STEP 4: Calculation of  $u_E$  when  $u_r$  is in Region I and Region III.

If  $\lambda_\ell < \lambda_r$  then (we have Region I)

Set:

$$\lambda_{E1} = \lambda_r$$

$$\lambda_{\bullet 1} = \lambda_\ell$$

$$u_{\bullet \ell 1} = u_\ell$$

$$u_{\bullet r 1} = u_r$$

$$u_{E1} = \frac{1}{2}(u_{\bullet \ell 1} + u_{\bullet r 1} + \int_{\lambda_{\bullet 1}}^{\lambda_{E1}})$$

$$\lambda_{\bullet 2} = \lambda_{\bullet 1} + \frac{(u_{E1} - u_{\bullet \ell 1})}{C_L(\lambda_{\bullet 1})}$$

$$u_{r\ell 1} = u_r + \sqrt{(P(\lambda_r) - P(\lambda_{\bullet 2}))(\lambda_r - \lambda_{\bullet 2})}$$

$$\lambda_{E2} = \lambda_r - (u_{E1} - u_r) \sqrt{\frac{P(\lambda_r) - P(\lambda_{\bullet 2})}{\lambda_r - \lambda_{\bullet 2}}}$$

if  $|\lambda_{E2} - \lambda_{E1}| \geq \text{tolerance}$  then

Set

$$u_{\bullet \ell 1} = u_{\bullet \ell 1} + \int_{\lambda_{\bullet 1}}^{\lambda_{\bullet 2}} C_L(s) ds$$

$$\lambda_{\bullet 1} = \lambda_{\bullet 2}$$

$$u_{\bullet r 1} = u_r + \sqrt{(P(\lambda_r) - P(\lambda_{E1}))(\lambda_r - \lambda_{E1})}$$

$$u_{E1} = \frac{1}{2}(u_{\bullet \ell 1} + u_{\bullet r 1} + \int_{\lambda_{\bullet 1}}^{\lambda_{E1}} C_L(s) ds)$$

$$\lambda_{\bullet 2} = \lambda_{\bullet 1} + \frac{(u_{E1} - u_{\bullet \ell 1})}{C_L(\lambda_{\bullet 1})}$$

$$u_{r\ell 1} = u_r + \sqrt{(P(\lambda_r) - P(\lambda_{*2}))(\lambda_r - \lambda_{*2})}$$

$$\lambda_{E2} = \lambda_r - (u_{E1} - u_r) \sqrt{\frac{\lambda_r - \lambda_{*2}}{P(\lambda_r) - P(\lambda_{*2})}}$$

else

$$\lambda_E = \lambda_{E2}$$

$$u_E = u_{E1}$$

end if

OUTPUT:  $u_E, \lambda_E, L = r^-$  and  $R = s^+$

else we have Region III.

Set

$$\lambda_{E1} = \lambda_\ell$$

$$\lambda_{*1} = \lambda_r$$

$$u_{* \ell 1} = u_\ell$$

$$u_{* r 1} = u_r$$

$$u_{E1} = \frac{1}{2}(u_{* \ell 1} + u_{* r 1} + \int_{\lambda_{E1}}^{\lambda_{*1}})$$

$$\lambda_{*2} = \lambda_{*1} + \frac{(u_{E1} - u_{r1})}{C_L(\lambda_{*1})}$$

$$u_{r\ell 1} = u_\ell - \sqrt{(P(\lambda_\ell) - P(\lambda_{*2}))(\lambda_\ell - \lambda_{*2})}$$

$$\lambda_{E2} = \lambda_\ell + (u_{E1} - u_\ell) \sqrt{\frac{P(\lambda_\ell) - P(\lambda_{*2})}{\lambda_\ell - \lambda_{*2}}}$$

if  $|\lambda_{E2} - \lambda_{E1}| \geq \text{tolerance}$  then

Set

$$u_{\bullet\ell 1} = u_{\bullet\ell 1} - \int_{\lambda_{\bullet 1}}^{\lambda_{\bullet 2}} C_L(s) ds$$

$$\lambda_{\bullet 1} = \lambda_{\bullet 2}$$

$$u_{\bullet\ell 1} = u_\ell - \sqrt{(P(\lambda_\ell) - P(\lambda_{\bullet 2}))(\lambda_\ell - \lambda_{\bullet 2})}$$

$$u_{E1} = \frac{1}{2}(u_{\bullet\ell 1} + u_{\bullet r 1} + \int_{\lambda_{E1}}^{\lambda_{\bullet 1}} C_L(s) ds)$$

$$\lambda_{\bullet 2} = \lambda_{\bullet 1} + \frac{u_{E1} - u_{\bullet r 1}}{C_L(\lambda_{\bullet 1})}$$

$$u_{r\ell 1} = u_\ell - \sqrt{(P(\lambda_\ell) - P(\lambda_{\bullet 2}))(\lambda_\ell - \lambda_{\bullet 2})}$$

$$\lambda_{E2} = \lambda_\ell + (u_{E1} - u_\ell) \sqrt{\frac{P(\lambda_\ell) - P(\lambda_{\bullet 2})}{\lambda_\ell - \lambda_{\bullet 2}}}$$

else

$$\lambda_E = \lambda_{E2}$$

$$u_E = u_{E1}$$

end if

OUTPUT:  $u_E, \lambda_E, L = s^-, R = R^+$

end if

STEP 5: Calculation of  $u_E$  in the case where  $u_r$  is in Region II.

if  $\lambda_\ell \leq \lambda_r$  then

$$u_{\bullet r 1} = u_r + \sqrt{(P(\lambda_r) - P(\lambda_\ell))(\lambda_r - \lambda_\ell)}$$

$$u_{\bullet\ell 1} = u_\ell$$



$$u_{E1} = (u_{\ell 1} + u_{r1})/2$$

$$\lambda_{\bullet 1} = \lambda_{\ell}$$

$$\lambda_{\bullet 2} = \lambda_{\bullet 1} - \frac{(u_{E1} - u_{r1})}{C_L(\lambda_{\bullet 1})}$$

$$u_{r\ell 1} = u_r + \sqrt{(P(\lambda_r) - P(\lambda_{\bullet 2}))(\lambda_r - \lambda_{\bullet 2})}$$

$$\lambda_{E1} = \lambda_r + u_{r\ell 1} - u_r \sqrt{\frac{\lambda_{\bullet 2} - \lambda_r}{P(\lambda_{\bullet 2}) - P(\lambda_r)}}$$

if  $\lambda_{E1} > \lambda_{\ell}$  then this is the rare case described earlier and since in this case  $\lambda_{\ell}$  is very close to  $\lambda_E$  then any of the suggested ideas can be used.

if  $\lambda_{\bullet 1} - \lambda_{E1} \geq \text{tolerance}$  then

$$\lambda_{\bullet 1} = \lambda_{E1}$$

$$u_{r1} = u_r + \sqrt{(P(\lambda_r) - P(\lambda_{\bullet 1}))(L_r - \lambda_{\bullet 1})}$$

$$u_{\ell 1} = u_{\ell} - \sqrt{(P(\lambda_{\ell}) - P(\lambda_{\bullet 1}))(\lambda_{\ell} - \lambda_{\bullet 1})}$$

$$u_{E1} = (u_{\ell 1} + u_{r1})/2$$

$$\lambda_{\bullet 3} = \lambda_{\bullet 1} - (u_{E1} - u_{r1})/C_L(\lambda_{\bullet 1})$$

$$\lambda_{\bullet 2} = \max(\lambda_{\bullet 2}, \lambda_{\bullet 3})$$

$$u_{r\ell 1} = u_r + \sqrt{(P(\lambda_r) - P(\lambda_{\bullet 2}))(\lambda_r - \lambda_{\bullet 2})}$$

$$\lambda_{E1} = \lambda_r + (u_{r\ell 1} - u_r) \sqrt{\frac{\lambda_r - \lambda_{\bullet 2}}{P(\lambda_r) - P(\lambda_{\bullet 2})}}$$

else

$$\lambda_E = \lambda_{E1} \quad u_E = u_{E1}$$

end if

OUTPUT:  $\lambda_E, u_e, L = s^-, R = s^+$

else if  $(\lambda_\ell > \lambda_r)$  then

$$\lambda_{\bullet 1r}$$

$$u_{\bullet \ell 1} = u_\ell - \sqrt{(P(\lambda_\ell) - P(\lambda_r))(\lambda_\ell - \lambda_r)}$$

$$u_{\bullet r 1} = u_r$$

$$u_{E1} = (u_{\bullet \ell 1} + u_{\bullet r 1})/2$$

$$\lambda_{\bullet 2} = \lambda_{\bullet 1} + (u_{E1} - u_{\bullet \ell 1})/C_L(\lambda_{\bullet 1})$$

$$u_{r \ell 1} = u_\ell - \sqrt{(P(\lambda_\ell) - P(\lambda_{\bullet 2}))(\lambda_\ell - \lambda_{\bullet 2})}$$

$$\lambda_{E1} = \lambda_\ell + (u_{r \ell 1} - u_\ell) \sqrt{\frac{P(\lambda_\ell) - P(\lambda_{\bullet 2})}{\lambda_\ell - \lambda_{\bullet 2}}}$$

Again if  $\lambda_{E1} > \lambda_r$  then  $\lambda_E$  is very close to  $\lambda_r$  so that use techniques described earlier.

if  $\lambda_{\bullet 1} - \lambda_{E1} > \text{tolerance}$  then

$$\lambda_{\bullet 1} = \lambda_{E1}$$

$$u_{\bullet \ell 1} = u_\ell - \sqrt{(P(\lambda_\ell) - P(\lambda_{\bullet 1}))(\lambda_\ell - \lambda_{\bullet 1})}$$

$$u_{\bullet r 1} = u_r + \sqrt{(P(\lambda_r) - P(\lambda_{\bullet 1}))(\lambda_r - \lambda_{\bullet 1})}$$

$$u_{E1} = (u_{\bullet \ell 1} + u_{\bullet r 1})/2$$

$$\lambda_{\bullet 3} = \lambda_{\bullet 1} + (u_{E1} - u_{\bullet \ell 1})/C_L(\lambda_{\bullet 1})$$

$$\lambda_{\bullet 2} = \max(\lambda_{\bullet 2}, \lambda_{\bullet 3})$$

$$u_{r\ell 1} = u_\ell - \sqrt{(P(\lambda_\ell) - P(\lambda_{*2}))(\lambda_\ell - \lambda_{*2})}$$

$$\lambda_{E1} = \lambda_\ell + (u_{r\ell 1} - u_\ell) \sqrt{\frac{P(\lambda_\ell) - P(\lambda_{*2})}{\lambda_\ell - \lambda_{*2}}}$$

else

$$\lambda_E = \lambda_{E1}, \quad u_E = u_{E1}$$

end if

OUTPUT:  $\lambda_E, u_E, L = s^-, R = s^+$

□

In Chapter V we will look at specific examples in order to illustrate the convergence of this technique.

### 4.3. Algorithm for Solving Initial, Boundary Value Problems by Godunov's Scheme.

ALGORITHM 4.2A:

To solve the hyperbolic conservation law,

$$u_t + f_X = 0$$

where  $u = (\lambda, u)^T$  and  $f = (-u, -P)$  subject to the initial condition,

$$u(X, 0) = F(X), \quad 0 < X < L,$$

and one of the following three boundary conditions.

$$\text{BV1: } u(0, t) = g(t), \quad u(L, t) = h(t), \quad t > 0,$$

$$\text{BV2: } \lambda(0, t) = g(t), \quad u(L, t) = h(t), \quad t > 0,$$

$$\text{BV3: } \frac{du}{dt}(0, t) = \gamma P(\lambda(0, t)), \quad u(L, t) = h(t), \quad t > 0.$$

Here  $\gamma$  is a given parameter.

INPUT:

1.  $F, h$  and  $g$  for BV1 and BV2;  $F, h, \gamma$  for BV3.
2.  $N$  the number of iterations.
3.  $dX$  the space step size.
4.  $L$
5.  $dt$  is chosen at each iteration  $n$  so that  $\lambda_{\max}^n$  the maximum value of  $\lambda$  will satisfy the CFL condition given by (2.38). Therefore we take

$$dt = \frac{dX}{(2\sqrt{P(\lambda_{\max}^n)})}.$$

OUTPUT:

$$u_j^N \text{ for } j = 0 \text{ to } M \text{ where } M = \frac{L}{dX} \text{ with}$$

OUTPUT INTERPRETATION:

$$u_j^N = u(jdX, Ndt) \text{ for } j = 0 \text{ to } M$$

STEP 1:

Initialize,

For  $j = 1$  to  $M - 1$

$$\text{set} \quad u_j^0 = \frac{1}{dX} \int_{X_{j-\frac{1}{2}}}^{X_{j+\frac{1}{2}}} F(s) ds$$

$$\text{where} \quad X_{j+1/2} = (j + \frac{1}{2})dX.$$

Set  $u_0^0 = F(0)$  and  $u_M^0 = F(MdX)$ .

OUTPUT:  $u_j^0$  for  $j = 0$  to  $M$ .

End.

For  $n = 1$  to  $N$  do Step 2 and Step 3 below.

OUTPUT: APPROXIMATE SOLUTION  $u_j^N$  for  $j = 0$  to  $M$ .

STEP 2:

Construction of  $u_j^{n+1}$ ,

Given  $u_j^n$  for  $j = 0$  to  $M$  we construct  $u_j^{n+1}$  as follows.

For each  $j = 0$  to  $M - 1$  do the following.

Set  $u_l = u_j$  and  $u_r = u_{j+1}$

evaluate  $u_{j+1/2}$  which is the value of the intermediate state for the

Riemannian problems, using Algorithm 4.1 or Algorithm 4.2. If  $1 < j <$

$M$  then

$$\text{set} \quad u_j^{n+1} = u_j^n + \frac{dt}{dX} (f_{j+\frac{1}{2}}^n - f_{j-\frac{1}{2}}^n)$$

$$\text{where} \quad f_{j+\frac{1}{2}}^n = f(u_{j+\frac{1}{2}}^n).$$

End if

**Continue.**

**OUTPUT:**

$$u_j^{n+1} \quad \text{for } j = 1 \quad \text{to} \quad M - 1.$$

**STEP 3:**

Computations at the boundaries,

1. At  $X = 0$  we have

$$u_0^{n+1} = u_0^n + \frac{dt}{dX} (f_1^n - f_{\frac{1}{2}}^n)$$

a) If  $u$  is specified at  $X = 0$ , i.e. if we have BVI then we proceed as follows.

Solve for  $P_{-1/2}^n$  from,

$$u_0^{n+1} = u_0^n + \frac{dt}{dX} (-P_{1/2}^n - (-P_{-1/2}^n)) \quad \text{where } u_0^n = g(udt)$$

Solve for  $u_{-1/2}^n$  as follows.

if  $\lambda_{-1/2}^n > \lambda_0^n$  then

$$u_0^n = u_{-1/2}^n - \int_{\lambda_{-1/2}^n}^{\lambda_0^n} c_L(s) ds$$

else

$$u_0^n = u_{-1/2}^n - (\lambda_0^n - \lambda_{-1/2}^n) \sqrt{\frac{P(\lambda_0^n) - P(\lambda_{-1/2}^n)}{\lambda_0^n - \lambda_{-1/2}^n}}$$

end if.

Set  $\lambda_0^{n+1} = \lambda_0^n + \frac{dt}{dX}(-u_{1/2}^n - (-u_{-1/2}^n))$ .

b) If  $\lambda$  is specified at  $X = 0$ , i.e. if we have BV1 then we proceed as follows.

Solve for  $u_{-1/2}^n$  from,

$$\lambda_0^{n+1} = \lambda_0^n + \frac{dt}{dX}(-u_{1/2}^n - (-u_{-1/2}^n)) \quad \text{where} \quad \lambda_0^n = g(ndt).$$

Solve for  $\lambda_{-1/2}^n$  as follows

if  $u_{-1/2}^n > u_0^n$  then

$$u_0^n = u_{-1/2}^n - \int_{\lambda_{-1/2}^n}^{\lambda_0^n}$$

$$\text{else } u_0^n = u_{-1/2}^n - (\lambda_0^n - \lambda_{-1/2}^n) \sqrt{\frac{P(\lambda_{-1/2}^n) - P(\lambda_0^n)}{\lambda_{-1/2}^n - \lambda_0^n}}$$

end if.

Set  $u_0^{n+1} = u_0^n + \frac{dt}{dX}(-P(\lambda_{1/2}^n) - (-P(\lambda_{-1/2}^n)))$ .

(c) If a mass is attached on  $X = 0$  end then we have BV3. In this case we approximate the boundary by the finite difference

$$\frac{u_0^{n+1} - u_0^\lambda}{dt} = \gamma P_0^n \quad \text{where} \quad P_0^n = P(\lambda(0, t)).$$

Then proceed as case (a) where  $u$  is specified by

$$u_0^{n+1} = u_0^n + dt\gamma P_0^n.$$

2) At  $X = L$  we have

$$u_M^{n+1} = u_m^n + \frac{dt}{dX} (f_{M+\frac{1}{2}}^n - f_{M-\frac{1}{2}}^n)$$

Solve for  $P_{M+\frac{1}{2}}$  from

$$u_M^{n+1} = u_M^n + \frac{dt}{dX} (-P_{M+\frac{1}{2}}^n - (-P_{M-\frac{1}{2}}^n)) \quad \text{where} \quad u_M^n = h(Mdt).$$

Solve for  $u_{M+1/2}^n$  as follows.

If  $\lambda_{M+1/2}^n > \lambda_M^n$  then

$$u_M^n = u_{M+\frac{1}{2}}^n - \int_{\lambda_{M+\frac{1}{2}}^n}^{\lambda_M^n} c_L(s) ds$$

else

$$u_M^n = u_{M+\frac{1}{2}}^n + (\lambda_M^n - \lambda_{M+\frac{1}{2}}^n) \sqrt{\frac{P(\lambda_M^n) - P(\lambda_{M+\frac{1}{2}}^n)}{\lambda_M^n - \lambda_{M+\frac{1}{2}}^n}}$$

end if

OUTPUT:

$$u_0^{n+1} \quad \text{and} \quad u_M^{n+1}.$$

End

In Chapter II we have seen that shocks that occur between mesh points are spread in many more than two intervals. Therefore the Artificial Compression method with an automatic switch was introduced. The following algorithm of



ACM is to be implemented as a subroutine of the main program 4.3a, and must be called at the end of Step 3.

**ALGORITHM 4.3B:**

To apply the artificial compression  $C'_\Delta$  given by (2.67)

$$u_j^{n+1} = u_j^n - \frac{\hat{\lambda}}{2}(\theta_{j+\frac{1}{2}} \hat{G}_{j+\frac{1}{2}}^n - \theta_{j-\frac{1}{2}} \hat{G}_{j-\frac{1}{2}}^n).$$

**INPUT:**

$$u_j^{n+1}, u_j^n \text{ for all } j, \varepsilon, \beta(u) \text{ and } \hat{\lambda}$$

here  $\beta$  is a scalar function of the vector  $u$  as described in Chapter II.

We shall take  $\beta(u) = \lambda$  in this case and  $\varepsilon > 0$  is chosen so that any variation of  $|\beta(u)|$  which is less than  $\varepsilon$  is negligible. In this algorithm we shall take  $\varepsilon = 0.01 \max |\lambda_j^{n+1} - \lambda_{j-1}^{n+1}|$ .

**OUTPUT:**

$$u_j^{n+1} \text{ for all } j.$$

**STEP 1:**

Computation of  $\hat{G}_{j-1/2}^n$  and  $\theta_{j-1/2}^n$

For  $j = 0$  to  $M - 1$  do the following.

Set

$$\Delta \lambda_j = \lambda_{j+1}^{n+1} - \lambda_j^{n+1}$$

$$\Delta u_j = u_{j+1}^{n+1} - u_j^{n+1}$$

$$\Delta \sigma(u_j^n) = \sigma(u_{j+1}^n) - \sigma(u_j^n)$$

if  $j > 0$  then

$$\hat{\gamma}_j = \min[|\Delta \lambda_j|, \Delta \lambda_{j-1} \operatorname{sgn} \Delta \lambda_j],$$

$$\gamma_j = \min[|\Delta u_j|, \Delta u_{j-1} \operatorname{sgn} \Delta u_j],$$

$$\alpha_j = \min[\hat{\gamma}_j, \gamma_j]$$

Reset

$$\alpha_j = \max[0, \alpha_j]$$

set

$$\hat{g}_j = \alpha_j [u_{j+1}^{n+1} - u_{j-1}^{n+1}]$$

if

$$\Delta \beta(u_j^n) - \Delta \beta(u_{j-1}^n) > \varepsilon$$

then

$$\text{Set } \theta_j = \frac{\Delta\beta(u_j^n) - \Delta\beta(u_{j-1}^n)}{\Delta\beta(u_j^n) + \Delta\beta(u_{j-1}^n)}$$

else

$$\text{set } \theta_j = 0$$

end if

if  $j > 1$  then

$$\text{set } \hat{G}_{j-\frac{1}{2}}^n = g_{j-1} + g_j - |g_{j-1}| \operatorname{sgn}(u_{j+1}^{n+1} - u_{j-1}^{n+1})$$

$$\theta_{j-\frac{1}{2}}^n = \max(\theta_j, \theta_{j-1})$$

End if

End if.

OUTPUT: Continue

STEP 2:

Application of  $C'_\Delta$ ,

$$\theta_{j-\frac{1}{2}}, \hat{G}_{j-\frac{1}{2}} \quad \text{for } j = 2 \text{ to } M-1$$

For  $j = 2$  to  $M-2$ .

Reset

$$u_j^{n+1} = u_j^n - \frac{\hat{\Lambda}}{2} (\theta_{j+\frac{1}{2}}^n \hat{G}_{j+\frac{1}{2}}^n - \theta_{j-\frac{1}{2}}^n \hat{G}_{j-\frac{1}{2}}^n)$$

Continue.

OUTPUT:

$u_j^{n+1}$  for  $j = 0$  to  $M$ .

End.

## CHAPTER V

### NUMERICAL ILLUSTRATIONS AND CONCLUSION

#### 5.1. Numerical Illustrations

Before solving some physical problems with general initial, boundary conditions, the method discussed in the preceding chapters have been tested using several simple initial value problems. The solution of one of such tests is illustrated in Figure 5.0 where the solution of (2.4) subjected to the following initial condition is shown.

$$u(X, 0) = \begin{cases} (1.5, 0)^T & X < 0 \\ (2.0, 0.0)^T & X > 0. \end{cases}$$

The calculation was done using Godunov's scheme given by Algorithm 4.3a. The single dotted line shows the solution with compression, the heavy line shows the solution without compression and the double dotted line shows the exact solution. Clearly the solution is in close agreement with the exact solution. In all the other examples considered similar results were found.

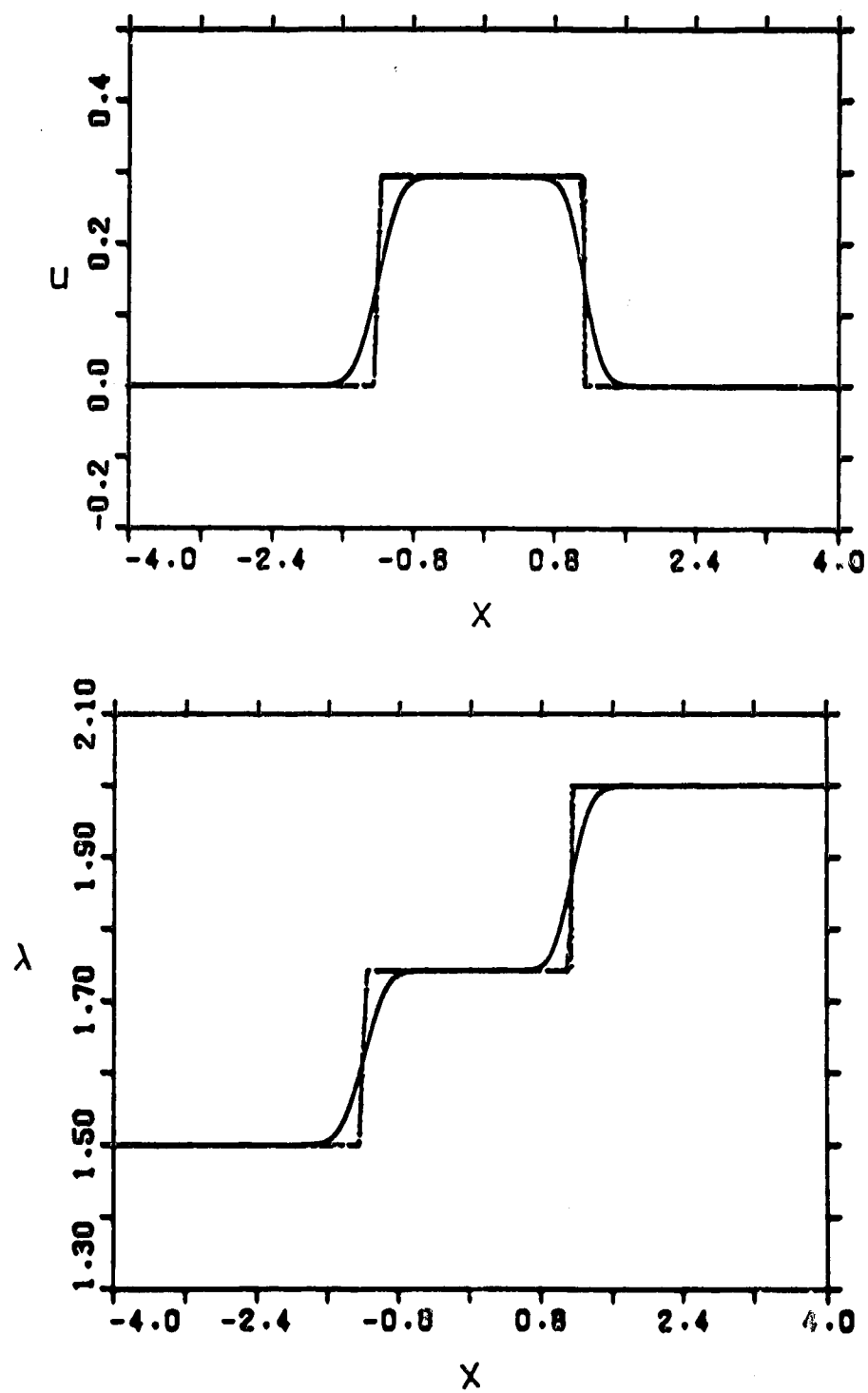


Fig. 5.0

We shall now look at numerical experiments carried out on a number of sample physical problems with general initial, boundary conditions. For the examples discussed below we use Algorithm 4.3a with the exact solution to the successive Riemann-problems given by Algorithm 4.1a and 4.1b, as a Riemann solver. In the algorithm a fixed time step chosen to satisfy the CFL condition was used, however, in order to reduce the computation time this was replaced by the variable time step as described in Algorithm 4.3a. The algorithm with the variable time step has proven to speed up the calculation considerably and it gives the same solution as the fixed time step.

In the following we employ Lagrangian coordinates and the non-dimensional form of the equations (3.9b). The unstretched string has length  $L_0$  and in nondimensional form we take it to lie along the  $x$  axis  $0 \leq x \leq L_0/L$ .

As a first example consider a Neo-Hookean string,  $P(\lambda) = \lambda - \lambda^{-2}$ ;  $C_L^2 = \frac{dP}{d\lambda} = 1 + 2\lambda^{-3}$ , lying along the  $x$  axis with

$$(5.1) \quad \lambda(x, 0) = \lambda_0, \quad u(x, 0) = 0, \quad 0 \leq x \leq \frac{L}{L_0},$$

subject to boundary conditions

$$(5.2) \quad \begin{aligned} u(0, t) &= g(t), \\ u\left(\frac{L_0}{L}, t\right) &= 0, \end{aligned}$$

where we take

$$(5.3) \quad g(t) = F_0 \sin(\omega t), \quad 0 \leq t \leq \frac{\pi}{\omega}$$

and zero otherwise. Before reflection, elementary characteristic theory implies that the positive characteristics are straight lines

$$(5.4) \quad \begin{aligned} x &= C(\hat{\lambda}(\tau))(t - \tau), & 0 \leq \tau \leq \frac{\pi}{\omega} \\ \hat{\lambda}(\tau) : \int_{\lambda_0}^{\hat{\lambda}(\tau)} C_L(s) ds &= -g(\tau), \end{aligned}$$

where  $\tau$  is a parameter,  $\tau(0, t) = t$  and  $\hat{\lambda}(\tau) = \lambda_0$  otherwise.

The envelopes of the characteristics are then given by

$$(5.5) \quad \begin{aligned} t &= \tau + C \frac{dC}{d\tau}, \\ X &= C(t - \tau), \end{aligned}$$

where

$$(5.8) \quad \frac{dC}{d\tau} = - \frac{dC}{d\lambda} (\hat{\lambda}(\tau)) g'(\tau) / C(\hat{\lambda}(\tau))$$

It is then clear that  $\hat{\lambda}(\tau)$  cannot decrease to 1 if

$$(5.7) \quad (\lambda_0 - 1)C_L(\lambda_0)/F_0 > 1,$$

so that the string does not go into compression at the left boundary. Further since

$$(5.8) \quad \frac{dt}{d\tau} = 4(1 - \hat{\lambda}^3)/3 + \hat{\lambda}^4 C_L^3 \sin \omega t / 3 \cos^2 \omega t,$$

for the  $g(t)$  considered the first breakdown does not occur on the front  $X = C_L(X_0)t$  but at an interior point where  $\frac{dt}{d\tau} = 0$ . A shock thus occurs before



reflection if breakdown point on the front is less than  $L_0/L$ . This is so if

$$(5.9) \quad X_B = C_L^4(\lambda_0)\lambda_0^4/3\omega F_0 < L_0/L.$$

To illustrate this case we shall take  $\lambda_0 = 2$ ,  $F_0 = 1$ ,  $\omega = 8$  and  $L = L_0/2$ . Fig. 5.1 shows the solutions at  $T = 1.45$  of the Godonov's scheme without artificial compression. In this figure the result obtained using the numerical algorithm 4.3a is compared to that obtained using the exact characteristic theory where the lower envelope of the positive characteristic has been used in the exact calculation. If the scale is magnified it can be shown that the discontinuity actually occurs behind the leading front.

If a positive shock reflects from the right hand boundary then we have

$$(5.10) \quad (\lambda_I - \lambda_{II})(P(\lambda_I) - P(\lambda_{II})) = (\lambda_{II} - \lambda_{III})(P(\lambda_{II}) - P(\lambda_{III}))$$

$$\lambda_I > \lambda_{II} > \lambda_{III}$$

where  $\lambda_I$  is the stretch ahead of the positive shock (that is essentially the initial stretch),  $\lambda_{II}$  is that behind it and ahead of the negative shock, and  $\lambda_{III}$  is the stretch behind the negative reflected shock. Thus if  $\lambda_I = 2$ , then  $\lambda_{III}$  will fall to 1 and the string goes into compression on reflection  $\lambda_{II} \simeq 1.44$  to 1.45. This is the case for the above example and it is not taken to reflection. If the amplitude is taken as 0.5 this does not occur and the solutions just before breakdown occurred and after reflection is shown in Fig. 5.2. Fig. 5.2a shows the solution at  $t = 1.64$  obtained using the exact characteristic theory. After the shock has occurred, Algorithm 4.3a is employed

with  $dX = 0.04$  and  $\tau = 0.01$  so that the CFL condition is satisfied. After each time step the Artificial Compression subroutine 4.3b with the parameters  $\beta(u) = \lambda$  and  $\epsilon^n = 0.01 \max_j |\Delta_{j+\frac{1}{2}}^n \beta^n|$  is called to sharpen possible discontinuities. We observe that the solution is oscillation free and that the discontinuities are very sharp.

The same problem is next considered for the s-shaped stress-stretch relation given by (3.12).  $\lambda_i = 2.642$  is again the value of the stretch at the inflection point, and we take an initial stretch  $\lambda_0 > \lambda_i$ . Referring to Fig. (3.2) it is clear that as  $\lambda$  decreases from  $\lambda_0$  an expansion wave propagates, and if  $\lambda$  does not fall below  $\lambda_i$  then as  $\lambda$  again increases to  $\lambda_0$  the positive characteristics converge to possibly form a shock (see equation 5.5). If  $\lambda$  decreases below  $\lambda_i$  then the positive characteristics converge first diverge, then converge and as  $\lambda$  increases diverge and converge again. In this case one expects two shocks to form. Up to the formation of the first shock, exact characteristic theory can be employed and the numerical algorithm 4.a thereafter. To illustrate this later case we shall consider the above example with  $F_0 = 0.75$  and  $\lambda_0 = 3.2$  and the other parameters as before. Fig. 5.3a shows the solution at  $t = 2.24$  obtained using the exact characteristic theory. After the first shock has occurred Algorithm 4.3a is employed with the Artificial Compression subroutine 4.3b. The parameters used in the algorithm is the same as before, and the solutions at different times is shown in Fig. 5.3b to d.

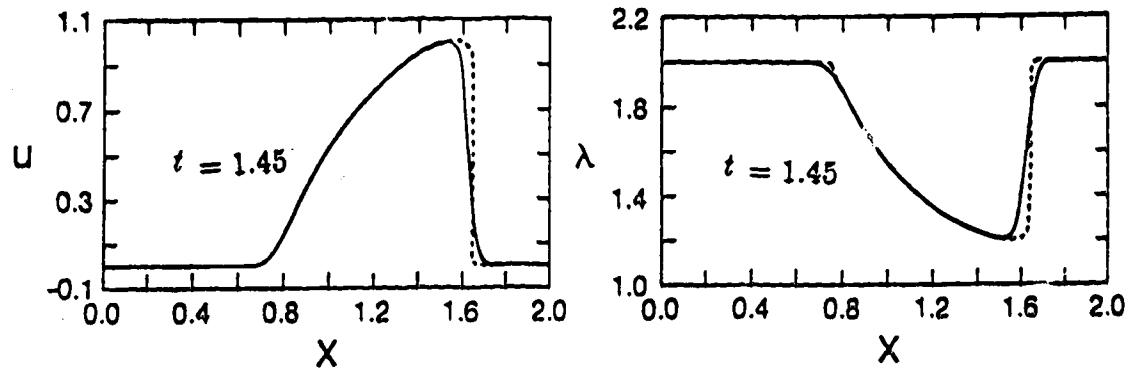


Fig. 5.1

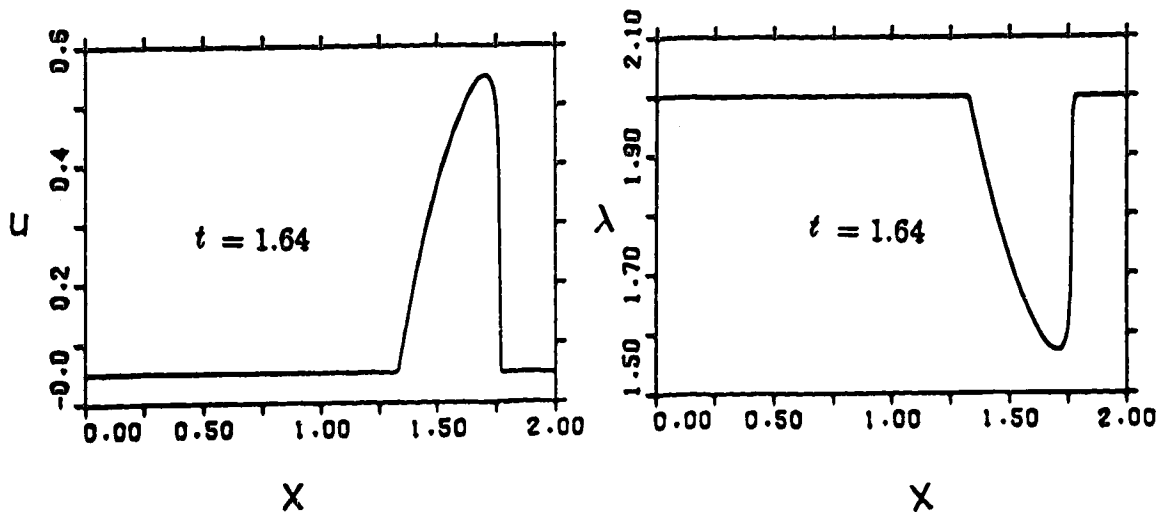


Fig. 5.2a

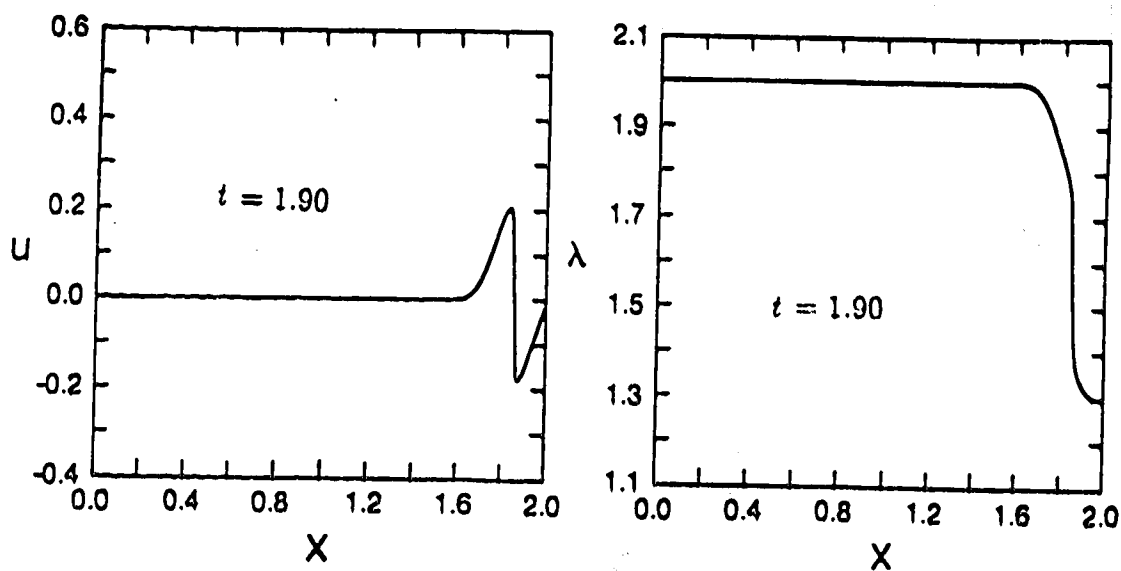


Fig. 5.2b

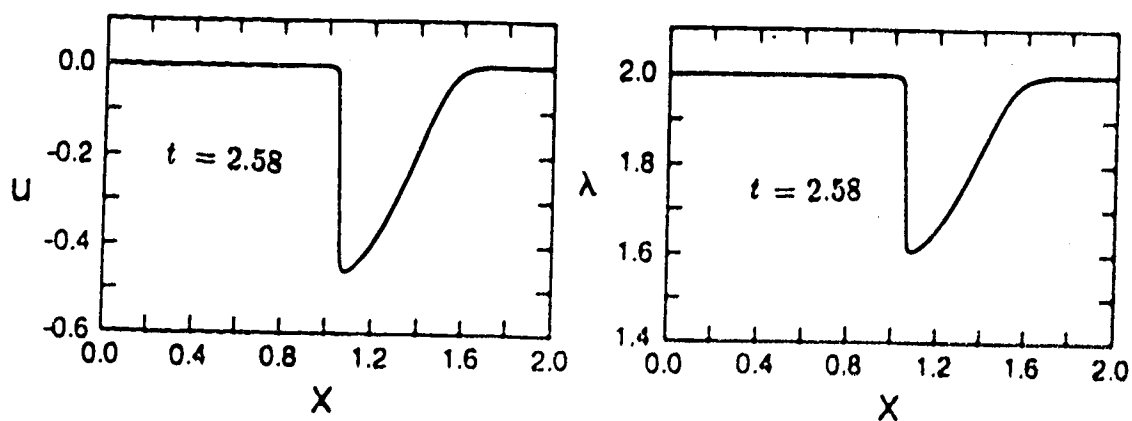


Fig. 5.2c

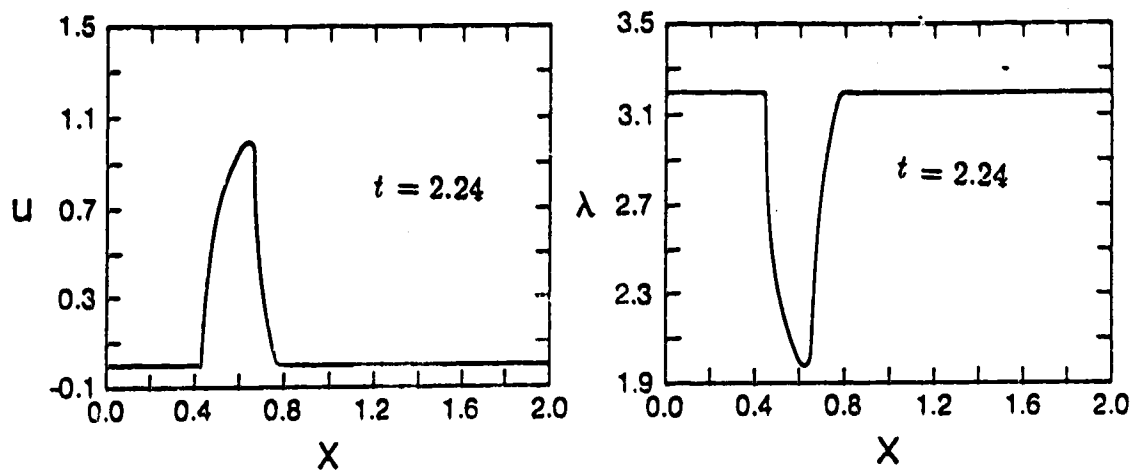


Fig. 5.3a

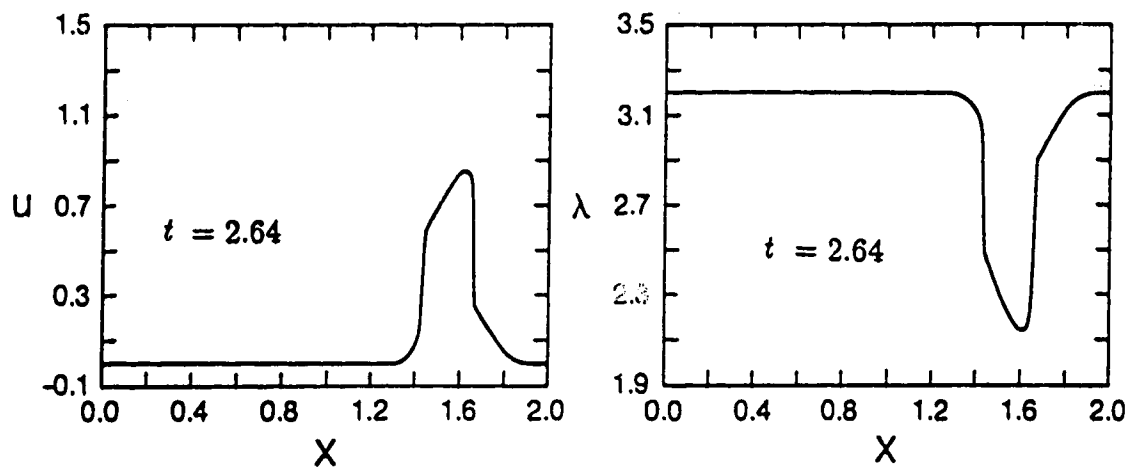


Fig. 5.3b

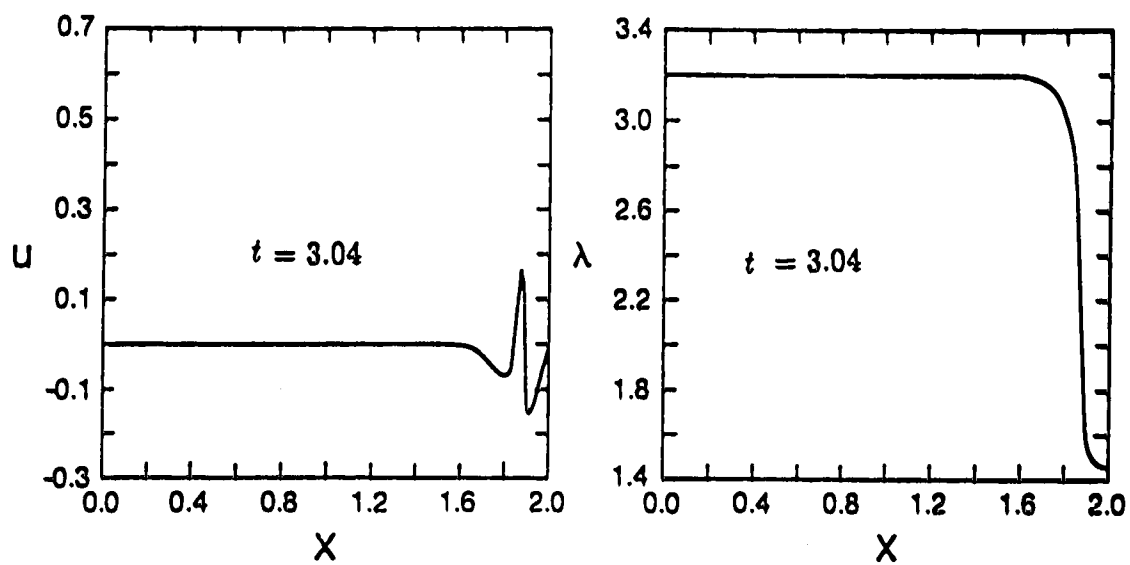


Fig. 5.3c

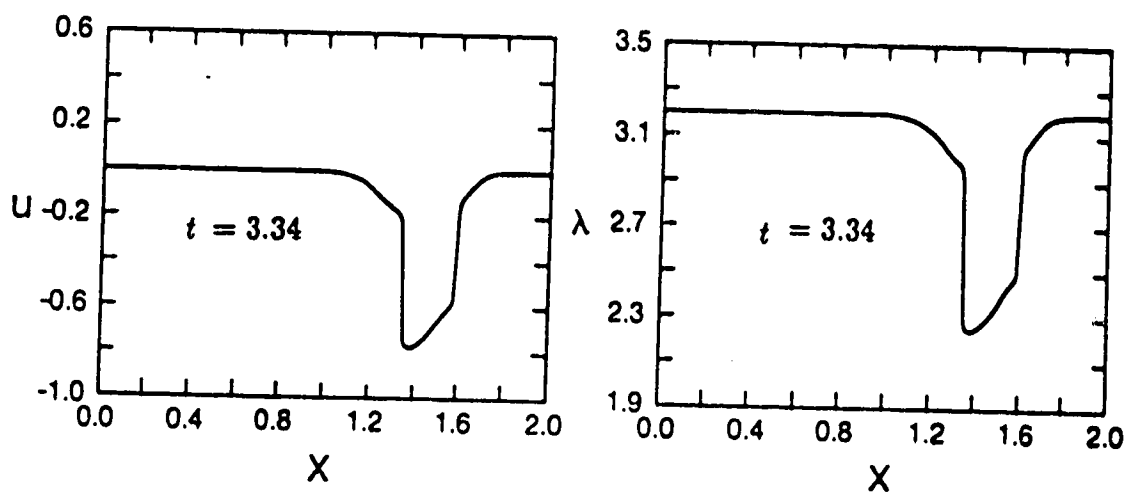


Fig. 5.3d

If instead stress is specified at the left boundary, or equivalently stretch, a similar analysis can be carried out up to the formation of the first shock.

In order to see the effect of the  $S$  shaped stress-stretch relation we take  $L_0 = L$ , with initial stretch  $\lambda_0 = 1.5$ . The boundary condition at the right end is as above and at the left end we take

$$(5.11) \quad \lambda(0, t) = h(t)$$

where

$$h(t) = \begin{cases} 1.5 & t \leq 0 \\ 1.5 + 2\sin(2\pi t) & 0 \leq t \leq \frac{1}{4} \\ 3.5 & t > \frac{1}{4} \end{cases}$$

In order to show the effect of the ACM, we use Algorithm 4.3a both with and without the compression subroutine 4.3b. Fig. 5.4a shows the solution at  $t = 0.9$  and the dotted lines indicate the solution without any ACM. The rest of Fig. 5.4 show the solution at different times after reflection.

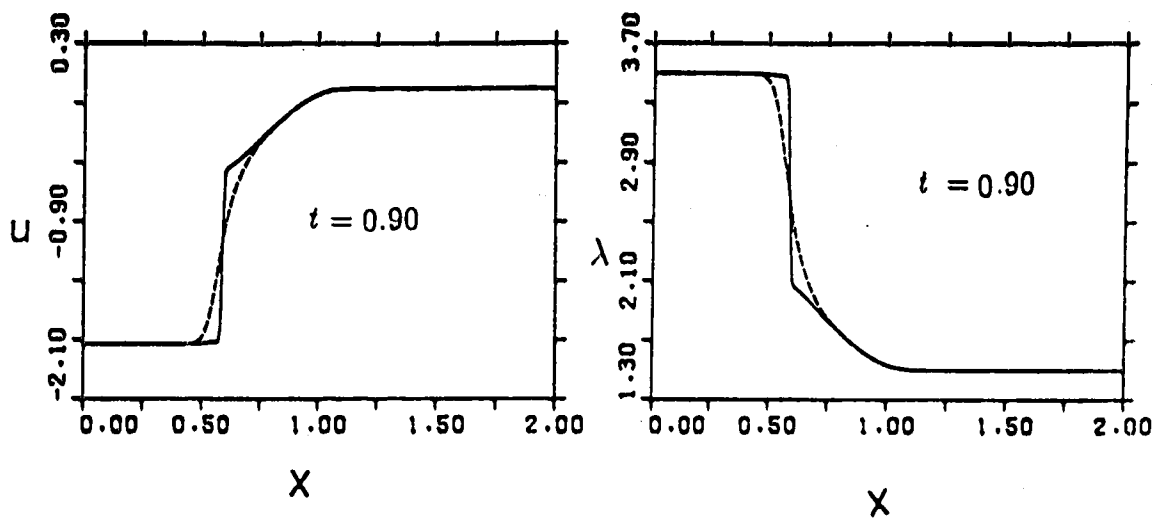


Fig. 5.4a

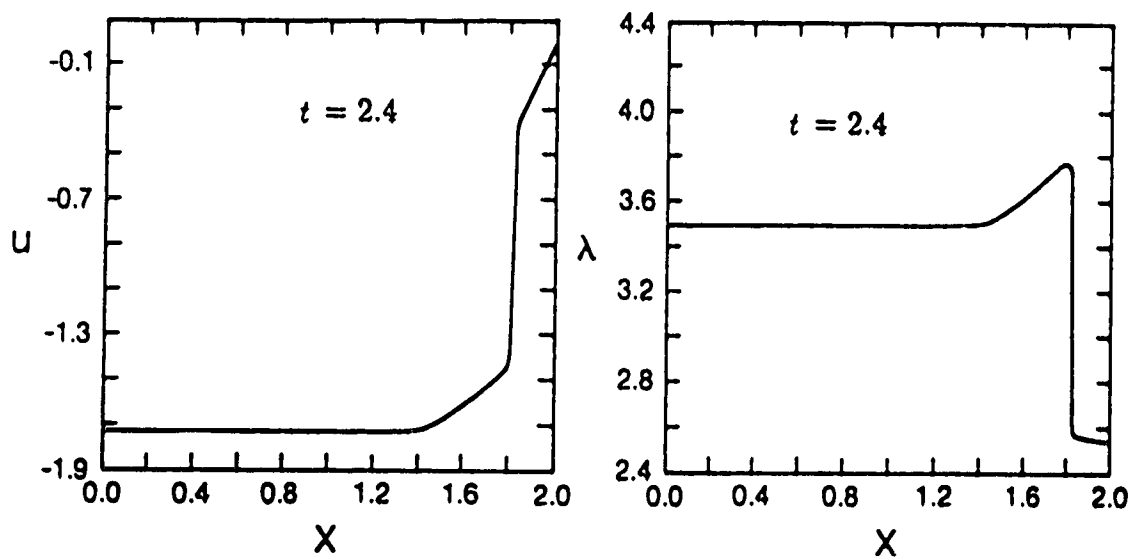


Fig. 5.4b



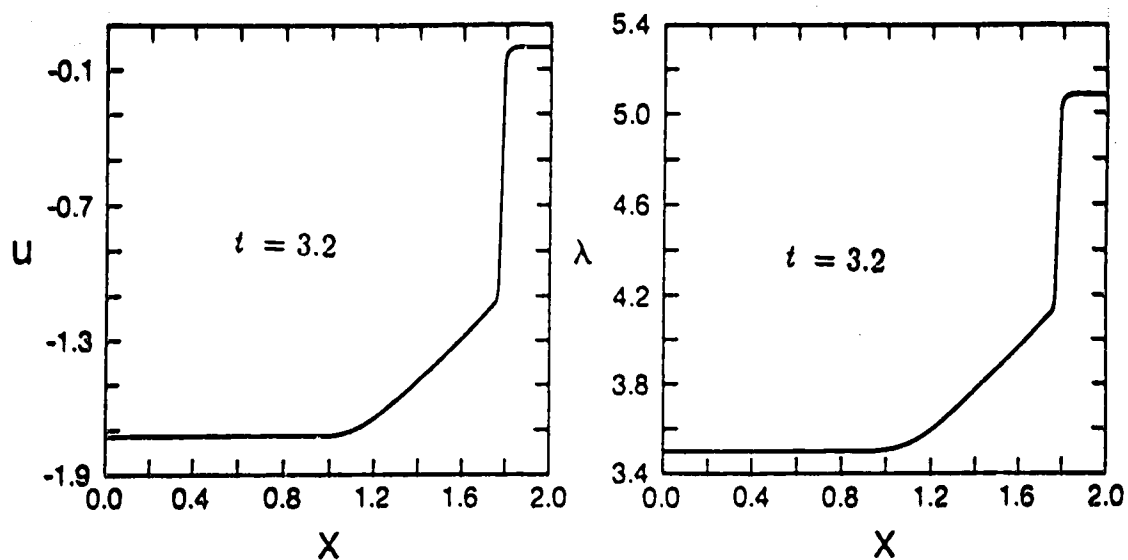


Fig. 5.4c

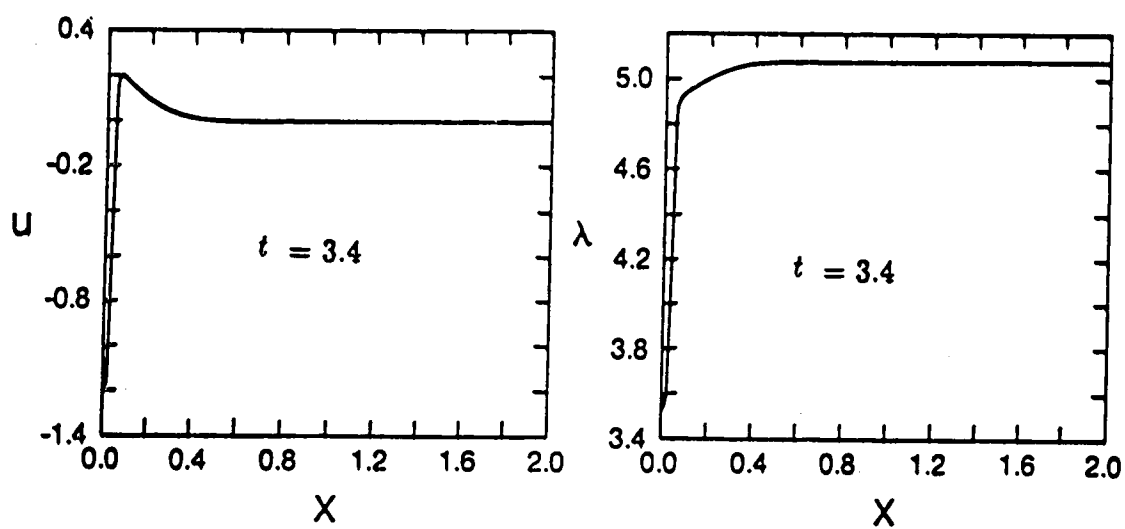


Fig. 5.4d

We now consider a different type of problem. A mass is attached at the left end while fixed at the right and then it is released. The ensuing periodic motion, while assuming that the fixed end did not interfere and while ignoring the mass of the string is described in [1]. In order to see the effect of waves in the string we consider this problem with  $L = L_0$  and an initial stretch of  $\lambda_0 = 3$ , so that  $\lambda$  lies beyond the inflection point or the s-shaped stress-stretch curve. If gravity and friction effects are ignored, then the boundary condition at the left end is

$$(5.11) \quad \frac{du}{dt}(0, t) = \gamma P\{\lambda(0, t)\},$$

where  $\gamma = A_0 L_0 \rho_0 / M$ ,  $A_0$  being the undeformed cross sectional area. A characteristic analysis can be carried out as before. Initially an expansion wave propagates. Depending on the value of  $M$  this either reflects from the right boundary or a shock forms before reflection. If no shock forms and if  $\lambda(0, t)$  decreases sufficiently quickly, the reflected wave causes the string to go into compression and further investigation is required. In either case the behaviour of the string and mass appears to differ from that considered in [1]. We take two diseparate values of  $\gamma$  corresponding to large and small mass, and the results using the numerical algorithm 4.1a without compression is shown on Fig. 5.5 and Fig. 5.6. Fig. 5.5 shows the solution corresponding to the big mass and Fig. 5.6 shows the solution corresponding to the small mass.

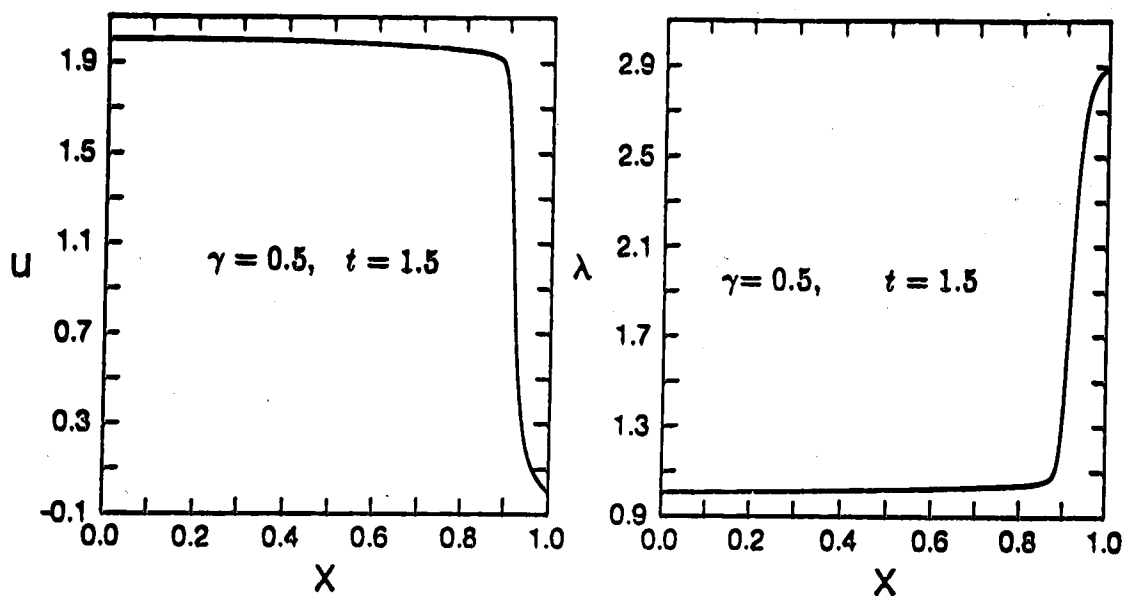


Fig. 5.5

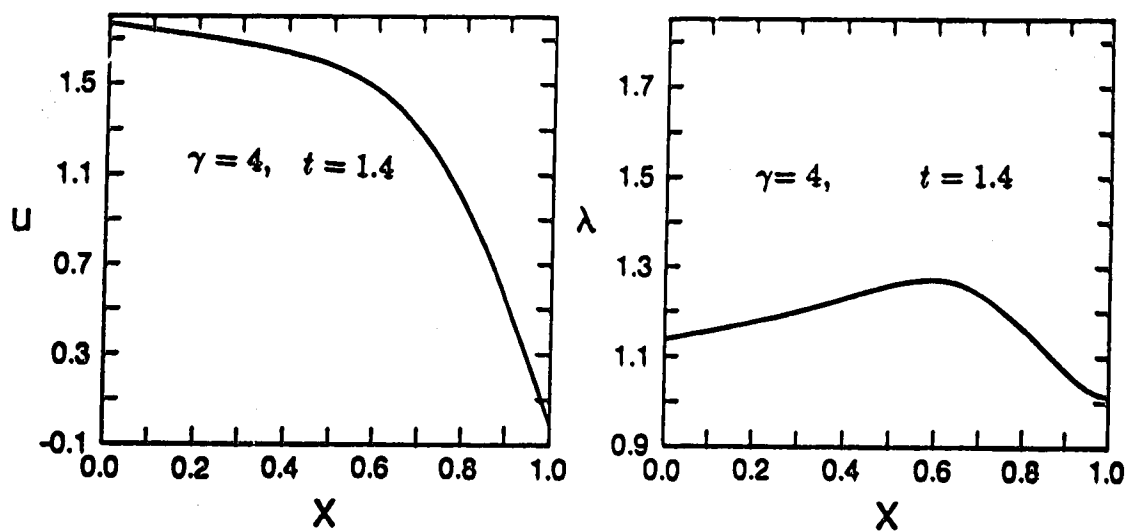


Fig. 5.6

As discussed in Section 4.2 we have also looked at an iterative Riemann solver in order to speed up the Algorithm 4.3a used in the above examples. In order to illustrate the iterative Riemann solver we shall consider simple Riemann problems. Four examples are chosen so that each one represents a Riemann problem with a right state lying in one of the four regions. The result agrees with the analysis given in Section 4.2. For example in region I case the intermediate value of the velocity is monotonically increasing while that of the stretch is monotonically increasing while that of the stretch is monotonically decreasing (see Table 5.1a). The solution found for each region shows that the technique converges to the exact solutions in a few iterations.

When this iterative Riemann solver is used in Algorithm 4.3a to solve the first example considered earlier, where a Neo-Hookian string is released from the left end while fixed at the right end, the solution found is exactly the same as the one found using the exact Riemann solver. However, the computation time has reduced by a factor of about six from the original calculation.

The iterative Riemann solver was also used in the other examples where we have the more complicated three-term stress-stretch relations. As in the Neo-Hookian case the result found matches with the one found with the exact Riemann solver. This numerical result appears to indicate that the iterative Riemann solver can also be used in the three-term string case. Although at this point we do not have any proof to verify this observation, we leave it as a

conjecture that the iterative Riemann solver can be extended to the problems involving the more complicated three-term stress-stretch relation.

$u_l = .5, \quad \lambda_l = 2., \quad u_r = 0., \quad \lambda_r = 4.,$

$i$	$\bar{\lambda}_i$	$\bar{u}_i$
1,	2.66658222532472,	1.072891106644160,
2,	2.665406693615804,	1.072940904554186,
3,	2.665404873508947,	1.072941132492271,
4,	2.665404873052639,	1.072941132845946,
5,	2.665404873052525,	1.072941132846035,
6,	2.665404873052525,	1.072941132846035,

### Region I

Table 5.1a

$u_l = 2., \quad \lambda_l = 2., \quad u_r = -2., \quad \lambda_r = 4.,$

1,	1.720951430460196,	.8234834546000301,
2,	1.720100514214743,	.8245378929376395,
3,	1.720096418692003,	.8245429668276247,
4,	1.720096398950312,	.8245429912853500,
5,	1.720096398855150,	.8245429914032446,
6,	1.720096398854691,	.8245429914038129,
7,	1.720096398854689,	.8245429914038157,
8,	1.720096398854689,	.8245429914038156,
9,	1.720096398854689,	.8245429914038156,

### Region II

Table 5.1b

$u_l = 0., \quad \lambda_l = 4., \quad u_r = 0., \quad \lambda_r = 2.,$

1,	2.971268190171003,	-.8228911066441601,
2,	2.970070266355220,	-.8229054102370379,
3,	2.970068198878485,	-.8229054852708398,
4,	2.970068198707657,	-.8229054854006387,
5,	2.970068198707644,	-.8229054854006493,

### Region III

Table 5.1c

1,	4.224307554369473,	.1771088933558399,
2,	4.224659301528498,	.1771088933558399,
3,	4.224659302270825,	.1771088933558399,

### Region IV

Table 5.1d

## 5.2. Conclusion

The propagation and reflection of waves travelling on a nonlinear hyper-elastic string has been investigated. It is clear that characteristic theory is preferable when available. When shocks and reflections are present numerical methods, such as Godunov's scheme are required. This was the method used in this thesis and it appears to work well and accurately. Godunov's numerical scheme uses numerical fluxs based on the solution of the Riemann problems. The exact solutions of the Riemann problems are very costly to solve. To overcome this difficulty an iterative Riemann solver has been proposed in this thesis at least for the Mooney-Rivlin stress-stretch relation. This method reduces the computation time considerably and it provides accurate results. Moreover numerical experiments have shown that the Riemann solver can also be used for the three-term string. However, since at this point there is no proof this is left as a conjecture. It would be interesting to compare this technique with other Riemann solvers such as the ones given in [7] and [18]. There is no oscillation superimposed on the solutions but shocks do smear. In order to sharpen the shocks Harten's Artificial Compression Method (ACM) with an automatic switch to turn the ACM on and off was used. In all the examples considered this has proven to resolve the shocks enormously.

The numerical experiments or physical examples suggest further investigations. If, for example, in considering the stretch string with a mass attached

to the left end, the string goes into compression on reflection, but there is still tension at the mass. The question arises as to how the string then behaves and as to how compressive regions propagate.

In general the algorithm is successful in solving problems of this type and, with modifications, should be extended to investigate more complicated problems.

## BIBLIOGRAPHY

- [1] Beatty, M.F., Chow, A.C., Free vibration of a loaded rubber string, *J. Nonlinear Mech.*, 19 (1984), 69-82.
- [2] Conlon, J. and Liu, P.P., Admissibility criteria for hyperbolic conservation laws, *Indian U. Math. J.*, 30 (1981), 641-652.
- [3] Fermi, E., Pasta, J.R., Ulam, S., Los Almos, Report No. 1940, May (1955).
- [4] Harten, A., The artificial compression method for computation of shocks and contact discontinuities: I. Single conservation laws, *Comm. Pure Appl. Math.*, 30 (1977), 611-638.
- [5] Harten, A., The artificial compression method for computation of shocks and contact discontinuities: III. Self adjusting hybrid method, *Method, Math. Comp.*, 32 (1978), 363-389.
- [6] Harten, A., Hyman, J.M., and Lax, P.D., On finite difference approximations and entropy conditions for shocks, *Comm. Pure Appl. Math.*, 29 (1976), 292-322.
- [7] Harten, A., Lax, P.D. and VanLeer, B., On upstream differencing and Godunov type schemes for hyperbolic conservation laws, *SIAM Review*, 25 (1983), 35-61.
- [8] Jennings, G., Discrete shocks, *Comm. Pure. Appl. Math.*, 27 (1974), 25-37.
- [9] Lax, P.D., Shock waves and entropy, Contribution to nonlinear functional analysis, S.H. Zaratonell, ed., Academic Press, New York (1971).
- [10] Lax, P.D. and Wendroff, B., Systems of conservation laws, *Comm. Pure Appl. Math.*, 13 (1960), 217-237.
- [11] Ogden, R.W., "Nonlinear Elastic Deformations", Ellis Harwood Limited, Chichester, England, 1984.
- [12] Olenik, O.A., Discontinuous solutions of nonlinear differential equations, *Uspekhi Mat. Nauk.*, 12 (1957), 3 (*Amer. Math. Soc. Trans. Ser.*, 2, 26 95-172).



- [13] Shearer, M., The Riemann problem for the planar motion of an elastic string, *Journal of Differential Equations*, 61 (1986), 149-163.
- [14] Smoller, J. "Shock Waves and Reaction-Diffusion Equations", Springer-Verlag, New York, 1983.
- [15] Smoller, J.A., On the solution of the Riemann problem with general step data for an extended class of hyperbolic systems, *Michigan Math. J.*, 16 (1969), 201-210.
- [16] Tait, R.J., Perturbation theory and nonlinear wave propagation in incompressible elastic materials, Proceedings of Canadian Applied Mathematics Society Conference on Continuum Mechanics, Vancouver 1988. Ed. G.A.C. Graham, S. Malik. Hemisphere pub. (to appear).
- [17] Wegner, J., Haddow, J.B., Tait, R.J., Finite amplitude wave propagation in a stretched elastic string, in "Proceedings IUTAM Symposium On Elastic Wave Propagation" March 1988, Ed. M. McCarthy, M. Hayes, (in press).
- [18] Vila, P.J., Simplified Godunov schemes for  $2 \times 2$  systems of conservation laws, *SIAM J. Numer. Anal.*, 236 (1986), 1173-1192.